FAKULTÄT FÜR MEDIZIN
INSTITUT FÜR HUMANGENETIK
Lehrstuhl: Prof. Dr. Thomas Meitinger

Characterization of a Novel Monogenic Form of Liver Failure

Marlies Gwendolyn Köpke

Vollständiger Abdruck der von der Fakultät für Medizin
der Technischen Universität München zur Erlangung
des akademischen Grades eines Doktors der Medizin (Dr. med.)
genehmigten Dissertation.

Vorsitzender: Prof. Dr. Ernst J. Rummeny

Prüfer der Dissertation:

1. Prof. Dr. Thomas Meitinger
2. Prof. Dr. Percy A. Knolle

Die Dissertation wurde am 07.08.2017 bei der Technischen Universität München eingereicht
und durch die Fakultät für Medizin am 04.07.2018 angenommen.

Table of contents

List of abbreviations

abbreviation	full words
%	percent
ACLF	acute-on-chronic liver failure
ADP	adenosindiphosphate
ALF	acute liver failure
ALT	alanine transaminase
ATP	adenosintriphosphate
bp	base pair
BSA	bovine serum albumin
cDNA	complementary deoxyribonucleic acid
Chr	chromosome
cm	centimetre
CNV	copy number variation
D-MEM	Dulbecco's Modified Eagle Medium
ddH2O	double distilled water
ddNTP	dideoxynucleotide
DMSO	dimethylsulfoxide
DNA	deoxyribonucleic acid
dNTP	deoxynucleotide
ECL	enhanced chemiluminescence
EDTA	ethylene diamine tetra acetic acid
ER	endoplasmic reticulum
ExAC	Exome Aggregation Consortium
FAO	fatty acid oxidation
FBS	fetal bovine serum
g	gram
g	relative centrifugal force
GEFS+	generalized epilepsy with febrile seizures plus
Glu	glutamate
GnomAD	Genome Aggregation Database
h	hour
HE	hepatic encephalopathy
HEK	human embryonic kidney
HEPES	4-(2-hydroxyethyl)-1-piperazineethanesulfonic acid
HIV	human immunodeficiency virus
HLH	hematophagocytic lymphohistiocytosis
HRP	horse radish peroxidase

hrs	hours
IF	immunofluorescence
IgG	immunoglobulin G
ILFS-1	infantile liver failure syndrome 1
ILFS-2	infantile liver failure syndrome 2
ILLD	interstitial lung and liver disease
INR	international normalized ratio
iRALF	infantile recurrent acute liver failure syndrome
ISI	international Sensitivity Index
kb	kilobase
l	litre
LARS	leucil-tRNA synthetase
LCAD	long-chain 3-OH-acyl-CoA dehydrogenase deficiency
LFIT	infantile transient liver failure
LoF	loss of function
M	molar
MARS	methionyl-tRNA synthetase
MARS®	molecular absorbent recirculating system therapy
MCAD	medium-chain acyl-CoA dehydrogenase deficiency
min	minute
MODS	multiple organ dysfunction syndrome
mRNA	messenger RNA
NADH/NAD+	nicotinamide adenine dinucleotide
NAG	neuroblastoma amplified gene
NAPQI	N-acetyl-p-benzoquinone imine
NBAS	neuroblastoma amplified sequence
NHDF	normal human dermal fibroblasts
NHDFneo	neonatal normal human dermal fibroblasts
NTBC	nitisinone
ORF	open reading frame
p	p-value
PAGE	polyacrylamide gel electrophoresis
PALF	pediatric acute liver failure
PALFSG	pediatric acute liver failure study group
PBS	phosphate buffered saline
PI	isoelectric point
PSC	primary sclerosing cholangitis
PT	prothrombin time
PVDF	polyvinylidene difluoride
RALF	recurrent acute liver failure

RCF	relative centrifugal force
RNA	ribonucleic acid
rpm	revolutions per minute
RT	room temperature
s	second
SDS	sodium dodecyl sulfate
SIRS	systemic inflammatory response syndrome
SNP	single nucleotide polymorphism
SOPH	short stature with optic atrophy and Pelger-Huët anomaly
TBS	tris buffered saline
Tris	tris(hydroxymethyl)aminomethane
TRMU	tRNA-5-methylaminomethyl-2-thiouridylate-methyltransferase
U	unit
UTR	untranslated region
V	volt
VLCAD	very-long-chain acyl-coa dehydrogenase deficiency
Wb	Western Blot
wt	wild type
γGT	γ-glutamyl transferase

List of prefixes

prefix	factor	pronunciation
µ	10^{-6}	micro
c	10^{-2}	centi
d	10^{-1}	deci
k	10^{6}	kilo
m	10^{-3}	milli
n	10^{-9}	nano
p	10^{-12}	pico

Introduction

Acute liver failure in children

Liver failure in infancy is a rare yet serious condition. While chronic liver failure is more common than acute liver failure (ALF), especially the latter is a life-threatening event. The most common causes for acute liver failure are drug-toxicity, metabolic disorders, infections such as hepatitis and autoimmune diseases. However, in approximately 35 to 50 % of ALF cases in children, a specific cause cannot be found.

Definition

The term "acute liver failure" refers to the sudden loss of liver function without prior known chronic liver disease or liver dysfunction. The definition of ALF differs between adults and children. In both cases, criteria include no history of known chronic liver disease as well as coagulation abnormality. One important difference, though, is that the duration of the illness must be less than 26 weeks in adults while it must be less than eight weeks in children. Moreover, hepatic encephalopathy is a necessary criterion to make the diagnosis of acute liver failure in adults (Polson et al. 2005). In children, in contrast, hepatic encephalopathy does not have to be present to meet the criteria for ALF. It can be argued though that hepatic encephalopathy may not be detectable in small children.

The Pediatric Acute Liver Failure Study Group (PALFSG) has proposed a definition for ALF in children, who are considered as patients from birth through 17 years of age (Bucuvalas et al. 2006, Narkewicz et al. 2009). Please see the appendix for reference ranges and explanations of the laboratory parameters. The following criteria have to be fulfilled:

- Biochemical evidence of liver injury provided by raised transaminases and/or raised bilirubin levels
- No history of known chronic liver disease
- Coagulopathy not corrected by vitamin K administration
- INR > 1.5 if the patient has encephalopathy or
  INR > 2.0 if the patient does not have encephalopathy
- Illness of less than eight weeks' duration

Acute liver failure may also develop on the basis of a chronic liver disease with or without liver cirrhosis (Canbay et al. 2011). This condition is called acute-on-chronic liver failure (ACLF). It has been stated, though, that acute-on-chronic liver failure is a different entity from acute liver failure and chronic liver failure (Kim and Kim 2013).

Epidemiology

Acute liver failure is a rare event even in large centres (Narkewicz et al. 2009). There are no exact data for incidence in both adults and children, hence numbers can only be estimated.

It is estimated that approximately 200-500 patients a year, adults as well as children, develop ALF in Germany (Canbay et al. 2011). The proportion of adults and children developing ALF is also not known. Recurrent acute liver failure, at the same time, appears to be much more rare (Lee et al. 2008).

There is epidemiological data available, though, on the group of pediatric patients developing acute liver failure. The Pediatric Acute Liver Failure Study Group (PALFSG) examined pediatric ALF patients. They found that in the US, children younger than three years represent more than a third (36.5 %) of pediatric ALF patients. Children younger than one year account for approximately 23 % of all PALF patients alone, constituting the largest age group of children by far (Squires et al. 2006). This stresses the importance to look into acute liver failure in infancy.

Pathophysiology

Clinical acute liver failure is the correlate of injury of hepatocytes on cellular level. The liver is the body's second largest organ after the skin, and amounts to 2 to 5 % of the body weight. It works as a "biochemical factory", being the organ where many metabolic reactions take place, nutrients are stored and released as well as endogenous and exogenous toxins are cleared. It also works as both an endocrine and exocrine gland, is involved in immune defence and is accounting for 25 % of the body's protein synthesis (Speckmann et al. 2013, Pape et al. 2014). Some proteins, thereunder the clotting factors, are almost entirely synthesised in the liver (Larsen and Bjerring 2011) – consequently, haemostasis will be severely impaired in liver failure. The liver is also involved in glucose metabolism, storing a considerable proportion of the body's glucose as glycogen. Liver failure hence results in ceased protein synthesis, reduced clearance of endogenous toxins, dysregulation of glucose metabolism and immune dysfunction.

The sudden and massive necrosis of a large number of hepatocytes at the same time leads to the release of ammonia, alanine, lactate and proinflammatory cytokines as well as DNA, RNA, and cytoskeletal debris (Larsen and Bjerring 2011).

The exact intrahepatic pathophysiology leading to necrosis differs between the different aetiologies of ALF. Yet, extrahepatic complications appear to develop quite homogenously. Patients present with an increased risk of gastrointestinal bleeding, seizures and myocardial dysfunction due to coagulopathy, hypoglycaemia and acidosis. A multiple organ dysfunction syndrome (MODS) frequently occurs in case of ALF (Bucuvalas et al. 2006). The syndrome manifests clinically by renal failure, cardiovascular compromise, acute respiratory distress syndrome, disseminated intravascular coagulation and possibly systemic inflammatory response syndrome (SIRS) (Bucuvalas et al. 2006, Devictor et al. 2011, Larsen and Bjerring 2011). It is attributed to both loss of hepatic functions and microvascular injury (Bucuvalas et al. 2006, Devictor et al. 2011). However, this mechanism is not yet understood (Bucuvalas et al. 2006, Larsen and Bjerring 2011). Additionally, ALF is often complicated by bacterial and fungal infections (Bucuvalas et al. 2006).

An important complication of acute liver failure is encephalopathy. The pathophysiology leading to the development of encephalopathy is also not yet fully understood. Hyperammonaemia is considered brain toxic. Accumulation of glutamine in astrocytes, which is associated with hyperammonaemia present in acute liver failure, leads to the swelling of these cells and, consequently, to brain oedema. However, the levels of both ammonia and glutamine do not correlate with the level of encephalopathy (Bucuvalas et al. 2006, Scott et al. 2013). Increased cerebral blood flow as well as an enhanced inflammatory response also appear to play an important role in the development of encephalopathy (Bucuvalas et al. 2006). Intracranial hypertension may develop, necessitating intensive care and leading to death in many cases (Bucuvalas et al. 2006, Gerner and Hoyer 2009). Nonetheless, it has been shown that progression to life-threatening intracranial pressure is less frequent than previously described (Scott et al. 2013).

Aetiology

Acute liver failure is the final common pathway of many different conditions. While in adults, paracetamol accounts for almost half of all ALF cases (46 %) and only 14 % of ALF remains

with an undetermined cause (Lee et al. 2008), causes in children are distributed quite differently.

The four leading reasons in children are drugs (which can be subdivided into paracetamol and non-paracetamol), metabolic and other inherited disorders, infections and autoimmune diseases (Squires et al. 2006). The prevalence of causes varies between different age groups and different ethnicities (Bucuvalas et al. 2006), as can be seen in Figure 1 below.

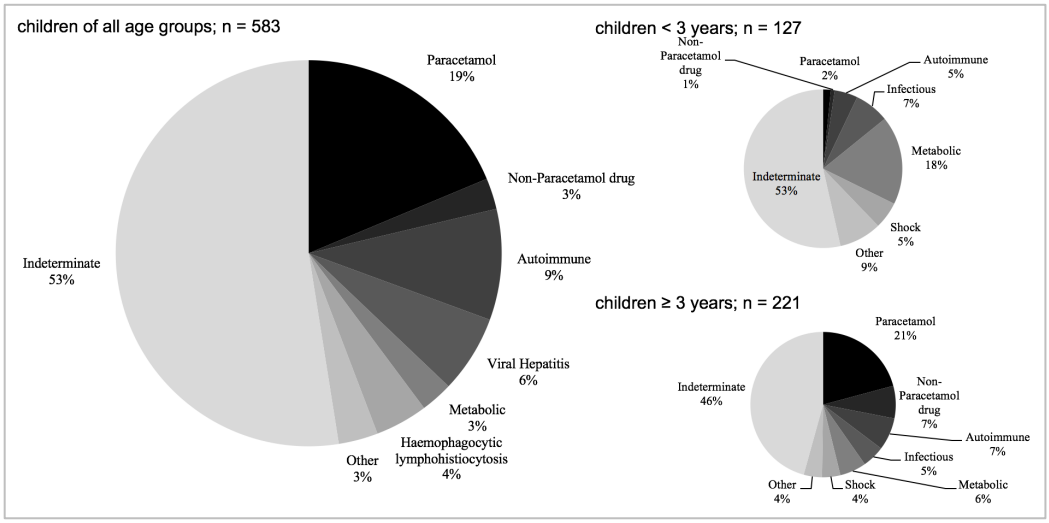

Figure 1: Distribution of aetiology of pediatric acute liver failure. Data on the left taken from Kulkarni et al. (2015), data on the right taken from Squires et al. (2006).

Most notably, the aetiology of acute liver failure remains undetermined in approximately half of pediatric acute liver failure patients (Squires et al. 2006, Narkewicz et al. 2009, Kulkarni et al. 2015). While in children aged less than three years, metabolic disorders mark the largest determined group of causes, being the cause for liver failure in almost one in five patients (18 %), they are not as important any more in children aged three years and older, where paracetamol is the reason for ALF in more than one in five patients (21 %) (Squires et al. 2006). It has been argued that possible causes for ALF may not have been examined thoroughly enough and henceforth known causes for ALF may have been overlooked (Narkewicz et al. 2009). Moreover, a considerable proportion of PALF of indeterminate cause is arguably due to unknown metabolic diseases or atypical clinical presentation of known metabolic diseases (Vilarinho et al. 2014).

Recurrent acute liver failure with clinical and biochemical hepatic recovery may result from different aetiologies, including infections such as fulminant viral hepatitis, immune

dysregulation such as autoimmune hepatitis as well as several inborn errors (Odaib et al. 1998, Rinaldo 2001, Engelmann et al. 2008, Brassier et al. 2013).

Drug-induced ALF

In children, drug induced ALF represents the largest entity of ALF causes. Paracetamol, at the same time, is clearly the most important ALF triggering drug. Yet it should be stressed that drug toxicity as reason for ALF is much more common in children older than three years than in younger children (Squires et al. 2006).

Drugs may lead to acute liver failure either in a dose-dependent fashion or, more often, as an idiosyncratic reaction at therapeutic doses with latency of five to 90 days (Lee 2003).

Paracetamol

Paracetamol typically causes dose-dependent hepatic injury (Lee 2003, Devictor et al. 2011). After the detoxification capacity of the liver is exceeded, the toxic metabolite of paracetamol, N-acetyl-p-benzoquinone imine (NAPQI), induces hepatocyte necrosis (Bucuvalas et al. 2006, Gerner and Hoyer 2009). Toxic doses may vary. Doses larger than 140 mg/kg body weight, however, are considered as potentially toxic (Gee and Ardagh 1998).

At the same time, it has been suggested that paracetamol may also lead to hepatotoxicity in therapeutic doses in some patients. In children, this has been linked to fasting periods as well as to generalized epilepsy with febrile seizures plus syndrome (GEFS+, Dravet-Syndrome) (Gerner and Hoyer 2009).

Non-paracetamol drug

While many different non-paracetamol drugs may also cause ALF (Squires et al. 2006), anticonvulsants should be highlighted (Bucuvalas et al. 2006, Gerner and Hoyer 2009). Phenytoin, carbamazepine and phenobarbital may lead to ALF (Bucuvalas et al. 2006), yet, valproate appears to be causing ALF the most often (Squires et al. 2006, Gerner and Hoyer 2009). It is known to be hepatotoxic (Aktories et al. 2013) particularly in patients with mitochondrial disorders (Sitarz et al. 2014). Many antimicrobials belong to the large group of ALF-causing drugs as well (Devictor et al. 2011).

In this group of non-paracetamol drugs, psychedelic mushrooms are also included. They appear not to be too rare as aetiology of ALF, yet not too common either (Squires et al. 2006, Devictor et al. 2011).

Metabolic and other inherited disorders

Besides drug toxicity, metabolic and other inherited disorders comprise the group of most frequent detected causes for ALF in children. They are the cause for ALF in almost one in five affected patients younger than three years (Squires et al. 2006). Patients with inherited metabolic disorders appear to present with acute liver failure in neonates and infancy, although children may also become symptomatic later (Gerner and Hoyer 2009). Nonetheless, the only markers for an inborn metabolic disorder in a study by Brett et al. (2013) appeared to be failure to thrive and history of vomiting on admission. Mitochondriopathies, Wilson disease and disorders of fatty acid oxidation (FAO) were identified as the most common metabolic disorders leading to ALF (Rinaldo 2001, Squires et al. 2006, Gerner and Hoyer 2009). Additionally, galactosaemia, hereditary fructose intolerance, tyrosinaemia, Niemann-Pick type C as well as Urea cycle defects were described as causes for ALF in children (Squires et al. 2006).

Some inborn errors of metabolism may also cause recurrent acute liver failure with recovery in the interval, that is, transient acute liver failure. Known metabolic causes are long-chain fatty acid oxidation deficiency (LCAD), disorders of the carnitine cycle, dihydrolipoamide dehydrogenase (E3) deficiency and Wolcott-Rallison syndrome (Odaib et al. 1998, Rinaldo 2001, Engelmann et al. 2008, Brassier et al. 2013).

Mutations in different other genes have also been described to cause transient ALF: *TRMU* (transient infantile liver failure (Zeharia et al. 2009)), *LARS* (infantile liver failure syndrome 1 (Casey et al. 2012)), *MARS* (interstitial lung and liver disease (van Meel et al. 2013)) and *IARS* (Growth retardation, intellectual developmental disorder, hypotonia, and hepatopathy (Kopajtich et al. 2016)). These disorders have been identified in several families from different origins.

In Germany, 99.5 % of all neonates are screened for inborn metabolic and endocrine disorders for which specific therapies exist (Harms and Olgemoller 2011). There are also ALF causing diseases amongst these screened disorders. Examples include galactosaemia and defects of FAO such as Medium-chain acyl-CoA dehydrogenase deficiency (MCAD), Long-chain 3-OH-

acyl-CoA dehydrogenase deficiency (LCHAD) as well as Very-long-chain acyl-CoA dehydrogenase deficiency (VLCAD) (Squires et al. 2006, Harms and Olgemoller 2011). The detection rate of inborn metabolic disorders has highly increased after the expansion of the neonate screening in 2005. Between 2005 and 2008, one in 1428 screened new-borns was diagnosed with a disease by neonatal screening. As a result, the respective appropriate therapies could successfully be administered to patients earlier (Harms and Olgemoller 2011). Possible therapies are outlined later on in the section "Therapy".

Autoimmune diseases

Autoimmune hepatitis usually starts as chronic inflammatory liver disease and may present as ALF in children, although this occurs in 5 % of cases only (Bucuvalas et al. 2006, Gerner and Hoyer 2009). The disease develops as a result of an immune reaction to liver cell antigens (Bucuvalas et al. 2006, Devictor et al. 2011). Patients present with progressive jaundice, uncorrectable coagulopathy over the course of one to six weeks and often develop hepatic encephalopathy (Gerner and Hoyer 2009, Devictor et al. 2011). Typically, antibodies and elevated immunoglobulin G (IgG) can be detected (Gerner and Hoyer 2009).

Haematophagocytic lymphohistiocytosis (HLH) may also present as acute liver failure with fever, hepatosplenomegaly and cytopenia, findings that are consistent with SIRS (Bucuvalas et al. 2006, Gerner and Hoyer 2009). The disease develops as a result of a disproportional immune response (Bucuvalas et al. 2006).

Coeliac disease and primary sclerosing cholangitis (PSC) have also been associated with acute liver failure (Gerner and Hoyer 2009).

Infections

An infection should be considered when the child presents with unspecific symptoms such as fever, loss of appetite and myalgia. Neonates and infants, in which symptoms are not easy to assess, are affected relatively often (Gerner and Hoyer 2009). While in Western countries, infections account for only 6 % of ALF in children (Bucuvalas et al. 2006), they present the most common cause for pediatric ALF in countries where hepatotropic viruses such as hepatitis A and E are endemic, such as India and Africa (Devictor et al. 2011, Bhatia et al. 2013). However, ALF may also be associated with Epstein-Barr virus, cytomegalovirus, adenovirus and herpes simplex virus, which are common in Europe (Bucuvalas et al. 2006, Squires et al.

2006, Gerner and Hoyer 2009, Mellinger et al. 2014). In young children, herpes simplex virus is the most common viral cause (Squires et al. 2006, Narkewicz et al. 2009).

Clinical phenotype

Clinical signs of acute liver failure may present to be unspecific (Gerner and Hoyer 2009). Very often, jaundice can be observed (71 %), followed by hepatomegaly (54 %), splenomegaly (20 %) and ascites (10 %) (Lee et al. 2005).

Hepatic encephalopathy (HE) and concomitant cerebral oedema may result in intracranial hypertension (Bucuvalas et al. 2006). HE, which is an ALF defining sign in adults, may be difficult to assess in children. The Pediatric Acute Liver Failure Study Group (PALFSG) has developed a scale to try to nonetheless assess hepatic encephalopathy in young children up until the age of 3 (Bucuvalas et al. 2006, Squires et al. 2006).

While Lee et al. (2005) present data where all children over the age of one year presented with hepatic encephalopathy (n = 58), only 54 % of children, comprising all age groups though, presented with HE in the patients the PALFSG examined (n = 222, Squires et al. (2006)). Interestingly, the PALFSG noted that 34 % of ALF children remained without HE during the course of the disease (Squires et al. 2006). HE may not always be properly assessed in small children though.

Children with ALF may also present with hypoglycaemia since the injured liver cannot uphold its glycogen metabolism and provide glucose. Additionally, it may fail to produce enough clotting factors so that the patients may present with acute haemorrhage, although this is an exception even in case of very low INR values. If the patient is actually bleeding, it occurs predominantly in the gastrointestinal tract (Gerner and Hoyer 2009).

Diagnostics

Proper diagnostics have to be conducted in order to find the individual reason for the occurrence of acute liver failure. The importance of a specific diagnosis is stressed as a high rate of undetermined causes is to be expected and possible therapies diverge between the different causes. Therapies will be outlined later in the section “Therapy”.

As always in medicine, a detailed anamnesis is crucial (Gerner and Hoyer 2009). The use of medical imaging is decided in each individual case, simply an ultrasonic examination of the

abdomen is compulsory. The size of the liver should be measured and documented carefully as a progression parameter, since it may decrease significantly during the time of the disease (Bucuvalas et al. 2006). An electroencephalography (EEG) is also required. It may be used as a progression parameter (Gerner and Hoyer 2009). In addition, EEG abnormalities on admission have been linked to poor outcome (Hussain et al. 2014).

The four leading causes of acute liver failure should be screened in ALF patients, i.e. drug toxicity, metabolic liver disease, autoimmune hepatitis and infections (Narkewicz et al. 2009). Drugs, most importantly paracetamol, as well as infections may be detected biochemically in the patient's blood serum. The identification of metabolic disorders may be helped by whole exome sequence analysis (Vilarinho et al. 2014). Autoimmune liver disease is often difficult to diagnose. While autoantibodies may be detected in some patients' blood, a biopsy of the liver may also be useful (Gerner and Hoyer 2009, Devictor et al. 2011).

The establishment of an individual diagnosis is crucial for the patient. There may not be a specific therapy, yet the prognosis may be estimated and hence important decisions such as procession with liver transplantation and genetic counselling of the family can be reached (Narkewicz et al. 2009).

Therapy

Therapeutic options differ widely between the different underlying causes of ALF. Since a specific cause cannot be identified in almost half of the cases, clinical management of patients is largely supportive (Squires et al. 2013). ALF remains a challenging medical condition in which intensive care is required in order to prevent or treat possible complications (Devictor et al. 2011). In any case, the patient should be transferred to a specialised centre with possibility for liver transplantation, as this is the only emergency treatment in many cases (Gerner and Hoyer 2009, Devictor et al. 2011).

General supportive care measures

Supportive care is centred on pathophysiological complications of liver failure. General supportive care includes tight balancing of fluid in order to prevent cardiopulmonary failure, renal failure, encephalopathy as well as ascites and intravenous or subcutaneous administration of vitamin K in order to balance the bleeding diathesis. Patients with metabolic disorders are generally provided with continuous parenteral glucose administration in order to achieve an

anabolic situation. Antimicrobial substances should be administered generously (Gerner and Hoyer 2009, Devictor et al. 2011). Extracorporeal liver assist devices may be helpful in systemic detoxification. Different methods, such as Molecular Absorbent Recirculating System therapy (MARS®) or transplantation of liver cells are available, although they are only recommended as a bridging therapy before undergoing liver transplantation at this point (Gerner and Hoyer 2009, Meyburg and Hoffmann 2010, Devictor et al. 2011, Bourgoin et al. 2014, Lexmond et al. 2015, Sponholz et al. 2016).

Disease-specific therapies

Specific therapy should be applied where possible.

Drug-induced ALF

N-acetylcysteine should be administered intravenously in case of a paracetamol overdose. It has been discussed whether this therapy is also beneficial in other non-paracetamol induced cases of ALF (Gerner and Hoyer 2009, Squires et al. 2013).

Autoimmune diseases

Autoimmune disorders should be treated with immunosuppression. This may be accomplished by administration of glucocorticoids or a combination of steroids and azathioprine (Gerner and Hoyer 2009, Speer and Gahr 2013).

Infections

There is specific medication against some viruses. Hepatitis due to herpes viruses should be treated by aciclovir while hepatitis due to hepatitis B virus should be treated by lamivudine (Gerner and Hoyer 2009, Narkewicz et al. 2009, Devictor et al. 2011).

Metabolic and other inherited disorders

The clinical management of patients with metabolic and other inherited disorders in acute liver failure centres on supportive care measurements. Especially patients with disorders of fatty acid metabolism should immediately be intravenously administered with high doses of glucose during crises (Speer and Gahr 2013).

For most metabolic diseases, there is no causal acute or chronic therapy. Nonetheless, there are specific long-term therapies for several diseases. These can be quite different depending on the disorder. For example, there are some diseases that are quite well treatable by specific

medication. To list some examples: for Wilson disease, D-penicillamine and zinc (Hermann 2012); for tyrosinaemia, nitisinone (NTBC) (Gerner and Hoyer 2009, Narkewicz et al. 2009, Devictor et al. 2011). Patients with mitochondrial disorders should, at the same time, not be treated with medication that inhibits the respiratory chain (Speer and Gahr 2013). Other diseases can be treated or their exacerbation can be prevented by a specific diet. In case of galactosaemia, the diet should be low in galactose and free from lactose; in case of hereditary fructose intolerance, the diet should be free from fructose (Gortner et al. 2012, Speer and Gahr 2013). Patients with urea cycle disorders are usually also treated with protein restricted diets supplemented with essential nutrients such as vitamins and minerals (Häberle 2012). Patients with mutations in *TRMU* may be treated with L-cysteine or N-acetyl-cysteine in future (Bartsakoulia et al. 2016). Specific therapies for the previously mentioned liver failure syndromes due to mutations in *MARS, LARS* and *IARS* have not yet been described.

Liver transplantation

Liver transplantation is the final option to treat and cure a patient with liver failure. In best case, the new liver will take up healthy function in the acceptor's body, not only curing the acute crisis but also preventing future ones. However, a liver transplant does not only have positive side effects. As with any transplant, the patient will have to take immunosuppressive medication for the rest of their life, putting them at risk for infections and various other diseases. If insufficient, though, the recipient's body may reject the transplanted organ, causing an inflammatory reaction possibly injuring the entire organism. Also, the transplanted organ is likely to last for several years only and may have to be replaced at some stage, not to mention the possible risks taken by the patient simply through the transplant operation (Ho et al. 2016).

Nonetheless, it is recommended to list the ALF patient for liver transplantation when there is a low likelihood of spontaneous recovery and at the same time, the child does not suffer from irreversible cerebral injury or respiratory failure (Bucuvalas et al. 2006). Although emergency liver transplantation continues to be the linchpin of ALF therapy (Devictor et al. 2011), ALF represents only 2 % of indications for pediatric liver transplantation in Germany (Ganschow 2011). In patients with malignant diseases and others that will not be cured by liver transplantation, which amount to 11 to 20 % of pediatric acute liver failure cases, liver transplantation is contraindicated. It is important to quickly evaluate all other candidates for possible listing for transplantation in order not to lose time (Devictor et al. 2011).

Prognosis

During the pretransplant era, acute liver failure in children led to death in up to 70 % of cases (Psacharopoulos et al. 1980). Fortunately the management of liver transplantation as well as general supportive care measures have greatly advanced. Hence, survival rates have notably increased. However, exact data are lacking here as well as in epidemiology. Some numbers have been estimated in studies providing benchmarks for the prognosis of children with acute liver failure.

Liu et al. (2006) published a total survival rate of 72 % in 2005, while Squires et al. (2006) published a survival rate of 82 % in 2006, which was yet only relating to 21-day-survival. Survival rates differ between the different causes of acute liver failure, ranging from 40 % in haematological/oncological causes up to 100 % in paracetamol induced liver failure (Liu et al. 2006). Intracranial pressure and cerebral oedema is a major cause of death in pediatric ALF (Bucuvalas et al. 2006, Gerner and Hoyer 2009).

Spontaneous recovery rates are greatest in paracetamol induced liver failure and, in contrast, lowest in non-APAP-drug induced liver failure (Squires et al. 2006). Liver transplantation was conducted in approximately 33 % of cases (Squires et al. 2006) and is linked to a long-term survival of 52 % in infants to 79 % in older children (Devictor et al. 2011). Interestingly, outcomes appear to be more benign in children than in adults (Dhawan et al. 2004). Outcomes of acute liver failure in children are visualized in Figure 2.

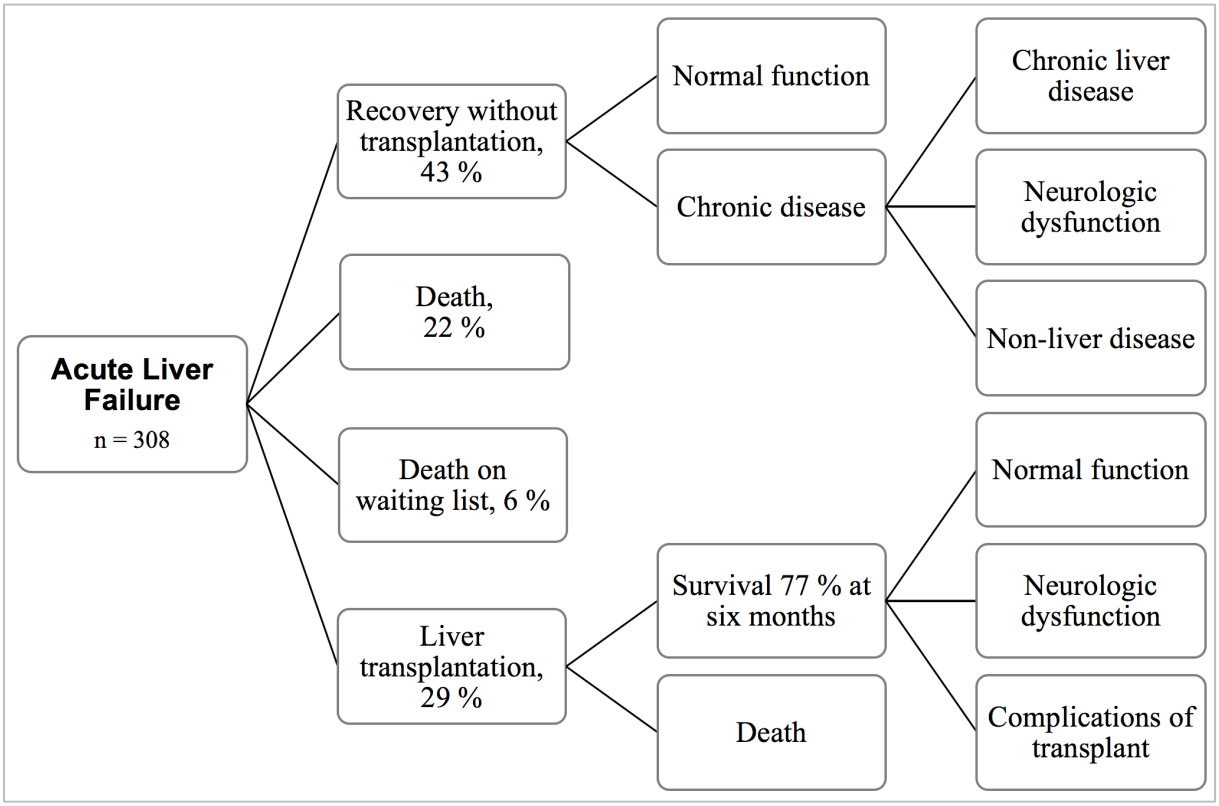

Figure 2: Outcome of acute liver failure in children.
Diagram adapted from Bucuvalas et al. (2006) and Lee (2003).

Several prognostic indicators in the event of acute liver failure in children were described. While age, sex and aetiology did not appear to be statistically significant prognostic indicators (Lee et al. 2005), the following conditions were found to be poor prognostic indicators for death or liver transplantation (Lee et al. 2005, Squires et al. 2006). Please see the appendix for reference ranges and explanations of the laboratory parameters.

- Prothrombin time > 55 seconds, INR ≥ 2.55
- Alanine transaminase (ALT) ≤ 2384 U/l on admission
- Total bilirubin ≥ 5 mg/dl
- Rising bilirubin in combination with falling transaminases
- Hepatic encephalopathy if present on admission
- Time to onset of hepatic encephalopathy > 7 days
- Moderate or severe abnormality of EEG on admission (Hussain et al. 2014)

Chronic liver failure in children

Chronic liver failure is by far more common than acute liver failure. This work centres on acute liver failure, however, an overview of chronic liver failure is given here for the sake of completeness and differentiation.

Definition

Patients, adults as well as children, may also develop chronic liver failure. In contrast to acute liver failure, chronic liver failure is irreversible. Chronic liver failure, or alternatively called end-stage liver disease, is characterised by permanent liver dysfunction, cirrhotic conversion of the liver and impairment of blood supply (Leonis and Balistreri 2008, Young et al. 2013). Chronic liver failure may decompensate. Acute-on-chronic liver failure, however, is to be differentiated from this exacerbation (Kim and Kim 2013).

Epidemiology

Chronic liver failure in children is rare, although more common than acute liver failure. Nonetheless, its importance must not be underestimated as end-stage liver disease often leads to high morbidity with need for tertiary care and consequently substantial impairment of quality of life, not only for the patient, but also for their environment (Leonis and Balistreri 2008, Young et al. 2013).

Aetiology

Like in acute liver failure, the aetiology of chronic liver failure is different in different age groups. In infancy, the causes of end-stage liver disease are mostly inborn. Possible causes include progressive familial intrahepatic cholestasis syndromes, other inborn metabolic disorders such as tyrosinemia and urea cycle disorders, Alagille Syndrome and, most importantly, biliary atresia. In older children and adolescents, the predominant causes of end-stage liver disease are, amongst others, autoimmune hepatitis, cryptogenic cirrhosis and α_1-antitrypsin deficiency (Leonis and Balistreri 2008, Young et al. 2013).

Clinical presentation

End-stage liver disease may lead to complications of cirrhosis such as portal hypertension, gastroesophageal varices and variceal haemorrhage, ascites, spontaneous bacterial peritonitis, hepatic encephalopathy as well as hepatopulmonary syndrome (Leonis and Balistreri 2008).

Most children with end-stage liver disease also develop moderate to severe malnutrition requiring intervention (Young et al. 2013).

Therapy

The ultimate therapy of chronic liver failure in children is liver transplantation. Biliary atresia is the reason for 60 % of pediatric liver transplantations (Ganschow 2011). However, complications of the end-stage liver disease before transplantation can and must be managed. Vaccinations in children should be maximised. Nutrient deficiencies should be screened and balanced. Ascites and other complications must be managed. There is much research going on in the field in order to improve the quality of life of children with end-stage liver disease (Leonis and Balistreri 2008, Young et al. 2013).

Fever and its association with liver disease

Definition

Fever, or alternatively called pyrexia, is defined as central body temperature elevated to 38 °C and higher due to an increase of the temperature regulatory set-point in the hypothalamus. It is mediated by endogenous pyrogens, e.g. IL-1, IL-6 and TNF-α, which are produced from arachidonic acid.

Fever is to be differentiated from hyperthermia that results from inadequate production or insufficient emission of heat (Renz-Polster and Krautzig 2013, Speckmann et al. 2013, Speer and Gahr 2013, Pape et al. 2014).

Physiologic and pathophysiologic effects

Fever is a physiologic process that is thought to help immune response. Some processes of immune response have been shown to proceed faster *in vitro* while the virulence of some microorganisms decreases at elevated temperatures. Additionally, some animals have been shown to be more likely to survive infections when having fever. It has been conjectured that fever also stimulates proliferation of lymphocytes and formation of antibodies (Renz-Polster and Krautzig 2013, Pape et al. 2014).

Temperatures higher than 41 °C, defined as hyperpyrexia, however, lead to metabolic derailment. The patient's general health and cardiovascular system may be severely impaired. Very high temperatures higher than 42 °C may even lead to cerebral damage (Renz-Polster and Krautzig 2013, Speer and Gahr 2013, Pape et al. 2014).

Fever is, as mentioned above, elevated body temperature due to an increase of the temperature regulatory set-point. When the fever is not needed any more, the set-point will be set back to normal. As the body needs time to adjust to the temperature regulatory set-point, patients will feel cold while temperature is increasing and will feel hot while temperature is decreasing again (Speckmann et al. 2013, Pape et al. 2014). This may be used as one possible clinical indicator whether the patient's fever is rather rising or falling.

Therapy

It has been discussed whether fever should be left or brought down medicinally. Different arguments should be considered. It has been shown that some infections, e.g. influenza, may be

over quicker when the patient has fever. At the same time, fever may also severely impair the patient's general health and their cardiovascular system, amongst others (Renz-Polster and Krautzig 2013).

Hence, it is suggested to ameliorate symptoms of fever by antipyretic medication if the temperature has risen to 39,5 °C or if the patient is at cardiopulmonary risk (Renz-Polster and Krautzig 2013, Speer and Gahr 2013).

Fever can be lowered by medicinal and by physical measures. Possible antipyretic drugs are cyclooxygenase inhibitors which inhibit the metabolism of arachidonic acid and hence inhibit the elevation of the temperature regulatory set-point. In children, paracetamol is the antipyretic drug of first choice. Paracetamol, however, is mainly excreted by the liver and may cause harm to it. Alternatively, ibuprofen and metamizole can be applied. Acetylsalicylic acid should not be applied to children, although it can be used as a potent antipyretic drug in adults. Physical measures include external heat derivation by leg compresses or cold sheets. Extra attention should be paid to the patient's fluid balance. While febrile, patients have a high need for fluid. Therefore, patients should be sufficiently administered with fluids (Renz-Polster and Krautzig 2013, Speer and Gahr 2013).

Association with liver disease

While moderate liver dysfunction may often accompany viral infections, fever has been associated with severe liver disease in rare cases.

Dengue fever has been associated with acute liver failure (Jhamb et al. 2011, Tan and Bujang 2013). Familial Mediterranean fever has also been linked to liver disease (Unal et al. 2012).

Recurrent acute liver failure syndrome

When I joined the laboratory of Dr. Holger Prokisch in October 2013, his group had recently detected mutations in the gene *NBAS* as the common genetic cause for recurrent acute liver failure in infancy in four unrelated patients. They were treated for recurrent fever-dependent acute liver failure and full recovery in the interval in the centre for pediatric and adolescent medicine at the University Hospital Heidelberg by Prof. Georg Hoffmann. Information about the patients was acquired by personal clinical contact between Prof. Hoffmann and Dr. Prokisch. While the patients suffered from a high number of episodes of acute liver failure during infancy when they had fever, the frequency of these episodes decreased with increasing age. By the time the patients grew up to the age of 18 years, they had suffered from no further episodes of acute liver failure.

Despite a thorough work-up during crises and in the interval, no evidence had been found indicating any of the other heretofore known causes of pediatric acute liver failure.

Hence, whole exome analysis had been performed on genomic DNA on these four patients. *NBAS* (NM_015909.3 (UCSC Genome Browser 2017), OMIM #608025 (OMIM 2015)), was found to be the only gene in which biallelic mutations were present in all affected individuals.

These index patients have from then on been labelled as patients 1 to 4. Their pedigrees are shown below in Figure 3.

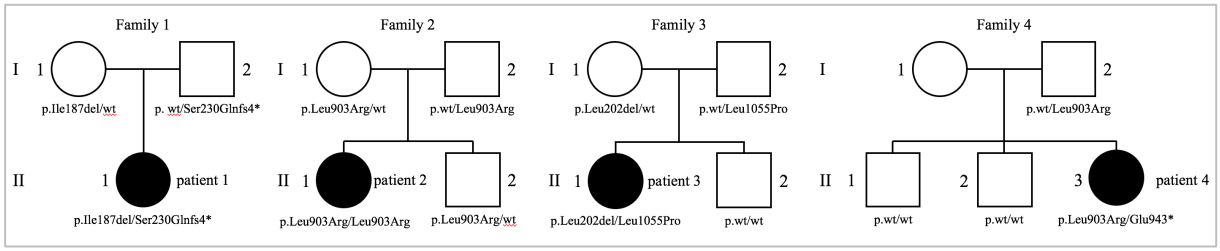

Figure 3: Pedigree of patients 1 to 4. The descriptions below the symbols for the family members display the biallelic mutations in NBAS on protein level and wild type, respectively.

Patient 5 was discovered soon after, since his exome had been sequenced already. Yet only after the detection of recurrent acute liver failure syndrome, we realised that his mutations in *NBAS* were the cause of his symptoms.

We termed the clinical syndrome “RALF syndrome” (RALF), referring to fever dependent episodes of acute liver failure with recovery in the interval.

NBAS

Discovery

The gene *NBAS* was discovered in 1999 by scientists examining genes co-amplifying with N-*myc* in neuroblastoma (Wimmer et al. 1999). Co-amplification of *NAG* with N-*myc* was linked to tumour stage (Scott et al. 2003). Hence, the gene and the resulting protein were called *neuroblastoma amplified sequence* (*NBAS*) (OMIM 2015).

Gene location, gene structure and protein structure

NBAS is located on the short arm of chromosome 2 at position 2p24.3 (OMIM 2015). Its genomic coordinates are chr2:15,307,032-15,701,472 and its accession number is NM_015909.3 (UCSC Genome Browser 2017). The gene extends over 420 kilo bases and comprises 52 exons (Scott et al. 2003). Three isoforms of the translated protein NBAS are predicted to exist. The longer one, consisting of 2371 amino acids translated from all 52 exons at a predicted molecular weight of approximately 270 kDa, has been chosen as the reference isoform (isoform identifier A2RRP1-1) (GeneCards 2017, UniProt 2017). It is visualized in Figure 4. Another isoform with only 2251 amino acids, lacking amino acid positions 860 until 979 of isoform 1 (isoform identifier A2RRP1-2), has been predicted (Gerhard et al. 2004). The sequence that is amplified in neuroblastoma is an even shorter splice variant, comprising only 1353 amino acids in 31 exons (Wimmer et al. 1999).

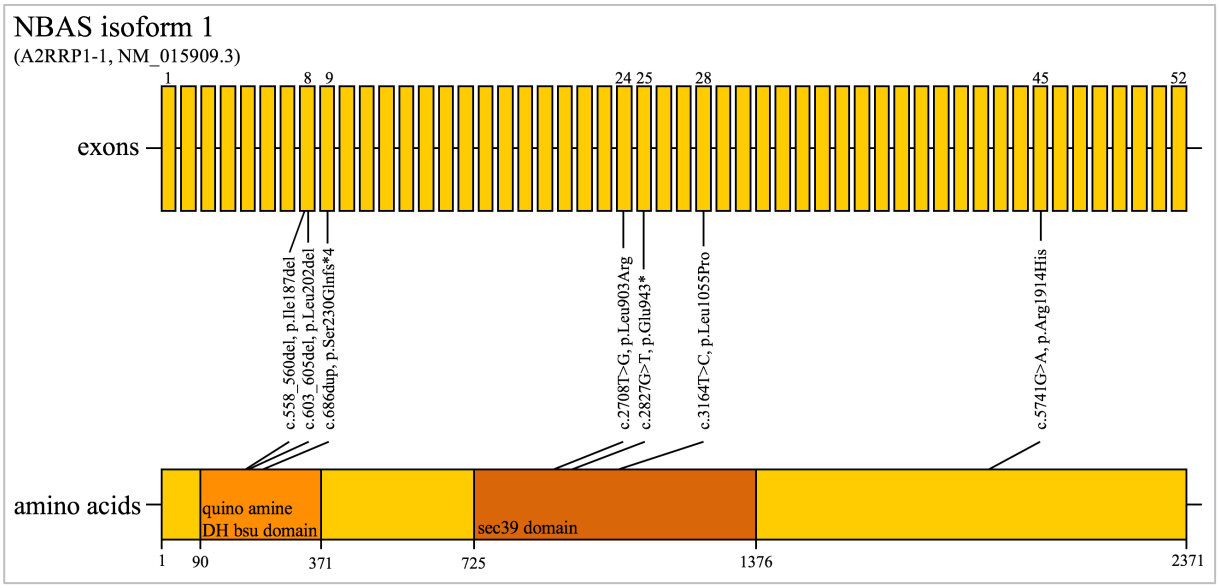

Figure 4: Gene and protein structure of NBAS with annotation of the mutations of NBAS patients 1 to 4 (known at the beginning of my thesis) as well as the mutation described to leading to SOPH syndrome (exon 45) (Maksimova et al. 2010).
Quino amine DH bsu domain is short for quinoprotein aminedehydrogenase, beta chain like domain.
Sec39 domain is short for secretory pathway 39 domain.
Variant of this figure published in Haack et al. (2015).

NBAS is conserved in vertebrates. It was found expressed in 15 primates and 16 different tissues (AceView 2017). Homologues for NBAS can be found in different species, including several mammals such as chimpanzee and mouse as well as reptiles, amphibians and ray-rinned fishes (HomoloGene 2015). NBAS contains conserved domains, the most important one being sec39 which can be found in all homologous proteins (HomoloGene 2015). In yeast, sec39 exists as a single domain protein (Kraynack et al. 2005). In humans, there furthermore are a beta chain like quinoprotein aminedehydrogenase domain and a WD40/YVTN repeat-like-containing domain at the N-terminal end of the protein (GeneCards 2017).

Expression in different tissues

The expression of NBAS in different human tissues is contradictory in different publications at the moment. Literature is, though, in agreement that NBAS is expressed in almost all tissues. No tissues were described showing exceptionally high levels of NBAS and only bile duct cells, alveolar cells, spleen and glial cells were described with no levels of NBAS (Scott et al. 2003, The Human Protein Atlas 2015, GeneCards 2017). Fruhwald et al. (2000) found highest levels of NBAS expression in heart and skeletal muscle while they found lowest levels in, interestingly, liver, small intestine and thymus. The Human Protein Atlas (2015) displays high

levels of NBAS in hepatocytes and many different glandular cells, medium levels in the central nervous system and low levels in fibroblasts.

Physiologic function of NBAS

The physiologic location and function of NBAS is not yet understood. In yeast, the homologous protein sec39 is involved in retrograde transport between ER and Golgi (Kraynack et al. 2005). Aoki et al. (2009) provided evidence that NBAS is also involved in retrograde transport in humans.

In eukaryotic cells, soluble N-ethylmaleimide-sensitive factor attachment protein receptor (SNARE) tethering factors mediate the docking and fusion of vesicles with target membranes. The fusion of membranes is mediated by membrane-bound proteins on the transport vesicles (v-SNARE) and target membrane (t-SNARE). NBAS is supposed to function as a component of an ER tethering complex that interacts with t-SNAREs p31 (USE1), BNIP1 and STX18 at the ER and the v-SNARE Sec22b. This tethering complex also includes ZW10, RINT1 and Sly1 (SCFD1) (Aoki et al. 2009, Hong and Lev 2014).

Lee et al. (2013) provided results suggesting NBAS to play an important role in plant growth and development. They also supported the thesis that NBAS plays a role in protein transport pathway, showing that NBAS deficiency in *Nicotiana benthamiana* resulted in ER stress and programmed cell death (Lee et al. 2013).

In contrast, Longman et al. (2013) have proposed that NBAS forms part of an autoregulatory Nonsense Mediated Decay circuit with DHX34, regulating endogenous RNA targets in human cells, zebrafish and *Caenorhabditis elegans*. They have, though, stated that NBAS may still be involved in ER-Golgi transport.

In summary, the exact function of NBAS remains to be elucidated although there is good evidence that it is part of the syntaxin 18 complex and involved in retrograde transport.

Associated diseases

Mutations in *NBAS* have been linked to different clinical phenotypes. As I already described, we identified biallelic mutations in *NBAS* to cause infantile RALF (Haack et al. 2015).

In 2010, Maksimova et al. (2010) had identified a specific mutation, c.5741G>A, p.Arg1914His in exon 45 of *NBAS*, in a Yakut population in Asia to cause short stature with optic atrophy and

Pelger-Huët anomaly (SOPH) syndrome in homozygous state (Maksimova et al. 2010). The mutation is located on the C-terminal domain of NBAS with unknown function. SOPH syndrome includes postnatal growth retardation, small hands and feet, loss of visual acuity and abnormalities of colour vision as well as Pelger-Huët anomaly. No phenotype of the liver has been described (Maksimova et al. 2010).

None of the additional syntaxin 18 complex components are associated with a known human disorder. Mouse models of deleted syntaxin 18 complex components p31 and RINT-1 were shown to be embryonic lethal (Lin et al. 2007, Uemura et al. 2009).

Purpose of this work

We had identified biallelic mutations in the gene *NBAS* to lead to infantile recurrent acute liver failure (Haack et al. 2015). This disease is characterised by fever-dependent recurrent episodes of acute liver failure. The physiologic function of NBAS has not yet been fully understood, although it has been found to be broadly expressed in almost all tissues. The purpose of this work was to validate the effect of mutations in *NBAS* on the patients' cellular and clinical phenotypes, to identify further patients and to characterize this novel monogenic form of liver failure.

This work is divided into four parts. Firstly, I investigated whether the detected mutations in *NBAS* did have an effect on the protein NBAS levels in the patients' cell lines to confirm the significance of the mutations and to establish a diagnostic tool for further infantile recurrent acute liver failure patients. Secondly, I examined why patients predominantly present with a liver phenotype while the protein NBAS is present in all tissues. I tried to establish a knockdown of the protein NBAS by down-regulating *NBAS* gene expression in hepatocytes in order to challenge the cell lines to find possible tissue-specific phenotypes. Thirdly, I sought to characterize the consequences of the mutations in *NBAS* on protein function in patient cell lines, especially the possible effect of high temperature on the patients. For all my experiments, I evaluated protein levels, by the means of Western Blot analysis, and protein function, by the means of a growth curve, both at normal and elevated temperature. Finally, I assessed the results I had gained on the protein NBAS in the context of it being a component of the syntaxin 18 complex. Overall, I hereby to some extent characterized this novel monogenic form of liver failure.

Materials and methods

Preamble

Most of the procedures were performed according to protocols established in Dr. Holger Prokisch's laboratory.

Cell culture work was assisted by the very helpful technical assistant Lena Protzmann.

Western Blots were carried out with the valuable help of technical assistant Sabine Schäfer.

Reagents and media

Table 1: Reagents and media

product	company
0,05%-Trypsin-EDTA	Gibco
6X DNA Loading Dye	Thermo Scientific
Acetic Acid	Millipore
Agar-Agar, Kobe I	Roth
Ampicilline	Sigma-Aldrich
Bio-Rad Protein Assay	Bio-Rad
Bio-Rad Protein Assay Standard II Albumin	Bio-Rad
Bromphenol blue	Fluka
Chloramphenicol	Roth
D-(+)-Galactose, anhydrous	Sigma-Aldrich
D-MEM - High glucose	Gibco
D-MEM - No glucose	Gibco
Dimethylsulfoxide	Sigma-Aldrich
DNA Agarose Byozym	Biozym Scientific
Dulbecco's Phosphate Buffered Saline	Gibco
ECL Plus Western Blotting Detection System	Amersham
EDTA	Sigma-Aldrich
EGTA	Sigma-Aldrich
Fetal Bovine Serum	Gibco
Glycerol	Merck

Glycine	Roth

Table 1, continued

IL6 Recombinant Human Protein	Gibco
Kanamycin	Sigma-Aldrich
Methanol	Merck
Pen Strep 5000 U/ml	Gibco
Ponceau S	Sigma-Aldrich
Protease Inhibitor	Roche
SERVA DNA Stain G	SERVA Electrophoresis
Sodium Chloride	Merck
Sodium dodecyl sulfate	Roth
Sodium Pyruvate	Sigma-Aldrich
Tris	Roth
Trizma-Base	Sigma-Aldrich
Trypton/Pepton from Casein	Roth
Tween® 20	Sigma-Aldrich
Uridine	Sigma-Aldrich
Yeast Extract	Merck

Buffers and solutions

Table 2: Buffers and solutions

name	recipe
Big Dye Master Mix	150 µl Big Dye
	300 µl HPLC H_2O
	450 µl Buffer
Laemmli Buffer	8 % SDS
	40 % glycerol
	0,02 % bromphenol blue
	250 mM Tris-HCl
LB Medium (per ml)	10 mg NaCl
	10 mg Trypton
	5 mg yeast extract
	20 mg Agar
Ponceau Red (pro 100 ml)	0,1 g Ponceau S
	5 % Acetic Acid
	95 % distilled water
Ponceau Destaining Solution	50% Methanol
	10% Acetic Acid
	40 % distilled water
RIPA Buffer	50 mM Tris-HCl
	1% NP-40
	0,5% Na-deoxycholate
	0,1% SDS
	150 mM NaCl
10X Running Buffer	25 mM TRIS
	192 mM glycine
	0,1% (w/v) SDS
TE Buffer, pH 8,0	10 mM Tris
	1 mM EDTA
	NaOH (auf pH 8,0)

Table 2, continued

10X Transfer Buffer	1,5 M Glycine
	200 mM Trizma
1X Transfer Buffer	10% 10X Transfer Buffer
	20% Methanol
	70% distilled water

Antibodies, ladders and enzymes

Table 3: Antibodies, ladders and enzymes

product	company
Anti-NBAS Prestige Antibody produced in Rabbit	Sigma-Aldrich
Anti-USE1 Prestige Antibody produced in Rabbit	Sigma-Aldrich
GeneRuler 100bp DNA Ladder	Thermo Scientific
HRP-conjugated anti-mouse produced in goat	Dianova GmbH
HRP-conjugated anti-rabbit produced in goat	Dianova GmbH
HRP-conjugated Anti-rat	Jackson Antibodies
Monoclonal Anti-Tubulin-alpha produced in rat	Abcam
Monoclonal Anti-β-Actin produced in Mouse	Sigma-Aldrich
PageRuler™ Plus Prestained Protein Ladder	Thermo Scientific

Kits

Table 4: Kits

product	company
BigDye® v3.1 Terminator Cycle Sequencing Kit	Applied Biosystems
CyQUANT® Cell Proliferation Assay Kit, for cells in culture	Molecular Probes
pLenti6/BLOCK-iT™-DEST Gateway®Vector Kit	Invitrogen (BLOCK-iT™ Lentiviral RNAi Expression System)
Gateway®LR Clonase®II Enzyme Mix	
One Shot® Stbl™ Chemically Competent *E. coli*	
ViraPower™ Bsd Lentiviral Support Kit	
293FT Cell Line	
BLOCK-iT™ U6 RNAi Entry Vector Kit	
One Shot® Top 10 Chemically Competent *E. coli*	
MycoAlert™ Assay Control Set	LONZA
MycoAlert™ Myoplasma Detection Kit	LONZA
Taq DNA polymerase	Qiagen
QIAGEN AllPrep DNA/RNA Kit	Qiagen
QIAGEN Plasmid Midi Kit	Qiagen
QIAprep Spin Miniprep Kit	Qiagen
QIAshredder™	Qiagen

Equipment and software

Table 5: Equipment and software

product	company
3730 DNA Analyer	Applied Biosystems
Autoclave Systec 5075 ELV	Systec
Bio-1D Software Version 15.0.3	PEQLAB Biotechnologie GmbH
CO_2 Incubator	Sanyo
Electrophoresis chamber	LONZA
Gap4	Staden Package
Incubator (37°C)	Memmert
KC4 Version #3.4 Rev. #18	Bio-Tek Instruments, Inc.
Liquid Nitrogen Tank	Chronos Messer
Magnetic stirrer RH basic	IKA Labortechnik
NanoDrop ND-1000 Software Version 3.8.1	Thermo Scientific Abgene
peqSTAR Thermocycler	PEQLAB Biotechnologie GmbH
Potter S, IKA Eurostar digital	IKA Labortechnik
Precision scales Basic Plus BP2100	Sartorius
Rotanta 46 RS	Hettich Zentrifugen
Rotator SB3	Stuart Benchtop Equipment
Scepter 2.0 Handheld Automated Cell Counter	Millipore
SIGMA Centrifuge 3K30	SIGMA Laborzentrifugen GmbH
SIGMA Centrifuge 4K15C	SIGMA Laborzentrifugen GmbH
SIGMA Centrifuge 6K15	SIGMA Laborzentrifugen GmbH
Spectrophotometer NanoDrop ND-1000	Thermo Scientific Abgene
Synergy HT Plate Reader	Bio-Tek Instruments, Inc.
Ultrospec 3300 *pro* UV/Visible Spectrophotometer	Biochrom Ltd.
Vilber Fusion FX7 2.0.7	PEQLAB Biotechnologie GmbH
Vilber Fusion Software Version 15.18	PEQLAB Biotechnologie GmbH
Vortex Genie 2 Scientific Industries	VWR
Water bath HRB 4 digital	IKA Labortechnik

Materials

Table 6: Materials

product	company
ABgene® PCR plates	Thermo Scientific
Adhesive PCR Film	Thermo Scientific
Amersham™ Hybond™ Blotting Paper	GE Healthcare
Amersham™ Hybond™-P (Membrane)	GE Healthcare
Cuvettes	NeoLab
Eppendorf Safe-Lock tubes (0,2 - 2 ml)	Eppendorf
Falcon conical tubes (15/50 ml)	BD Bioscience
Falcon™ Tissue Culture Plate 24-well	Fisher Scientific
Falcon™ Tissue Culture Plate 6-well	Fisher Scientific
Filtertop cell culture flask (25/75/175 cm^2)	Greiner Bio One
Insulin syringe U-100 (0,5 ml; 0,3 mm x 8 mm)	BD Bioscience
MILLEX GP; syringe filter unit (0,22/0,45 µm)	Millipore
Monoject™ Syringe 6 ml	Santa Cruz Biotechnology
Nunc™ Cell Culture Dishes 100mm	Thermo Scientific
PAGEr GELS (4-12% T-G)	LONZA
Scepter Sensors, 60 µm	Millipore
Serological Pipettes (1 - 50 ml)	Greiner Bio One
SteriCup® and SteriTop® 0,22 µm	Millipore

Cell lines

Table 7: Cell lines

cell line	cell type	company
NHDFneo	Normal human dermal fibroblasts derived from neonatal foreskin	Lonza
HEK 293-FT	Clonal isolate derived from human embryonal kidney cells transformed with the SV40 large T antigen	Life Technologies
Hep G2	Hepatoblastoma derived from a fifteen-year old Caucasian male	Sigma-Aldrich
patient cell lines	Fibroblasts derived from a skin biopsy	not applicable

Molecular biology methods

Plasmid extraction from bacteria (Miniprep/Midiprep)

Plasmids were isolated from bacterial overnight cultures using the QIAprep Spin Mini Kit and the QIAGEN Midi Kit, respectively. The procedures were performed according to the manufacturer's protocols. The bacterial overnight cultures were supplemented with 1 % ampicillin, the positive selection marker. Overnight cultures of 5 ml and 100 ml for the Miniprep and the Midiprep, respectively, were used. In the morning, the cultures were pelleted and the supernatant medium was discarded. After alkaline lysis, several washing steps followed. Eventually, DNA was eluted by addition of TE Buffer and centrifugation in the Miniprep Kit. In the Midiprep Kit, DNA was eluted by addition of isopropanol, washed with ethanol and the air-dried pellet was resuspended in provided EB Buffer.

DNA extraction from human cells (AllPrep)

DNA was isolated from cell pellets from cells in cell culture using the QIAGEN AllPrep DNA/RNA Kit. The procedures were performed according to the manufacturer's protocols. Cell pellets were obtained as described in "Generation of Cell Pellets for Further Analysis" in the chapter Cell Biology Methods. After homogenization in RLT Plus buffer using a QIAshredder column, the sample was placed into an AllPrep DNA spin column and several washing and centrifugation steps followed. Eventually, DNA was eluted by addition of EB Buffer.

Determination of concentration of DNA

The concentration of DNA in a solution was determined using the NanoDrop ND-1000 Spectrophotometer. The program was set to "Nucleic Acids". The NanoDrop measures the absorbance of light of RNA and DNA photometrically at 260 and 280 nm, respectively. The software NanoDrop Version 3.8.1 was used. After cleaning the sensor with distilled water, 1 µl of distilled water was loaded and set as "blank". Then, 1 µl of every sample was loaded and measured. The measurement was taken when the displayed graph showed a peak. In the end, the sensor of the machine was cleaned with distilled water again.

Polymerase chain reaction (PCR)

PCR was used in order to amplify DNA fragments. Sequence-specific primers were used.

For a PCR, a cycle of different temperatures is repeated for several times. The first temperature is the denaturing temperature. At the second temperature, the primers are annealing to the present fragments. In the third step at the third temperature, the DNA fragment that is intended to be amplified is synthesized by a thermostable DNA polymerase.

DNA sequencing from transduced cells

In order to validate transduction success, DNA from transduced cells was sequenced in several steps. In a first step, genomic DNA was amplified by PCR following the protocol of Qiagen. In a second step, the success of the amplification was ensured by gel electrophoresis before the samples were purified using a vacuum. As last steps, the DNA was sequenced according to the following protocol "Sequencing of plasmid DNA from bacteria".

I used primers suggested in the BLOCK-iT™ Lentiviral RNAi Expression System Kit from Invitrogen with an added M13-Sequence (Table 8).

Table 8: Sequences of the primers used for sequencing of genomic DNA

primer	sequence
U6_M13 Forward	CGACGTTGTAAAACGACGGCCAGTGGACTATCATATGCTTACCG
V5_M13 Reverse	CAGGAAACAGCTATGACCACCGAGGAGAGGGTTAGGGAT

For the sequencing reaction, the *Taq* DNA Polymerase Kit from Qiagen and a 96-well plate were used. A reaction was set up using reagents as presented in Table 9.

Table 9: Reagents of the amplification PCR reaction

reagents	volume
dNTPs 2 mM	5 µl
10X buffer	5 µl
Forward Primer	1 µl
Reverse Primer	1 µl
Taq polymerase	0,2 µl
HPLC H_2O	32,8 µl
DNA	5 µl
total	*50 µl*

The samples were then placed in a peqSTAR Thermocycler using the protocol outlined in Table 10.

Table 10: Temperature protocol of amplification PCR reaction

temperature	time	number of cycles
95 °C	5 min	1
95 °C	30 s	35
52 °C	30 s	
72 °C	45 s	
72 °C	10 min	1
20 °C	1 min	1

In the next step, the success of the amplification was checked with a short gel electrophoresis. TE buffer was mixed with 1,5 % agarose and heated in a microwave until the liquid was clear. After the heating process, 0,02 ‰ DNA Stain was added. The gel was cast in a mould and wells were created by the use of a comb. Afterwards, the gel was transferred to an electrophoresis chamber and placed in TE buffer. 3 µl of a 100 bp ladder were loaded. 3 µl of every sample were mixed with 5 µl of DNA loading dye and the resulting 8 µl were loaded. The gel was left to run for 30 minutes at a constant voltage of 100 V. Thereafter, the gel was placed under a UV lamp to detect bands of DNA. It was not only looked for any bands, but also for bands in the estimated amplification product size.

DNA was then purified from the samples in which the amplification had worked. For this, HPLC H_2O was added to the samples up to a total volume of approximately 100 µl. The samples were then transferred to a purifying plate and the fluid was extracted by a vacuum pump. Subsequently, the DNA was collected in 40 µl of HPLC H_2O and transferred back to small vessels.

In the final step, the DNA was sequenced according to the following protocol “Sequencing of plasmid DNA from bacteria”.

Sequencing of plasmid DNA from bacteria

In order to check the quality of plasmid DNA from bacteria, Sanger sequencing was performed. Isolated Plasmid DNA was sequenced by firstly running a sequencing PCR (Polymerase Chain Reaction), secondly precipitating the DNA and resuspending it in 20 µl HPLC H_2O, and thirdly

measuring the emission of fluorescence of the fragments after separation by capillary electrophoresis.

Sanger sequencing works by amplifying DNA fragments using a PCR and sequence-specific primers. However, fluorescently labelled didesoxynucleotides (dNTP) are added as well as "normal" desoxynucleotides. Hence, in theory, the DNA fragments are bound to terminate with a labelled dNTP at every base position. The fragments can be separated by length through electrophoresis. A machine can then measure the different fluorescent emissions at every position and henceforth read a sequence. The detected sequence is finally compared to the desired sequence.

Primers suggested in the BLOCK-iT™ Lentiviral RNAi Expression System Kit from Invitrogen were used (Table 11).

Table 11: Sequences of the primers used for sequencing of plasmid DNA

primer	sequence
M13 Reverse	CAGGAAACAGCTATGAC
U6 Forward	GGACTATCATATGCTTACCG
V5(C-term) Reverse	ACCGAGGAGAGGGTTAGGGAT

For the sequencing reaction, the BigDye® v3.1 Terminator Sequencing Kit from Applied Biosystems was used. A 96-well plate was used. A reaction with the reagents listed in Table 12 was set up.

Table 12: Reagents of the sequencing PCR reaction

reagents	volume
BigDye® v3.1	0,5 µl
BigDye® Buffer	1,5 µl
HPLC H_2O	1 µl
Forward/Reverse Primer (concentration: 10 ng/µl)	1 µl
Plasmid DNA	1 µl
total	*5 µl*

The samples were then placed in a peqSTAR Thermocycler using the protocol outlined in Table 13.

Table 13: Temperature protocol of sequencing PCR reaction

temperature	time	number of cycles
96 °C	2 min	1
96 °C	10 s	25
50 °C	5 s	
60 °C	4 min	
20 °C	1 min	1

After the sequencing PCR reaction, DNA was purified by precipitation with ethanol. In a first step, 25 µl of 100 % ethanol were added to every sample and left to incubate for at least 15 min in a dark place. Centrifugation at 3000 *g* for 30 min at 20 °C followed. The plate was quickly centrifuged turned upside down in order to remove excess water. Next, 125 µl of 70 % ethanol were added to every well followed by centrifugation at 2000 *g* for 15 min at 20 °C. Then, the plate was gently beaten upside-down on a tissue to remove excess water again. It was consequently centrifuged upside-down at 600 *g* for 1 min at 20 °C. At last, the sample was left at room temperature for several minutes so that the remaining alcohol would evaporate in order not to disturb the measurement. The samples were then resuspended in 30 µl HPLC H_2O, 25 µl of which were pipetted into a sequencing plate.

Determination of base sequence

The DNA in the sequencing plates was analysed by an Applied Biosystems 3730 DNA Analyzer. The sequence was consequently viewed using the programme Gap4 by Staden Package.

Microbiological methods

Cultivation of bacteria

Bacteria were cultivated in LB Medium. Both LB Medium supplemented with agarose and liquid LB Medium was used. In general, the medium was supplemented with the desired selection marker. There were only overnight cultures which were kept in an incubator at 37 °C. Agarose plates with bacteria were kept in the fridge to store them.

Cell biology methods

Cultivation of human cells

Human cells were cultivated in Dulbecco's modified Medium (High-Glucose) supplemented with 10 % FBS, 1 % Penicillin-Streptomycin and 200 µM Uridine. The cultures were maintained at 37 °C and 5 % CO_2. The cultures were kept in bottles of 75 cm^2 (medium flask) in general.

Collection of cells

The medium of the cells was drawn off the cells. Then, the cells were washed with PBS in order to remove possible remains of medium. The PBS was, again, drawn off afterwards. Trypsin-EDTA solution (0,5 ml for a small flask, 2 ml for a medium flask, 4 ml for a large flask) was consequently added to the cells. The flasks were returned to the incubator and left to incubate for several minutes. When all cells were detached, the reaction was stopped by adding medium (2 ml for a small flask, 10 ml for a medium flask, 20 ml for a large flask), pipetting the solution up and down. The solution was then centrifuged at 500 *g* for 3 minutes 30 seconds. Afterwards, the supernatant was drawn off and the cell pellet was used further.

Splitting of cells

The cells were splitted when 80 to 90 % confluent. Human fibroblasts were mostly splitted 1:3 or 1:4, hepatocytes were splitted 1:6 to 1:10. For splitting, the cell pellet was resuspended in medium. The solution was then divided up onto the number of flasks that was intended.

Generation of stocks

The pellet of one full medium flask was considered sufficient for two stocks. Hence, this pellet was resuspended in 3 ml freezing medium (medium supplemented with 10 % DMSO). 1,5 ml of cell suspension was filled in one cryo tube. The tubes were then placed into a -80 °C freezer and later placed into liquid nitrogen at -160 °C for long-term storage.

Generation of pellets for further analysis

The pellet of one small flask was considered sufficient for one Western Blot. In order to further remove remaining medium by washing with PBS again, this pellet was suspended in 1,5 ml PBS and filled into a 1,5 ml tube. The suspension was centrifuged in a table-top centrifuge at

13.000 rpm for 4 minutes. Afterwards, the supernatant was drawn off and the pellet was placed into a -80 °C freezer.

Contamination test for mycoplasma

Newly arrived cell lines were routinely tested for contamination with mycoplasma using the MycoAlert™ Kit from LONZA according to the manufacturer's protocol. A 2 ml sample of medium in which the cell lines had been growing for at least two days was taken.

Blasticidin killing curve

In a 6-well-plate, 75.000 cells were seeded in each well and supplemented with 2 ml Medium each on a Tuesday. The following Friday, selection of cells with blasticidin was started. After a change of medium, 0 µg, 2 µg, 4 µg, 6 µg, 8 µg and 10 µg of blasticidin, respectively, were added. Medium was changed every second to third day. The concentration of blasticidin where all cells were dead after seven to ten days was used.

Determination of cell count using the Scepter™ Handheld Cell Counter

A cell pellet was resuspended in either Medium or PBS, depending on the further purpose of the cells. The resuspension volume depended on the estimated cell count. For example, the pellet from a medium flask was usually resuspended in 1 ml and then diluted 1:10 in PBS. If the cells were diluted in medium, the solution had to be diluted 1:10 in PBS so that the Scepter™ Cell Counter was able to work properly. From every solution of cells, two samples were taken and measured once each. For fibroblasts, the counted size range of cells was set to 12 to 24 µm, for hepatocytes, the counted size range of cells was set to 6 to 18 µm.

Determination of cell count using the CyQUANT® Cell Proliferation Assay Kit

Before starting to use the kit, both kit components, the 20X cell-lysis buffer stock solution and the 400X GR dye, were allowed to thaw from -20 °C to room temperature. Just before the experiment, a solution of 1X cell-lysis buffer and 1X GR dye was created for fibroblasts. For hepatocytes, a solution of 1X cell-lysis buffer and 2X GR dye was used.

Before doing experiments with CyQUANT®, a calibration curve was created as suggested by the manufacturer. For this, a highly concentrated cell suspension of approximately $9 \cdot 10^6$ in PBS was generated. In a 24-well plate, the different cell numbers were plated out as triplicates. In every well, one millilitre of the CyQUANT® solution was added. After incubation for five

minutes at room temperature, the fluorescence was measured with a Synergy HT plate reader at the bottom of the plate and sensitivity 50 using the software KC4 Version #3.4. NHDFneo were used as standard for fibroblasts whereas Hep-G2 were used as standard for hepatocytes. The results are shown in Figure 5. For fibroblasts, the linear range was found to be up to 110.000 cells per well. For hepatocytes, a linear range up to 300.000 cells was found.

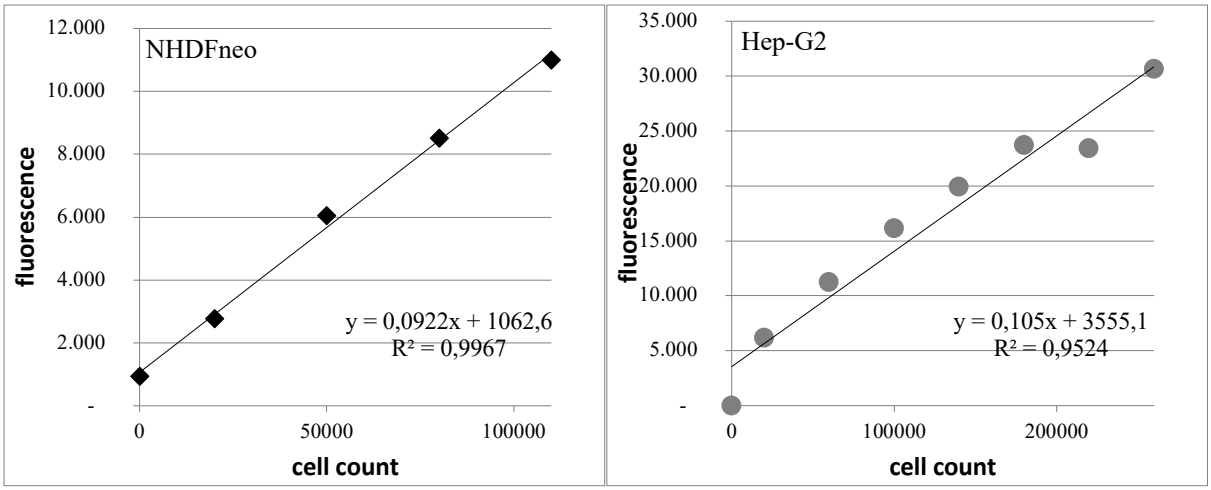

Figure 5: Fluorescence of cells plotted against cell count.
NHDFneo are displayed on the left. Hep-G2 are displayed on the right.

In order to determine the cell count of plates on which experiments were conducted the medium in the plates had to be drawn off and the plates were frozen to -80 °C for at least 16 h. The day of the experiment the desired plates were unfrozen, the desired CyQUANT® solution was created and 1 ml was added to every well on every plate in which cells had been. After 5 min of incubation at room temperature, the fluorescence was determined as described above. The cell count was determined by using the formulas in the diagrams above.

Growth curve

Method 1a

This method was conducted as a trial method and only with fibroblast cell lines. Fibroblasts were plated out on a Monday on 25 cm^2 tissue flasks using 5 ml medium. The cell count of every cell line was determined with the Scepter™ Cell Counter. For every day and condition that was to be counted one flask was used. Hence, 40.000 cells were seeded in every bottle.

The flasks were placed into 37 °C, 40 °C and 42 °C, respectively. Every day at the same time on the following days of the week, the cell count of one flask per condition was determined with the Scepter™ Cell Counter.

Method 1b

This method differs from method 1a in the fact that cells were plated out on a Friday and cell count was assessed on the days of the following week.

Method 2

This method was established as an improvement from the earlier growth curve experiments. It has the advantages that it needs many less cells, consumes less time for the scientist and is more accumulative since it gives triplicates of every time point and condition.

Cells were plated out on a Monday in 24-well plates. The cell count of every cell line was determined with the Scepter™ Cell Counter. Hence, the same number of cells was seeded in every well. For fibroblasts, the starting cell count was either 5.000 cells or 2.500 cells, for hepatocytes, the starting cell count usually was 4.000 cells. 500 µl medium were used per well. Every cell line was seeded three times on each in order to achieve triplicates. For every day and condition that was to be counted one plate was used.

After plating and leaving the cells attach for 1h at 37 °C, the time was noted and taken as time zero. At this point, the growth condition for the cells was changed as desired. For example, a certain number of plates was placed in 40 °C. The following days of the week, one plate per condition was taken every day at the same time and the medium was drawn off. Then, the plates were frozen in a -80 °C freezer for at least sixteen hours until they were measured with CyQUANT®.

Knockdown of a gene in cell culture

Preamble

The term "knockdown" refers to an experimental method inducing the down-regulation of the expression of a selected gene (Encyclopedia of Cancer 2012). This may be accomplished by different means, generally by introducing antisense oligonucleotides such as siRNA (short interfering RNA) into cells. In my work, I have decided to use a method of lentiviral transduction of shRNA (short hairpin RNA) (Guénet et al. 2015).

The Knockdown was conducted using lentiviral transduction of shRNA. Lentiviral transduction leads to a permanent integration of the desired DNA into the genome, hence, a stable Knockdown can be established.

The BLOCK-iT™ Lentiviral RNAi Expression System from Invitrogen was used. The permission to perform the experiments in a S2 laboratory had been granted. All procedures up to the lentiviral transduction were performed according to the manufacturer's protocol. The lentivirus used in this kit is based on HIV and uses blasticidin as the positive selection marker for cells in culture.

The lentiviral transduction was performed according to protocols established in the laboratory and described by Danhauser et al. (2011). It is similar to the procedure suggested in the manufacturer's protocol.

Design and handling of oligonucleotides for shRNA

The shRNA to be used for the BLOCK-iT™ Lentiviral RNAi Expression System Kit were created using the RNAi designer by life technologies (http://rnaidesigner.lifetechnologies.com/). The accession number of *NBAS* (NM_015909.3) was entered in the tool "shRNA". Open Reading Frame (ORF), *Homo sapiens* as database and the vector pENTR™/U6 were selected. Minimum and maximum percentage of GC were selected as 35 % and 55 %, respectively. From the suggested sequences, the sequences starting at base position 1908 and base position 3027, respectively, were chosen. A third shRNA sequence was created in the tool "siRNA to shRNA" by entering the sequence used for knockdown of NBAS in the paper "Identification of the Neuroblastoma-amplified Gene Product as a Component of the syntaxin 18 Complex Implicated in Golgi-to-Endoplasmic Reticulum Retrograde Transport" (Aoki et al. 2009) and selecting the vector pENTR™/U6.

Hence, a shRNA sequence starting at base position 4160 was chosen. With the same tool, a scramble shRNA sequence was designed. The sequence was recommended by the company Life Technologies.

The DNA oligos were produced by Invitrogen and delivered lyophilized (Table 14). They were resuspended in TE Buffer to a final concentration of 200 µM.

Table 14: Sequences of ordered DNA oligos containing shRNA sequences.

oligo	sequence
NBAS_shrna_1908_bottom	AAAAGCAGATGATGGCAGATTTACATTCGTGTAAATCTGCCATCATCTGC
NBAS_shrna_1908_top	CACCGCAGATGATGGCAGATTTACACGAATGTAAATCTGCCATCATCTGC
NBAS_shrna_3027_bottom	AAAAGCACTAGAGTGCATCTATACCTTCGGGTATAGATGCACTCTAGTGC
NBAS_shrna_3027_top	CACCGCACTAGAGTGCATCTATACCCGAAGGTATAGATGCACTCTAGTGC
NBAS_shrna_4160_bottom	AAAACTAGTAAAGCAGTACAAGGATTCGTCCTTGTACTGCTTTACTAGC
NBAS_shrna_4160_top	CACCGCTAGTAAAGCAGTACAAGGACGAATCCTTGTACTGCTTTACTAG
Scramble_Sequence_bottom	AAAATAACGACGCGACGACGTAATTTTCGAATTACGTCGTCGCGTCGTTAC
Scramble_Sequence_top	CACCGTAACGACGCGACGACGTAATTCGAAAATTACGTCGTCGCGTCGTTA

Double-stranded oligos were generated from the matching single-stranded oligos in an annealing procedure.

Transformation of chemically competent *E. coli*

For the procedure, two different strands of chemically competent *E. coli* were used, namely OneShot® TOP10 Competent *E. coli* and OneShot® Stbl3™ Competent *E. coli*.

The vials with the *E. coli* were taken from the -80 °C freezer and left to thaw on ice. 2 µl of the plasmid which was to be transformed was added into each vial. The solution was gently stirred to mix it. An incubation on ice for 30 min followed. Then, the cells were heat-shocked for 30s and 45 s, respectively, in a water bath at 42 °C after which the tubes were immediately placed on ice. After addition of room temperature S.O.C. medium, the tubes were horizontally shaken at 37 °C for 1 h. Two different volumes of 50 µl and 100 µl were spread on pre-warmed LB agar plates containing the desired selection marker.

Cloning of entry construct

The aim of this step was to clone the shRNA of interest into a vector in order to generate a vector containing the entry construct.

A ligation reaction of ligation buffer, the vector pENTR™/U6, the double-stranded oligo that was created as described earlier, DNase/RNase-free water and T4 DNA ligase was set up and left to incubate for at least five minutes before proceeding to transforming OneShot® TOP10 Competent *E. coli*. Kanamycin resistance was used as the positive selection marker.

Cloning of expression construct

The aim of this step was to clone the shRNA of interest from the vector containing the entry construct in a different vector in order to generate a vector containing the expression construct.

A recombination reaction containing the entry clone, the vector pLenti6/BLOCK-iT™-DEST and TE buffer was set up and left to incubate at room temperature for 1 h before proceeding to transforming OneShot® Stbl3™ Competent *E. coli*. Ampicillin resistance was used as the positive selection marker. Chloramphenicol resistance was used as a negative selection marker.

Preparation of media for the lentiviral transduction

For the lentiviral transduction, different media were needed. Media were filtered through a 0,22 µm filter using a SteriCup® and SteriTop® from Millipore. The contents are listed in Table 15.

Table 15: Composition of media used for lentiviral transduction.

medium	basis	FBS	pen/strep	uridine
Medium 1	D-MEM	+ 10% FBS		
Medium 2	D-MEM	+ 10% FBS	+ 1 % P/S	+ 200 µM Uridine
Medium 3	D-MEM			
Medium 4	D-MEM	+ 2 % FBS		

Selection medium was generated by addition of 3,6 µg Blasticidin per ml medium to normally used cell culture medium (D-MEM with 10 % FBS, 1 % P/S and 200 µM Uridine).

From now on, Medium 1, 2, 3, and 4 as well as selection medium will refer to the mediums described in this chapter.

Production of lentivirus

The lentivirus was produced in HEK 293-FT cells. HEK 293-FT cells were cultivated and maintained in normal medium until they were split on a 10 cm tissue culture dish using Medium 1. On the day of transduction, the HEK 293-FT cells were 70 – 80 % confluent.

For each cell line to be transduced, one reaction mixture was needed. Usually, the double amount was prepared in order to have a back-up stock. Table 16 shows the ingredients for one reaction mixture.

Table 16: Composition of reaction mixtures used to produce a lentivirus.

(a)

reagent	amount
Medium 3	1,5 ml
Lipofectamine® 2000	36 µl

(b)

reagent	amount
Medium 3	1,5 ml
ViraPower™ Packaging Mix	9 µl
Expression Vector	3 µg

Mixture *(a)* was left to incubate for 5 min at room temperature while mixture *(b)* was prepared. Afterwards, both reaction mixtures were mixed and left to incubate at room temperature for 20 min.

The medium on the HEK 293-FT cells was carefully drawn off and 5 ml of Medium 1 was added. Subsequently, the 3 ml of the reaction mixture was added. The cells were then left in an incubator overnight.

The following day, the medium was drawn off the HEK 293-FT cells and replaced by Medium 4. The cells were left in an incubator for 48 to 72 h.

Lentiviral transduction

The human cell lines to be transduced were cultivated and maintained in normal medium until they were split on a 10 cm tissue culture dish using Medium 2. On the day of transduction, the cells were 70 to 80 % confluent.

The medium containing the virus produced by the HEK 293-FT cells was taken after 48 to 72 h of incubation and centrifuged at 2.000 *g* for 15 min at 4 °C. The supernatant was filtered through a 0,45 µm filter and diluted 1:1 with Medium 2. The mixture was well mixed and poured on the cell lines to be transduced of which their medium had been taken off.

The following day, the medium containing the virus was taken off the cells and replaced by normal medium.

The day after this day the selection of the cells which had been transduced was begun with. The virus uses Blasticidin as the positive selection marker. Hence, the medium was drawn off the transduced cells and replaced by selection medium.

Maintenance of transduced cells

The transduced cells were maintained exactly as non-transduced cell-lines except that selection medium was used.

Proteomic analysis

Preamble

Protein experiments were conducted in collaboration with Dr. Tobias Haack and technically assisted by Sabine Schäfer and Lena Protzmann.

Preparation of protein samples

The cell pellet prepared for a Western Blot as described earlier was thawed on ice. RIPA buffer was supplemented with 2 % Protease Inhibitor just before using it. The procedure was performed on ice. The cell pellet of a small flask was suspended in 20 to 25 µl buffer whereas the cell pellet of a medium flask was suspended in 80 to 100 µl buffer. The cell suspension was then passed through a 0,5 ml insulin syringe for two or three times in order to break the cells. Afterwards, the cells were placed in a rotating wheel and agitated at 35 rpm for one hour at 4 °C. Then, the samples were centrifuged at 15.150 rpm for 10 min at 4 °C. The supernatant was transferred to a fresh tube and further processed or frozen to - 80 °C.

Determination of protein concentration

The protein concentration in a sample was determined by Bradford Measurement. BioRad Protein Assay Solution was diluted 1:5 in order to obtain a working concentration. The measurement was conducted using a photometer measuring the absorbance of light in 1 ml of the solution in a cuvette. A standard curve was created using BSA in different concentrations. 2 µl of a sample were added to 1 ml of Protein Assay Solution and measured. This was duplicated for every sample in order to find an average. The concentration of protein in µg per µl solution was calculated.

Preparation of samples for SDS-PAGE

After having measured the protein content, the samples to load on a gel were prepared. The procedure was performed on ice. A 15 µl suspension containing 15 µg protein sample and 1X Laemmli buffer was prepared. An example is shown below in Table 17.

Table 17: Exemplary composition of Western Blot samples

sample	NHDFneo	Hep-G2
concentration	7,13 µg/µl	24,38 µg/µl
15 µg Sample	2,11 µl	0,62 µl
Laemmli 5X	3,0 µl	3,0 µl
RIPA Buffer	9,89 µl	11,38 µl
Total	*15 µl*	*15 µl*

The samples were mixed and then placed in a heating block for 5 min at 70 °C in order to denature the proteins. Afterwards, the samples were immediately placed on ice for two minutes. Subsequently the samples were shortly vortexed and quickly centrifuged.

SDS-PAGE

The proteins in the samples were separated by SDS-PAGE (sodium dodecyl sulfate-polyacrylamide gel electrophoresis) according to their molecular weight. SDS (sodium dodecyl sulfate-polyacrylamide) is binding to proteins and hence adding negative charges. This is masking the intrinsic charge of the proteins and thus leads to a charge-to-mass-ratio that is almost constant for all proteins.

Precast gels with an 4-12% acrylamide gradient from LONZA were used. The gels were placed in the gel electrophoresis chamber. The inner part of the chamber was firstly filled with running buffer. When no buffer was leaving the inner lumen, the outer part was filled as well. The wells of the gel were carefully washed separately with running buffer using a syringe. Afterwards, the samples were loaded. 8 µl of the Prestained Plus Ladder were used. 10 µl of the protein sample solution prepared as described earlier were loaded, hence 10 µg of protein were loaded of each sample. A voltage of 60 V was applied for 30 min, followed by a voltage of 100 V for 60 to 90 min.

Western Blot transfer

The proteins in the gel were transferred to a PVDF membrane for further analysis. The technique of wet-blotting was used.

The membrane was incubated in 100 % methanol for 30 seconds in order to activate it. Two sponges were washed with distilled water. The activated membrane, two sponges and four

fitting pieces of blotting paper were incubated in transfer buffer for several minutes. The materials were then stacked on each other in the following order: one sponge, two pieces of blotting paper, the gel, the activated membrane, two pieces of blotting paper and lastly one sponge. The stack was then placed in a blotting chamber which was surrounded by ice. The blotting chamber was filled with transfer buffer up to the highest possible level. A voltage of 100 V was applied for 75 min.

Ponceau staining

The membrane was placed in a dish and incubated with Ponceau red solution for one minute. The solution was poured back into the bottle. The membrane was consequently destained with destaining solution. The destaining solution was replaced several times. The result was scanned and the membrane was washed for one min in TBS-Tween.

Fixation of proteins on the membrane

After the success of the transfer was checked, the membrane was placed in milk for 1 h in order to block the proteins on the membrane.

Incubation with antibodies

After the blocking, the membrane was cut as desired, for example it was cut at the ladder position of 70 kDa in an upper and a lower part. The membrane was placed in 5 to 10 ml milk supplemented with the desired primary antibody. The falcons with membrane and milk were placed on a roller apparatus and agitated overnight.

The following morning, the membranes were taken out of the milk containing the primary antibody and placed in a fresh falcon. The membranes were then washed in TBS-Tween three times for at least 10 min. Then, milk supplemented with matching secondary antibody was added. The membranes were incubated for 1 h at room temperature. The milk containing the secondary antibody was then discarded and the membranes were washed in TBS-Tween three times for at least 10 min.

Different dilutions and secondary antibodies were used for the four used antibodies. These are outlined in Table 18.

Table 18: Primary and corresponding secondary antibodies with utilized dilutions

primary antibody	dilution	secondary antibody	dilution
Anti-NBAS	1:2.000	Anti-Rabbit	1:7.500 - 1:10.000
Anti-USE-1	1:250		
Anti-α-tubulin	1:10.000	Anti-Rat	1:10.000
Anti-β-actin	1:15.000	Anti-Mouse	1:7.500 - 1:10.000

Detection of immunofluorescence signal

Vilberscan Fusion FX7 with Firmware 2.0.7 was used for development of the membrane. The software Fusion Version 15.18 was used.

The membrane was slightly drained and then placed into a foil. Enhanced chemiluminescence solution was dispersed on the membranes just before developing them. For a first picture, automated time at full resolution was used. Afterwards, different sensitivities (Full resolution/high sensitivity/super sensitivity) and different times (one second up to four minutes) were tried out until a satisfying picture was obtained.

Quantification of immobilized proteins

For the quantification of proteins on a membrane, the software Bio-1D Version 15.0.3 was used using the pictures obtained with the Fusion FX7 as described earlier.

The software can calculate the molecular weight, the volume, the area and the height of a sample when being given a standard on the same membrane. The standard of one lane was always set as 10 µg.

The proteins β-actin and α-tubulin were taken as loading controls.

Statistical and mathematical methods

Calculation of a growth rate

The growth rate of the cells per hour r was calculated based on the formula for exponential growth:

$C(t) = C_0 \bullet e^{r \bullet t}$ (Ford 2009)

C_0 = cell count at time 0, $C(t)$ = cell count after time t, t = time in hours

Calculation steps taken:

$$C(t) = C_0 \bullet e^{r \bullet t}$$

$$\frac{C(t)}{C_0} = e^{r \bullet t}$$

$$\ln\left(\frac{C(t)}{C_0}\right) = \ln\left(e^{r \bullet t}\right)$$

$$\ln\left(\frac{C(t)}{C_0}\right) = \ln e \bullet r \bullet t$$

$$\ln\left(\frac{C(t)}{C_0}\right) = r \bullet t$$

$$r = \frac{\ln\left(\frac{C(t)}{C_0}\right)}{t}$$

Hence, the growth rate per day was calculated as

$r_{\text{day}} = 24 \bullet r$

Determination of p-values

P-Values were calculated by a Student's t-test. Two-sided, both paired and non-paired t-tests were conducted.

Results

Validation of NBAS mutations

Preamble

We had found biallelic mutations in *NBAS* in four unrelated patients with infantile recurrent liver failure, yet no other common gene. Although this is highly suggestive that *NBAS* is indeed the cause for the patients' symptoms, all patients carried missense mutations of unknown significance, several even predicted to be benign, thus in the beginning I sought to test whether the patients' mutations in *NBAS* actually had an effect on the expressed protein levels.

During the course of my thesis, the Prokisch laboratory identified further *NBAS* patients by exome and Sanger sequencing, so I used cell lines of eight patients for my experiments since different cell lines were available at different time points.

Protein levels at standard conditions

In a preliminary experiment conducted by our colleague Daniel M Bader in the Gagneur Lab at the Department for Informatics, Computatonal Biology, TUM, the transcriptomes of three patients were analysed. The analyses showed a decrease of *NBAS* RNA in patients 1, 2 and 5 to on average 78 % of controls, as can be seen in Figure 6 below.

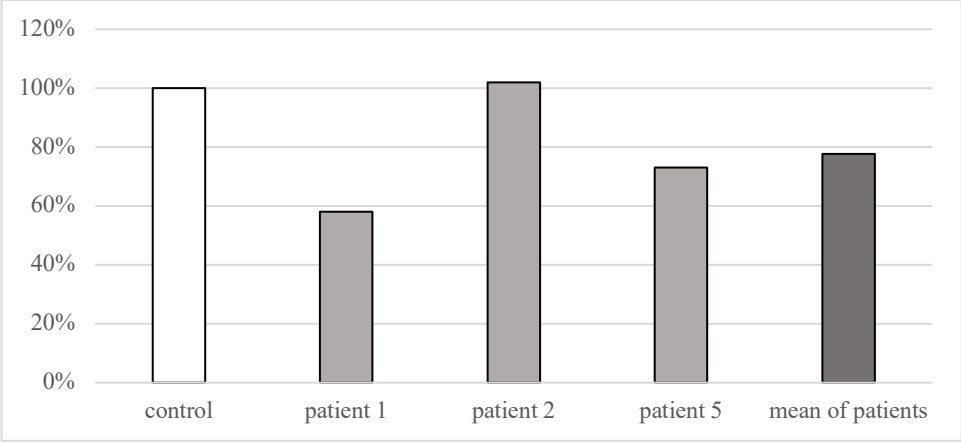

Figure 6: NBAS RNA content of patient cell lines as a percentage of NBAS RNA levels of 100 control cell lines.
Cell lines were cultivated and collected. The transcriptome was analysed by our colleague Daniel M Bader in the Gagneur Lab at the Department for Informatics, Computational Biology, TUM.

In order to quantify the amount of present NBAS in cells, I conducted Western Blots and quantified Western Blot bands of seven *NBAS* patient fibroblast cell lines, including the patient cell lines whose transcriptome had been analysed. These, in contrast, showed a drastic reduction of NBAS levels to approximately 20 % of controls, as can be seen in Figure 7 below. NBAS levels were independent from the level of *NBAS* RNA present in the cell line. Testing of patient 1 revealed a significant reduction of NBAS steady state levels ($p=0.03$, two-tailed unpaired t-test). This indicates a severe impairment of NBAS expression and/or protein stability. Furthermore, shown in Figure 7, the reduction of NBAS levels was accompanied by a reduction of p31 levels to approximately 33 % of controls. As outlined in the introduction, p31 is described to be an interaction partner of NBAS in the syntaxin 18 complex. Hence it can be deduced that not only NBAS itself but also the complex it is involved in is affected by mutations in *NBAS*.

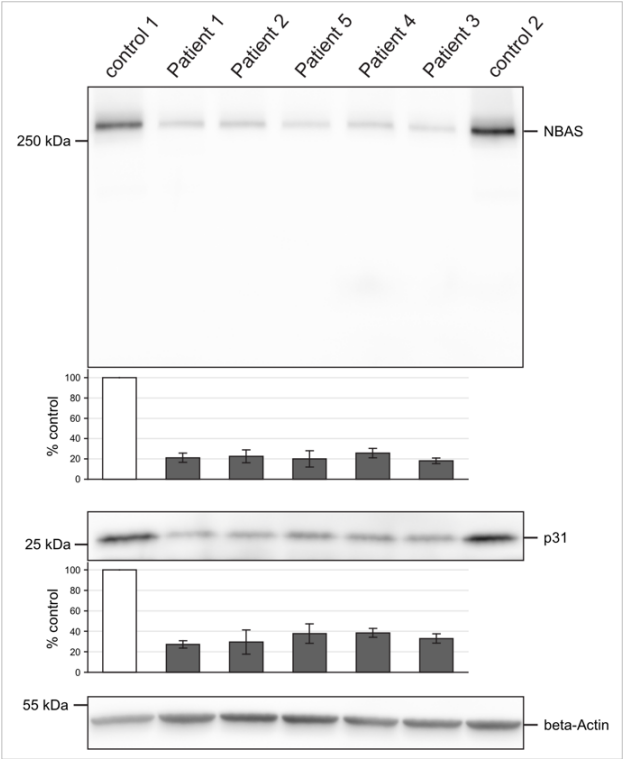

Figure 7: Levels of NBAS and p31 protein in patients 1 to 5.
Fibroblast cell lines were cultured until they reached approx. 70 % confluency, consequently harvested, pelleted and processed for Western Blots. Western Blots were incubated overnight with primary antibodies against NBAS, p31 and β-actin and developed using enhanced chemiluminescence. This figure was created while I was taught the method. Figure published in Haack et al. (2015).

Establishment of NBAS Western Blot as a diagnostic tool

During the course of my thesis, I established the NBAS Western Blot procedure as a diagnostic tool for the identification of further patients. In patients with *NBAS* mutations of unclear significance, this Western Blot can now be conducted to diagnose NBAS deficiency in patients. During the six months that I was in the laboratory, we found four further patients from three families with recurrent acute liver failure with mutations in *NBAS*, all carrying at least one missense variant of unknown significance, and significantly lowered NBAS protein levels. Figure 8 displays the pedigrees of the eight patients that we knew while I was in the laboratory, Figure 9 the structure of NBAS with the identified variants. Up to Summer 2017, a total of 16 patients have been diagnosed with recurrent acute liver failure due to mutations in NBAS.

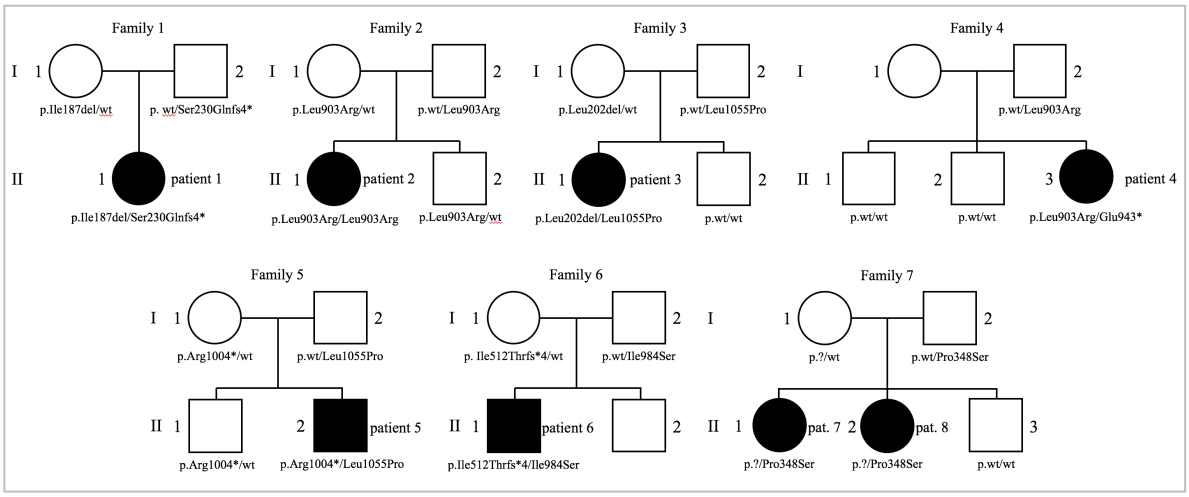

Figure 8: Pedigrees of patients 1 to 8 (families 1 to 7).

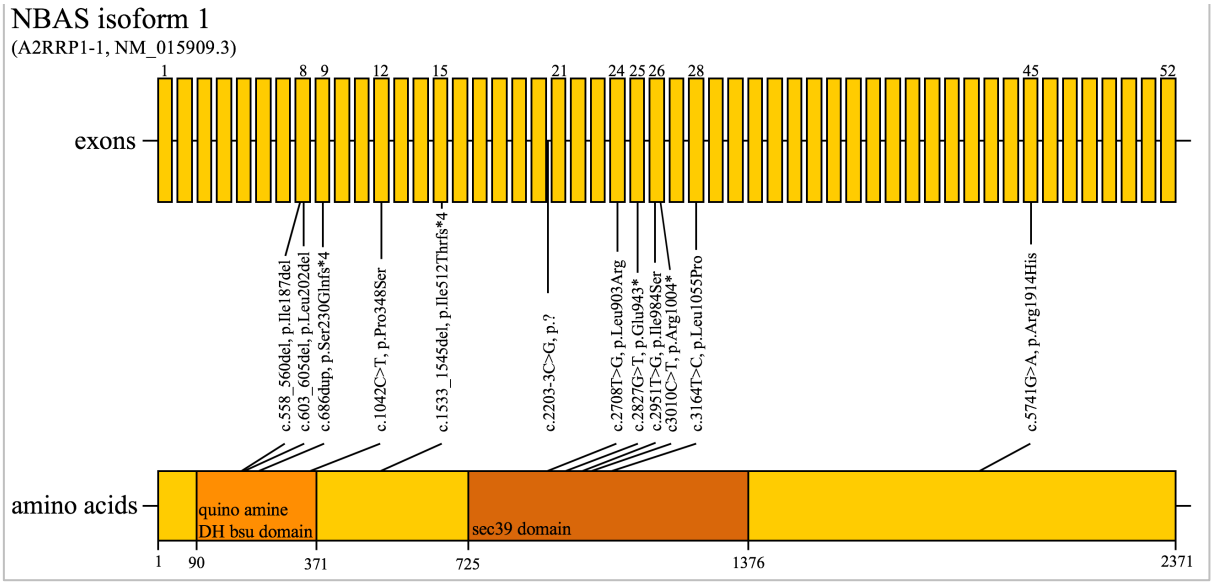

Figure 9: Gene and protein structure of NBAS with twelve variants identified in seven index patients.

Frequency of *NBAS* variants

In future, further patients with recurrent acute liver failure syndrome will be discovered. The Prokisch laboratory had already discovered eight patients from seven unrelated families during my time there, the families being from different countries, continents and ethnicities. This led us to conjecture that mutations in *NBAS* are a rather frequent cause of acute liver failure in infancy. I thus checked the frequency of *NBAS* variants both with the Exome Aggregation Consortium data (ExAC) and the Genome Aggregation Database (GnomAD) (Lek et al. 2016). An overview of the analysis by ExAC is provided in Table 19.

Table 19: Constraints of the gene NBAS provided by the Exome Aggregation Consortium (ExAC 2017).

constraint from ExAC	expected no. variants	observed no. variants	constraint metric
Synonymous	307.7	394	z=-3.05
Missense	738.9	909	z=-3.06
Loss of Function (LoF)	96.0	56	pLI=0.00
Copy Number Variations (CNV)	13.1	60	z=-2.10

The Z score is for the deviation of observed counts from the expected number where a positive z score indicates an increased tolerance to variation. The pLI score indicates tolerance to LoF variants. The closer pLI is to one, the more intolerant the gene appears to be (Lek et al. 2016).

The data show that there are less loss of function (LoF) variants than expected (56 observed variants vs. 96 expected variants), however this is not significant (pLI=0.00). At the same time, there are more observed copy number variants than expected (60 observed variants vs. 13.1 expected variants). These include both duplications and deletions, most frequently affecting exons 29 to 31. There are no individuals who have homozygous loss of function variants. However, there are 187 out of 60 000 persons who have a heterozygous loss of function mutation in ExAC (2017), translating to a frequency of 0.0031. GnomAD (2017) presents a frequency of 0.0032 with 479 variants in 150 000 individuals. This in turn leads to conjecture that approximately one in 98 000 persons is predicted to have two loss of function mutations in *NBAS*, which are presumably lethal. This has not yet been shown though. The analysis of ExAC yet appears to contradict that LoF variants are lethal. LoF variants may show a different phenotype or are simply too rare.

As seen in ILFS2 patients so far, 20 665 missense variants found in 150 000 samples in GnomAD (2017) are rare heterozygous variants. A rare variant is a variant with an allele

frequency of < 1 % in the population. Hence, the probability for a rare heterozygous missense mutation is 0.138. The number in ExAC (2017) is similar with a frequency of 0.154. Thus, it can be approximated that four in 9 000 persons carry both a loss of function and a rare heterozygous missense variant. This may indicate a high number of ILFS2 patients. However, this number appears far too high. Many of these persons may have a benign variant, hence the significance of their mutations may only be tested by examining NBAS levels using a Western Blot.

This assumption is supported by the in-house database of the institute of human genetics, comprising 11 000 exomes. There are 21 cases with a combination of a loss of function and a rare missense mutation, which is close to the prediction based on gnomAD. Eleven of these cases are ILFS2 cases. Other phenotypes include developmental delay, Charcot-Marie-Tooth-Syndrome, nephrotic syndrome and mitochondrial diseases, with no indication of a liver involvement. Future research is needed to find out more about the significance of these variants in *NBAS*.

Characterization of NBAS reduced hepatocyte cell lines

Preamble and purpose

As I have shown, the patients' mutations in *NBAS* lead to lowered NBAS protein levels. In the next step, I aimed to have a closer look at the patients' phenotype. I had observed that our patients predominantly suffered from liver failure while other organs appeared not to be impaired, as outlined in the introduction. However, I also laid out that NBAS is expressed in most tissues at approximately the same level. Since our laboratory had only cultivated patient fibroblast cell lines, I created NBAS knockdown cells from hepatocytes in order to be able to observe possible tissue specific effects of reduced levels of NBAS. A knockdown is the down-regulation of a selected gene by experimental methods (Encyclopedia of Cancer 2012). Since our patients presented with symptoms when suffering from fever, I especially looked for a possible phenotype at elevated temperatures.

Knockdown procedure

The knockdown procedure was conducted using the BLOCK-iT™ Lentiviral RNAi Expression System from Invitrogen as described in the chapter "Materials and methods". As explained, three different shRNAs against different RNA sequences as well as a scramble sequence were used. The sequences will be referred to from now on as T-1908, T-3027, T-4160 and T-Scramble. I chose Hep-G2 cells as model cells for hepatocytes. The Hep-G2 cell line is a stable epithelial adherent cell line derived from the hepatoblastoma (Lopez-Terrada et al. 2009) of a 15-year old Caucasian male (American Type Culture Collection). In result, I obtained the transduced cell lines Hep-T-1908, Hep-T-3027, Hep-T-4160, Hep-T-Scramble and Hep-T-Scramble II.

Success of lentiviral transduction

Although the protocol of the RNAi Expression Kit stated that the success of the transduction needed only to be examined via Western Blots, I decided to sequence the transduced cells nonetheless in order to check whether the virus had actually inserted into the genome.

First, I performed an amplification PCR on DNA extracted from cell pellets with primers which were only supposed to bind to viral sequences. Gel analysis showed an amplification product of matching size of the inserted viral sequence (approx. 300 bp) present in transduced cell lines

(Figure 10). No amplification product was obtained in Hep-G2 wild type cells. This indicated that the transduction had worked.

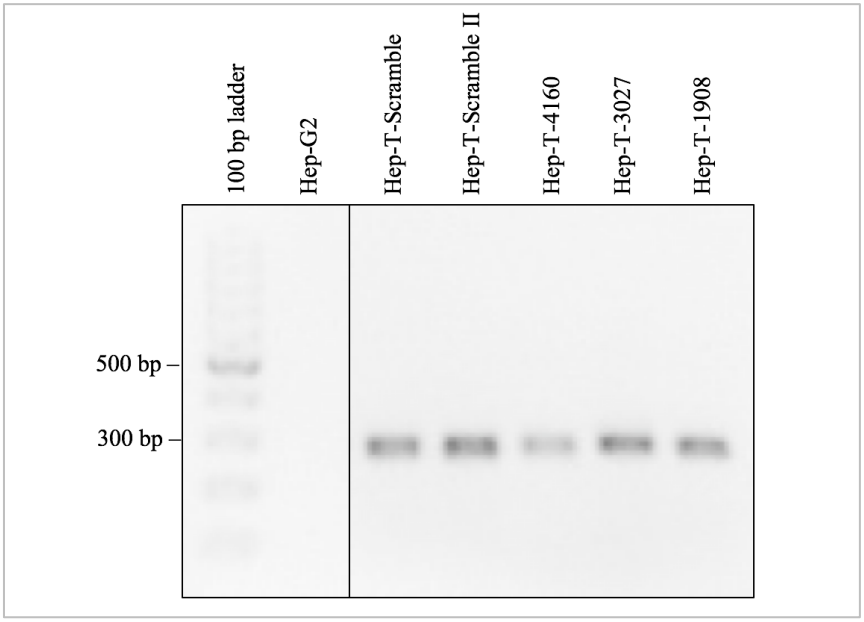

Figure 10: Validation of transduction. Gel shows PCR products obtained by amplification of viral sequences in transduced and non-transduced control cell lines. Genomic DNA of the cell lines was amplified by PCR using primers specific for the viral sequences that were intended to be inserted. PCR products were separated on agarose gel using electrophoresis and examined under UV light.

Sequencing of the cell lines confirmed that the insertion of the virus including the shRNA sequences had worked in every cell line without a mutation, verifying the success of the transduction procedure.

Level of knockdown

In order to quantify the level of protein knockdown achieved, I conducted Western Blots with cell pellets of knockdown cells collected at different time points after the transduction (Figure 11). In the first time after transduction, the cell lines were cultivated in a S2 lab due to lentiviral content before they could safely be transferred to a S1 lab. The first possible time after transduction to collect cells hence was at this point of transfer. Two Western Blots were done with cell pellets that had been collected at this time. This was, on average, 24.4 days (SD: 3.1 days) after transduction. One Western Blot, but with each sample running twice, was conducted with cell pellets that had been collected approximately two weeks later.

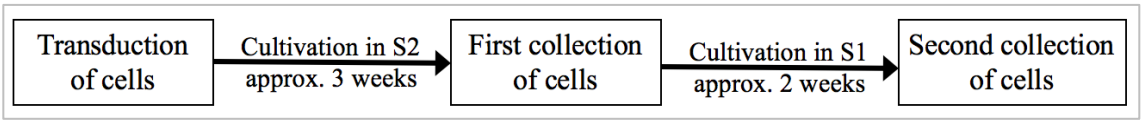

Figure 11: Collection of cells after transduction

The membranes with the immobilized proteins were incubated with antibodies, immunofluorescence was detected and protein levels were quantified. The NBAS level in non-transduced Hep-G2 was taken as 100 %. The results obtained with cells collected at first time point are shown in Figure 12, those obtained with the later collected cells are shown in Figure 13.

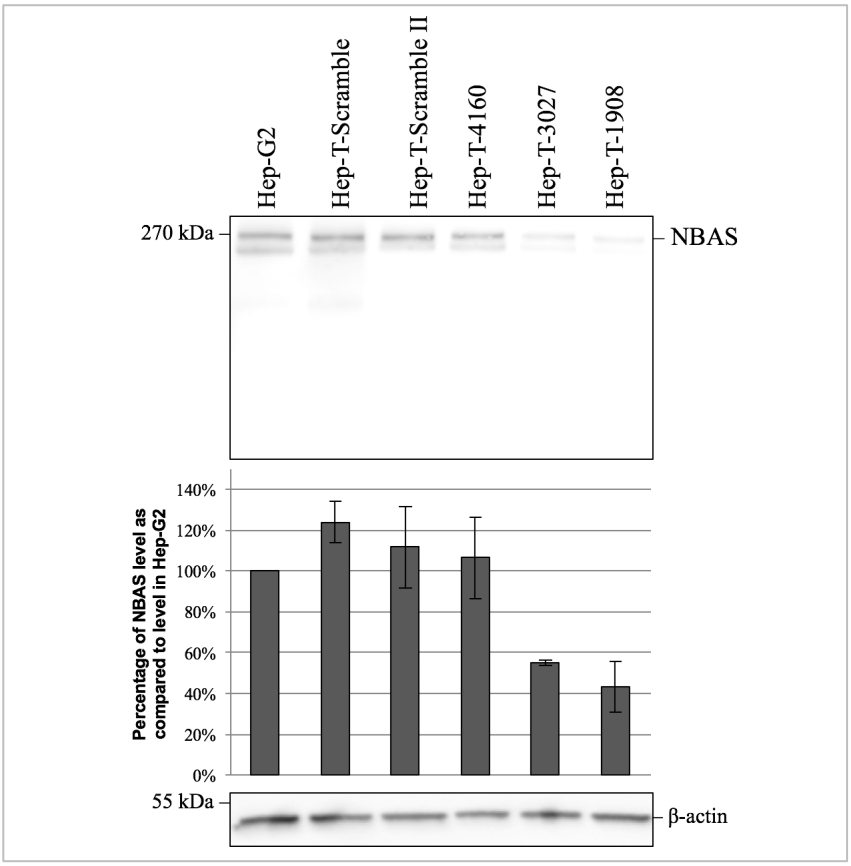

Figure 12: NBAS levels three weeks after knockdown with shRNA.
Cell lines were cultured until they reached approx. 70 % confluency, consequently collected at first time point, pelleted and processed for Western Blots. Western Blots were incubated overnight with primary antibodies against NBAS and β-actin as loading control and developed using enhanced chemiluminescence. Bars indicate the standard deviation.

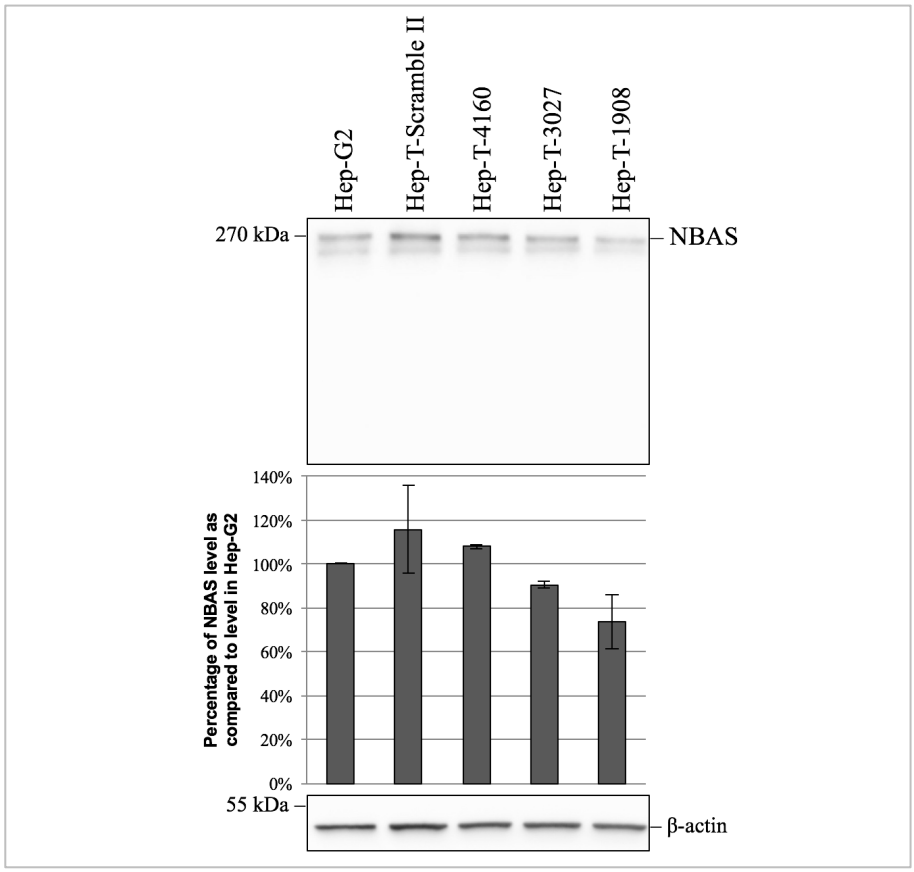

Figure 13: NBAS levels six weeks after knockdown with shRNA.
Cell lines were cultured until they reached approx. 70 % confluency, consequently collected at second time point, pelleted and processed for Western blots. Western blots were incubated overnight with primary antibodies against NBAS and β-actin as loading control and developed using enhanced chemiluminescence. Bars indicate the standard deviation.

The quantification showed that in Scramble cell lines, there was, as expected, no reduction in NBAS. In the first collected samples, Hep-T-3027 and Hep-T-1908 appeared to have NBAS levels of less than 60 % of normal NBAS level. However, in the later collected samples no knockdown could be detected any more, as can be seen in Figure 14. NBAS levels in Hep-T-3027 and Hep-T-1908 showed a statistically significant increase compared to the earlier samples (for Hep-T-3027: $p=0.028$; for Hep-T-1908: $p=0.006$) while there was no significant difference in Hep-T-4160 ($p=0.445$).

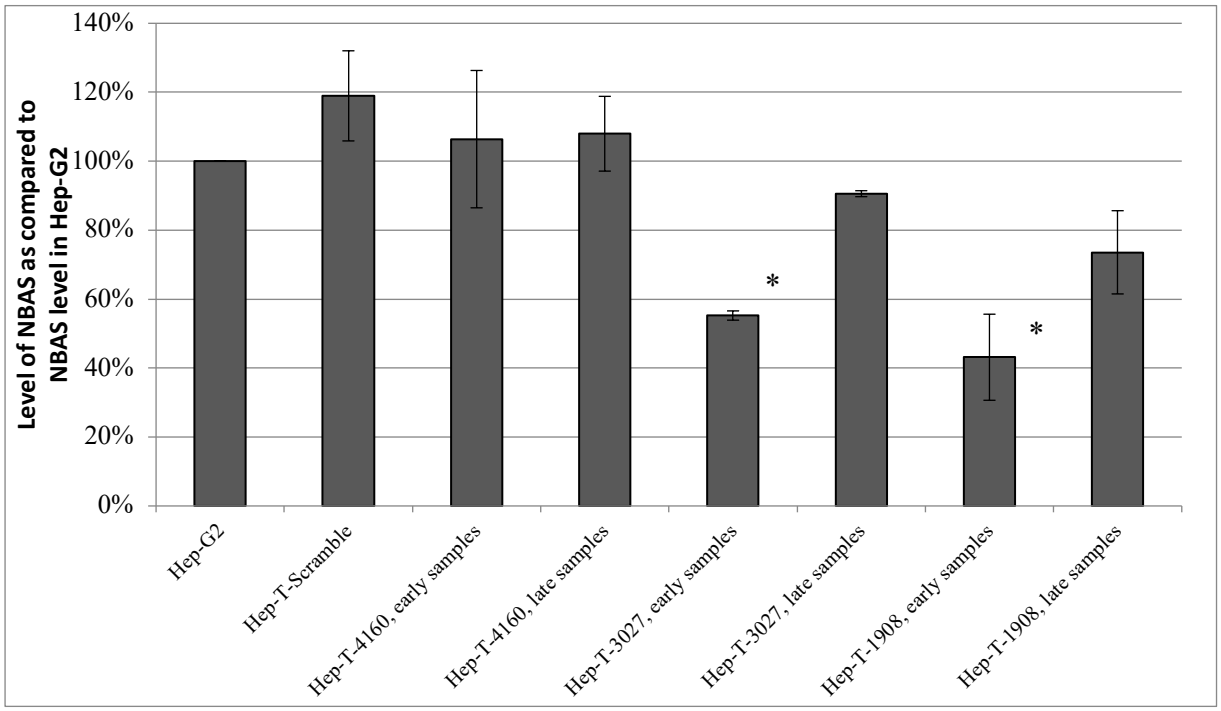

*Figure 14: Comparison of NBAS levels at first and second collection after knockdown with shRNA. Cell lines were cultured until they reached approx. 70 % confluency, consequently harvested, pelleted and processed for Western Blots. Western Blots were incubated overnight with primary antibodies against NBAS and β-actin as loading control and developed using enhanced chemiluminescence. Bars indicate the standard deviation. * indicate a significant difference.*

However, the reduction of NBAS levels in Hep-T-3027 and Hep-T-1908 was never to a protein level comparable to our infantile acute liver failure patients who presented with levels of approximately 20 % of controls. Hence, the knockdown procedure did not have the desired effect.

Phenotype of transduced cells

After transduction, I sought to find a phenotype that the transduced cells presented, possibly indicating tissue specificity.

For the transduced hepatocytes, there appeared to be a phenotype in the beginning. It seemed that Hep-T-3027 and Hep-T-1908 were growing more slowly than normal Hep-G2 cells, Hep-T-Scramble and Hep-T-4160. I sought to quantify this observation by conducting a growth curve. However, I was not able to quantify the apparent growth defect. In fact, by the time of the conduction of the growth curve, all transduced hepatocyte cell lines were growing like the control. This may be due to the fact that it took time until all cell lines were set up for a growth curve. However at this time, NBAS levels were at normal levels again.

Sensitivity to temperature

I also sought to examine sensitivity to temperature in transduced cell lines. However, no phenotype could be shown. As it was not possible to conduct growth curves, as explained above, no sensitivity to temperature on functional level could be observed either.

Since protein levels were shown to increase again to levels which are higher than patient protein levels, protein levels of NBAS at elevated temperatures in transduced cell lines were not examined.

Conclusion of knockdown experiments

The lentiviral transduction of hepatocytes with shRNA sequences, which were supposed to lead to a knockdown of NBAS in the cell lines, did not reach its aim.

Although the transduction was successful, NBAS levels in transduced cell lines were never as low as NBAS levels in patient cell lines (mean NBAS level in patient cell lines: approximately 20 % of controls; minimum NBAS level in transduced cell line (Hep-T-1908): 43 %). Additionally, protein levels in transduced cell lines were increasing with time. Thus, the knockdown did not work as desired.

No phenotype of transduced cells could be observed. This, however, is very likely due to the fact that there was no sufficient knockdown of NBAS in the cell lines. Hence, no tissue specificity could be observed either.

In conclusion, the knockdown cells did not prove to be a stable model system. Other targets or vector systems should be tested in future in order to overcome technical problems. However, this was not possible during the course of this thesis. Consequently, I proceeded to conduct further experiments with patient fibroblasts as these cell lines do have mutations that result in a phenotype *in vivo*.

Characterization of patient fibroblast cell lines

Preamble and purpose

In order to further characterize infantile liver failure syndrome 2, I chose patient fibroblast cell lines as model cells. Fibroblast cell lines were the most stable available model since the cell lines have mutations that lead to a phenotype *in vivo* and there was a lot of experience with the cultivation of fibroblast cell lines in the laboratory. During the course of my work, I cultivated patient cell lines from eight patients (patients 1 to 8). I have already established that mutations in *NBAS* lead to lowered levels of NBAS protein in the patients.

Consequently, I sought to investigate the function of NBAS in patient cell lines. The mentioned syntaxin 18 complex in which NBAS is a component is described to play a role in retrograde transport (Aoki et al. 2009). Hence, I searched a method to examine retrograde transport and its possible impairment in cell lines. I found several protocols using the B-subunit of Shiga toxin to visualize retrograde transport (Sandvig et al. 1994, Johannes et al. 1997, Mallard and Johannes 2003, Shi et al. 2012). However, the protein was not delivered due to supply problems and legal issues during my time in the laboratory. Thus, I was not able to conduct this experiment and had to find other surrogate parameters to study NBAS function. I hence decided to produce growth curves as a possible parameter for cell function. Since our patients presented with liver failure during fever yet mostly without symptoms otherwise, I examined NBAS levels and function both at normal and elevated temperature.

Protein function at elevated temperatures

I examined whether an elevation of temperature was affecting NBAS. I was interested in both protein levels and protein function. As outlined, I decided to quantify the latter by conducting a growth curve experiment.

At the very beginning, however, a temperature to model fever had to be found. The desired temperature would allow control fibroblasts to survive while patient fibroblasts would show a defect. A growth curve according to Method 1a (see Materials and methods), using 42 °C as the elevated temperature, was conducted. The results are shown in Figure 15 below. There did not appear to be a distinction between patients and controls neither at 37 °C nor at 42 °C. Between 72 h and 164 h, cell count was decreasing in all six cell lines at 42 °C. After three days

at maximum, both control and patient fibroblasts stopped growing and died after one week at 42 °C.

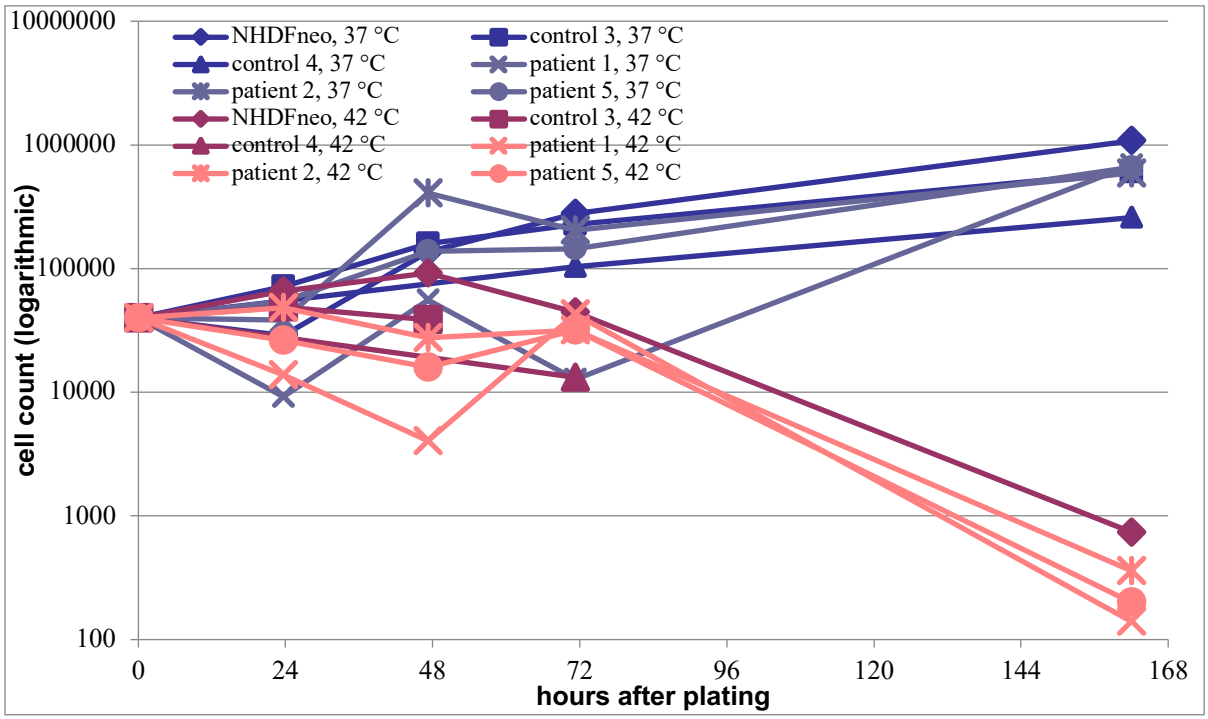

Figure 15: Growth Curve assessed by cell counter, using 42 °C as elevated temperature (Method 1a). One flask with 40.000 plated fibroblast cells was used for every cell line, time point and condition. Cell count was assessed with the Scepter™ Cell Counter.

After I detected the cell count, I calculated growth rates for the six cell lines. Firstly, I calculated growth rates for the first 48 hours of measurement, both at 37 °C and at 42 °C, as visualized in Figure 16. Secondly, I calculated growth rates for the first 72 hours of measurement, shown in Figure 17. Lastly, I tested whether there was a significant difference between those growth rates. Yet, all p-values were not significant (Table 20).

Table 20: p-values (two-tailed, non-paired t-tests) for controls versus patients using Method 1a (results shown in Figure 16 and Figure 17).

growth rate per hour for first	48 h	72 h
37 °C: WT vs MUT	0,99	0,47
42 °C: WT vs MUT	0,14	0,61

WT = NBAS wild type, MUT = NBAS mutant (patients)

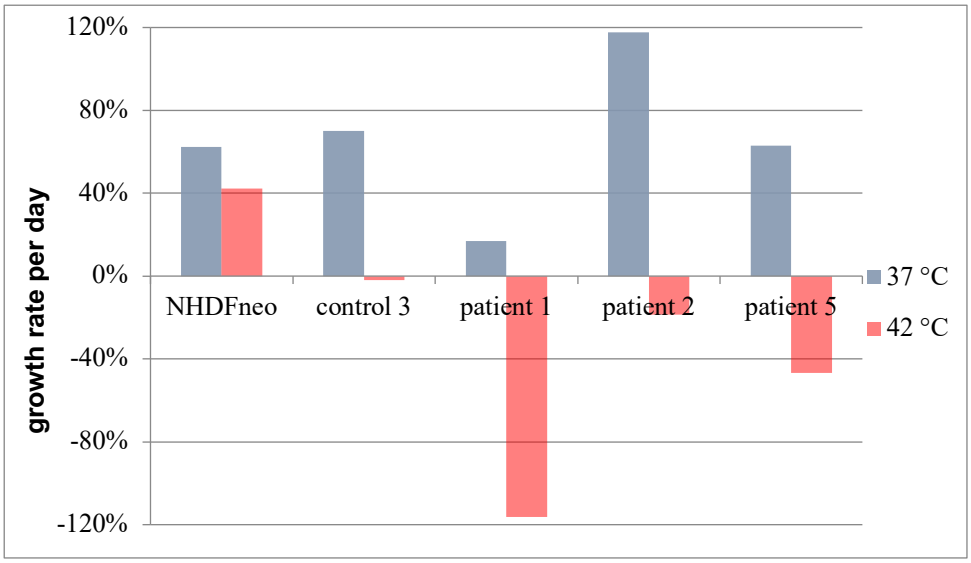

*Figure 16: Growth rates per day during the first **72 hours** after plating calculated from the experiment shown in Figure 15. Growth rates are varying. At 42 °C, one control appears to be the only one to have a very high negative growth rate (control 4).*

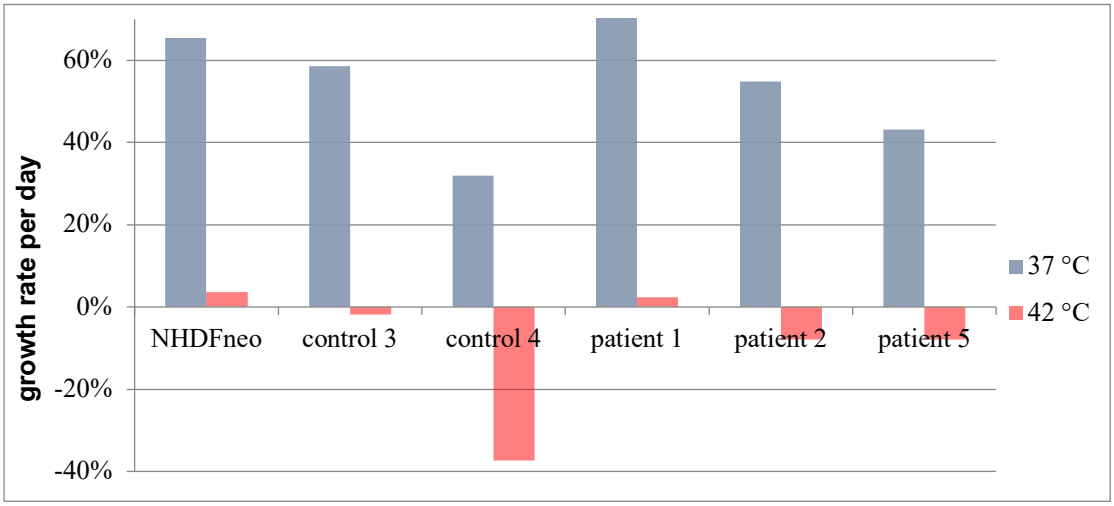

*Figure 17: Growth rate per day during the first **48 hours** after plating from the experiment shown in Figure 15.*

In conclusion, a temperature of 42 °C was too high for this experiment. This, however, is according to biology where body temperatures higher than 41 °C lead to metabolic derailment of the patient (Speer and Gahr 2013). I decided to take 40 °C as the elevated temperature in following experiments. Cell counts one day after plating the cells appeared to be variable. To be able to follow the growth over a longer time period, I decided to plate the cells on a Friday and start assessing cell growth on Monday the following week.

Hence, I established Method 1b. Consequently, a growth curve according to Method 1b was conducted. This experiment, displayed in Figure 18, showed that at 37 °C, all cell lines were growing nicely whereas at 40 °C, all cell lines, patient as well as controls, were dying. It appeared that on the first two measurements (72 h and 96 h after plating) at 40 °C, patient fibroblasts were more sensitive to the temperature shift than control fibroblasts.

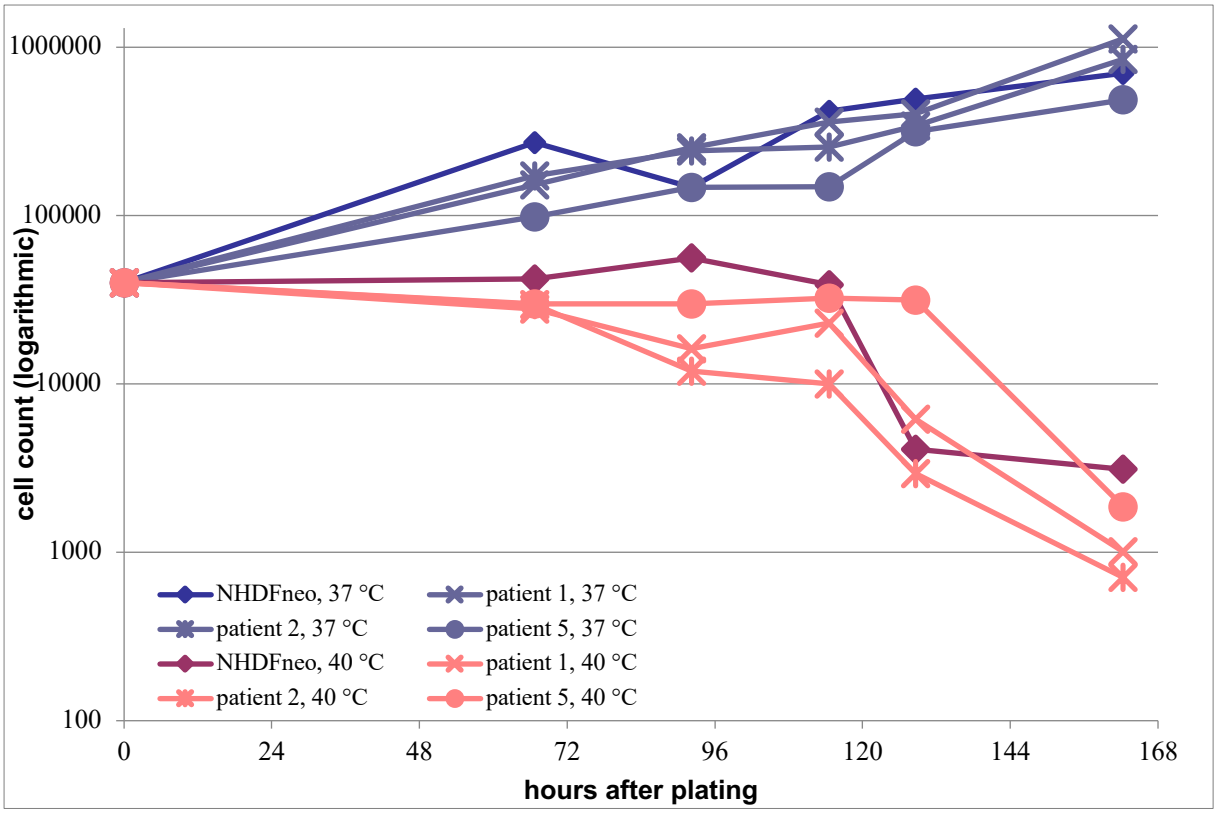

Figure 18: Growth curve assessed by cell counter using 40 °C as elevated temperature (method 1b). One flask with 40.000 plated fibroblast cells was used for every cell line, time point and condition. Cell count was assessed with the Scepter™ Cell Counter.
Note that both patient and control cell lines behave similarly at the different temperatures.

Again, I calculated growth rates for the four different cell lines both at 37 °C and at the elevated temperature 40 °C (Figure 19). I thus concluded that the most sensitive time window to study a temperature sensitive effect may be right after the start of the temperature shift.

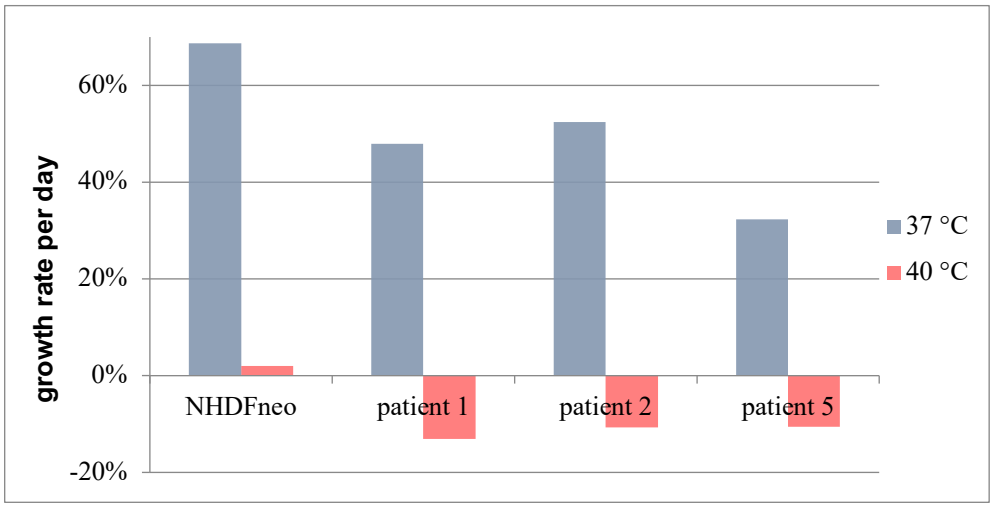

Figure 19: Growth rates per day during the first 72 hours from the experiment shown in Figure 18.

As a result, I decided to establish a new protocol to conduct a growth curve, Method 2. This method allows obtaining triplicates of every time point and condition, hence reducing the random error by calculation of an average. The method also offers advantages for the scientist simplifying the procedure, e.g. less cells are needed to start with and less time is needed to obtain the cell count (please see "Cell biology methods" for detailed explanation). In order to be sure that a reduced cell count is due to an impairment in growth and not due to an impairment in attachment of cells, I also decided to leave any plate at 37 °C for one hour after plating them to allow the cells to settle and attach before possibly placing them into 40 °C.

I repeated the experiment several times according to Method 2. Results are shown in Figure 20. I found that typically at 72 hours, cell proliferation stopped before continuing again for the next 24 hours – independently from the cell line looked at, independently from the number of cells at the start of the experiment and independently from the temperature. This observation suggests that cell proliferation is limited on cellular level where one proliferating cell can only double a restricted number of times before the space around it is taken. Nonetheless at the same time, the experiments showed that during the first two days after plating cell growth is exponential.

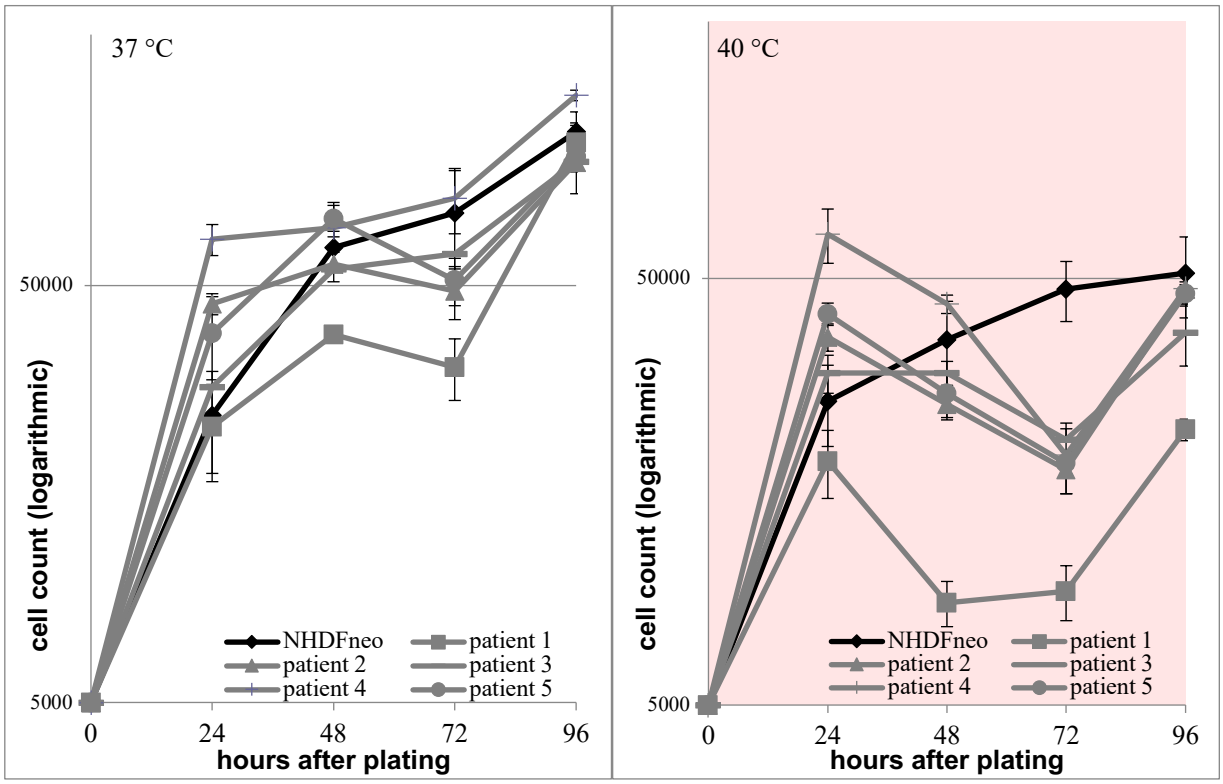

Figure 20: Cell growth at 37 °C, on the left side, and 40 °C, on the right side, assessed by DNA quantification (Method 2). Each fibroblast cell line was plated three times with 5.000 cells per well on one 24-well-plate. One plate was used for every time point and condition. No background colour indicates cultivation at 37 °C, red background indicates cultivation at 40 °C. Cell count was assessed using CyQUANT®. Bars indicate the standard deviation.

Since the uncertainty remained whether the cells had actually properly attached after one hour at 37 °C, I consequently tried another condition with a change of temperature during cultivation. For this, I cultivated all cell lines at 37 °C for two days before changing the condition by placing the cell lines into an incubator with 40 °C. I then assessed cell counts at two further time points after cultivation at 40 °C (Figure 21).

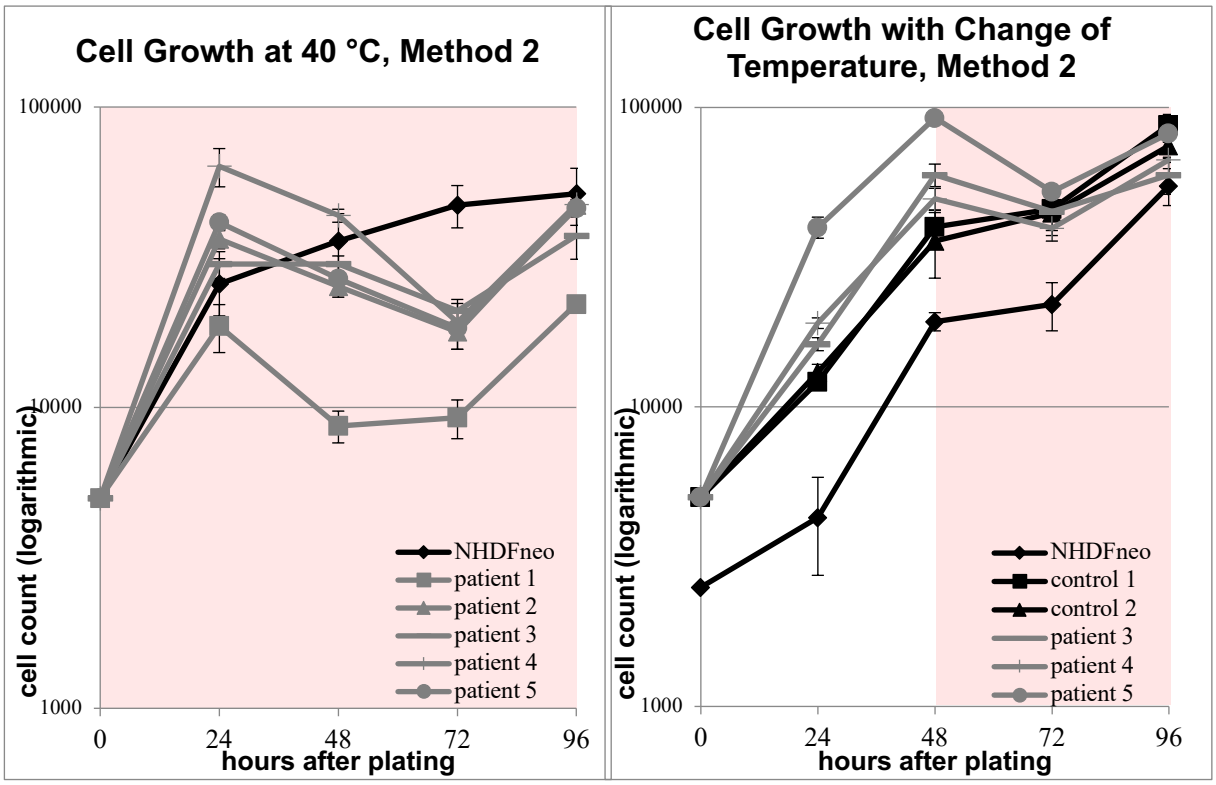

Figure 21: Temperature shift experiment after 48 hours, assessed by DNA quantification (method 2). Each fibroblast cell line was plated three times with 5.000 cells per well on one 24-well-plate (2.500 cells in case of NHDFneo in the experiment with temperature shift, displayed on the right). One plate was used for every time point and condition. No background colour indicates cultivation at 37 °C, red background indicates cultivation at 40 °C. Cell count was assessed using CyQUANT®. Bars indicate the standard deviation obtained from triplicates.

By calculating the growth rates per day from the previous experiment, it became obvious that growth rates between the different cell lines distinctly differ from one another (Figure 22). Cell lines that were proliferating more quickly than others were not suitable for this experiment as they were also limiting their proliferation more quickly. Hence, I had to select cell lines presenting with comparable growth rates at 37 °C. I thus picked fibroblast cell lines, which were established in our lab, without a mutation in *NBAS* as controls, "control 1" and "control 2", as well as the patient cell lines "patient 3" and "patient 4" to conduct further experiments.

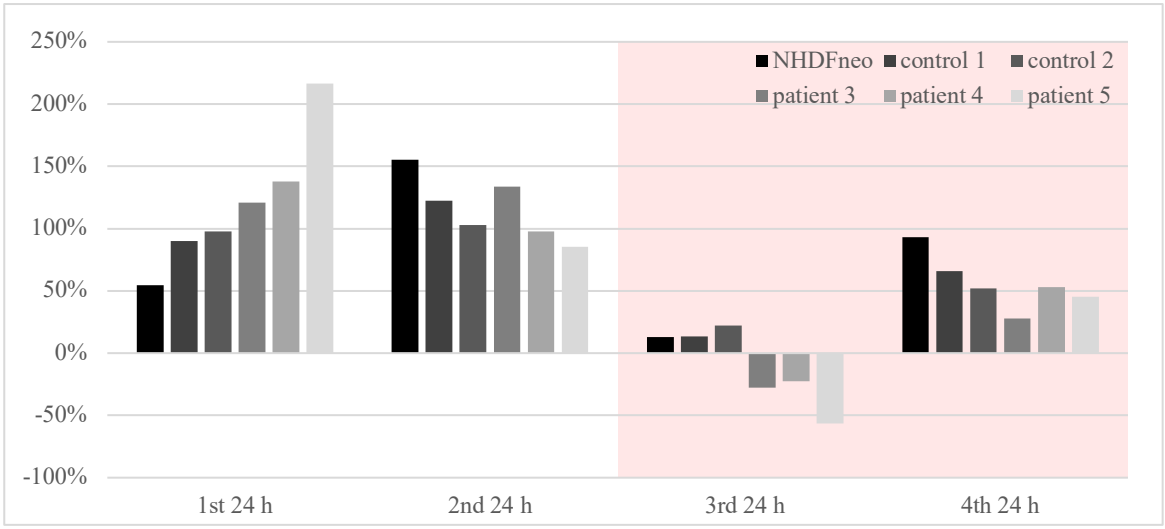

Figure 22: Growth rates per day with change of temperature using method 2. No background colour indicates cultivation at 37 °C, red background indicates cultivation at 40 °C.

I found that the most substantial difference in growth rates between patient and control cell lines appeared to be in the third 24 hours of the experiment, that is in the first 24 hours after the change in temperature. Thus, I found that the most convincing results to evaluate a possible sensitivity to temperature are obtained when placing the cells in 40 °C after they had grown in 37 °C for one day. As cell proliferation appeared to be limited after cultivation for two days, I moreover deduced that cell count should only be determined at two time points during these first two days. I concluded that assessing cell count at two time points, 25 hours and 49 hours after seeding, with a change of temperature to 40 °C after 25 hours, is best in order to obtain utilizable results.

The final experiment was repeated three times. Cell counts are displayed in Figure 23, growth rates are displayed in Figure 24. The results showed that while there was no significant difference in growth rates at 37 °C between patient and control cell lines ($p=0.224$), patient cell lines grew significantly slower than control cell lines at 40 °C ($p=0.037$). In addition, only patient cell lines displayed a significant impairment of growth rate at 40 °C compared to 37 °C (for patient 3: $p=0.044$; for patient 4: $p=0.017$, all two-tailed paired t-tests). Hence, I was able to show that patient cell lines with mutations in *NBAS* present with a temperature sensitive phenotype.

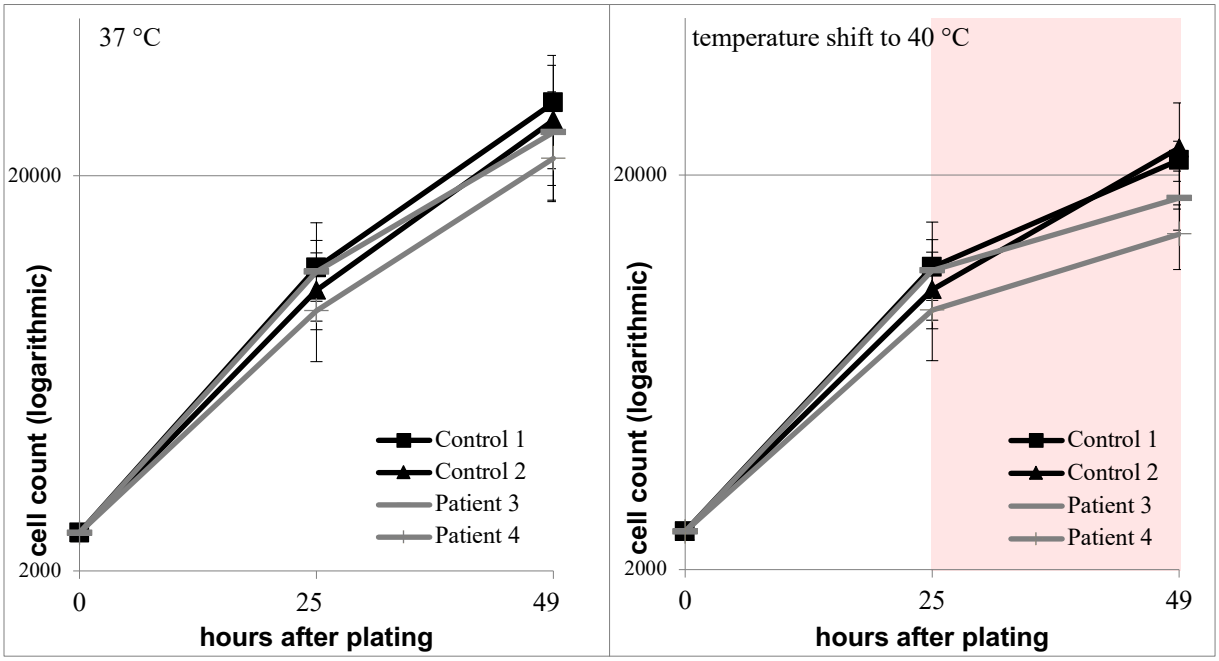

Figure 23: Temperature shift experiment after 24 hours, assessed by DNA quantification (method 2). Each fibroblast cell line was plated three times with 2.500 cells per well on one 24-well-plate. One plate was used for every time point and condition. No background colour indiciates cultivation at 37 °C, red background indicates cultivation at 40 °C. Cell count was assessed using CyQUANT®. Bars indicate the standard deviation obtained from triplicates.

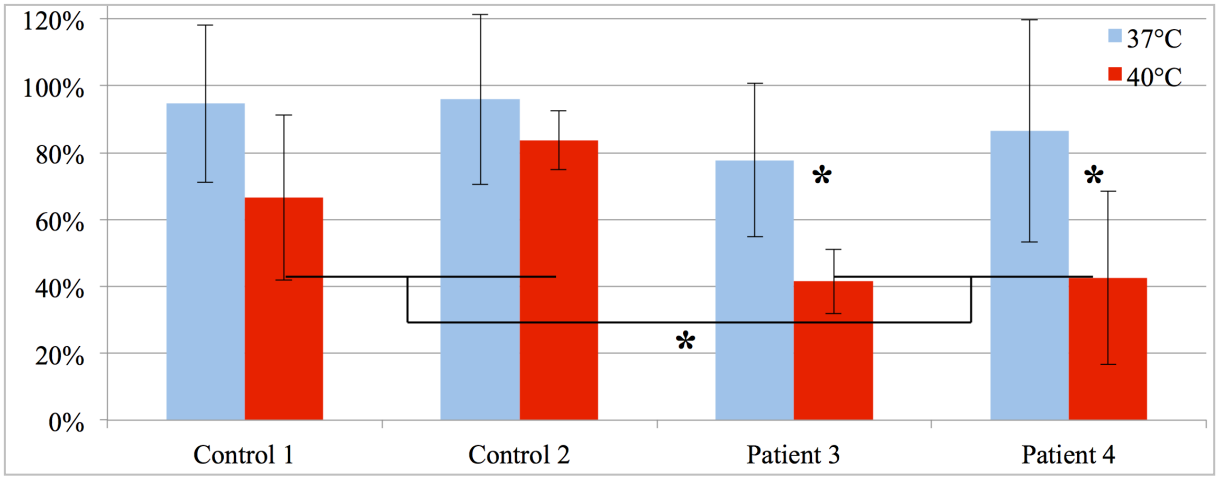

*Figure 24: Growth rates per day during the last 24 hours of the experiment shown in Figure 23. Bars indicate the standard deviation obtained from triplicates. * indicates a significant difference.*

Protein levels at elevated temperatures

When the suitable elevated temperature was found to be 40 °C, I started to look at the protein level of NBAS at elevated temperatures. Since the growth curves showed impairment of growth right after being placed in 40 °C, I decided to look at the protein level after eight hours and after 24 hours at 40 °C of five patient cell lines and one control cell line. Quantification showed a further decrease of NBAS levels in patient cell lines after growth at 40 °C in comparison to 37 °C, whilst NBAS levels in the control remained unchanged (Figure 25).

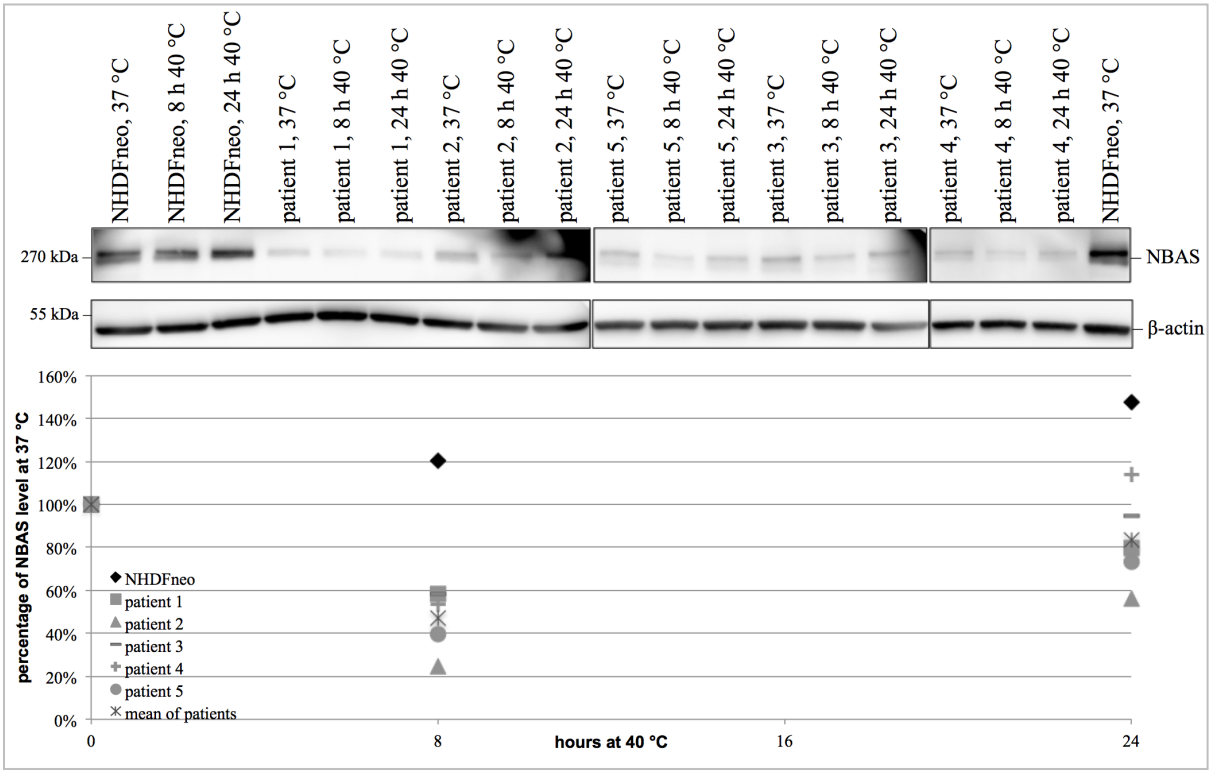

Figure 25: Quantification of NBAS levels after 8 hours and 24 hours growth at 40 °C, respectively. Fibroblast cell lines were cultured until they reached approx. 70 % confluency, consequently harvested, pelleted and processed for Western Blots. Western Blots were incubated overnight with primary antibodies against NBAS and β-actin as loading control and developed using enhanced chemiluminescence. Levels are displayed in percentage of the NBAS level of the concerned cell line at 37 °C.

Next, I took one patient cell line (patient 5) and generated samples after several different periods of time at 40 °C (1 h, 2 h, 4 h, 6 h, 8 h, 9 h, 10 h, 12 h, 14 h, 16 h, 18 h, 20 h, 24 h). Quantification of protein levels showed a rapid decrease of NBAS levels within three hours yet a small recovery after some point (Figure 26).

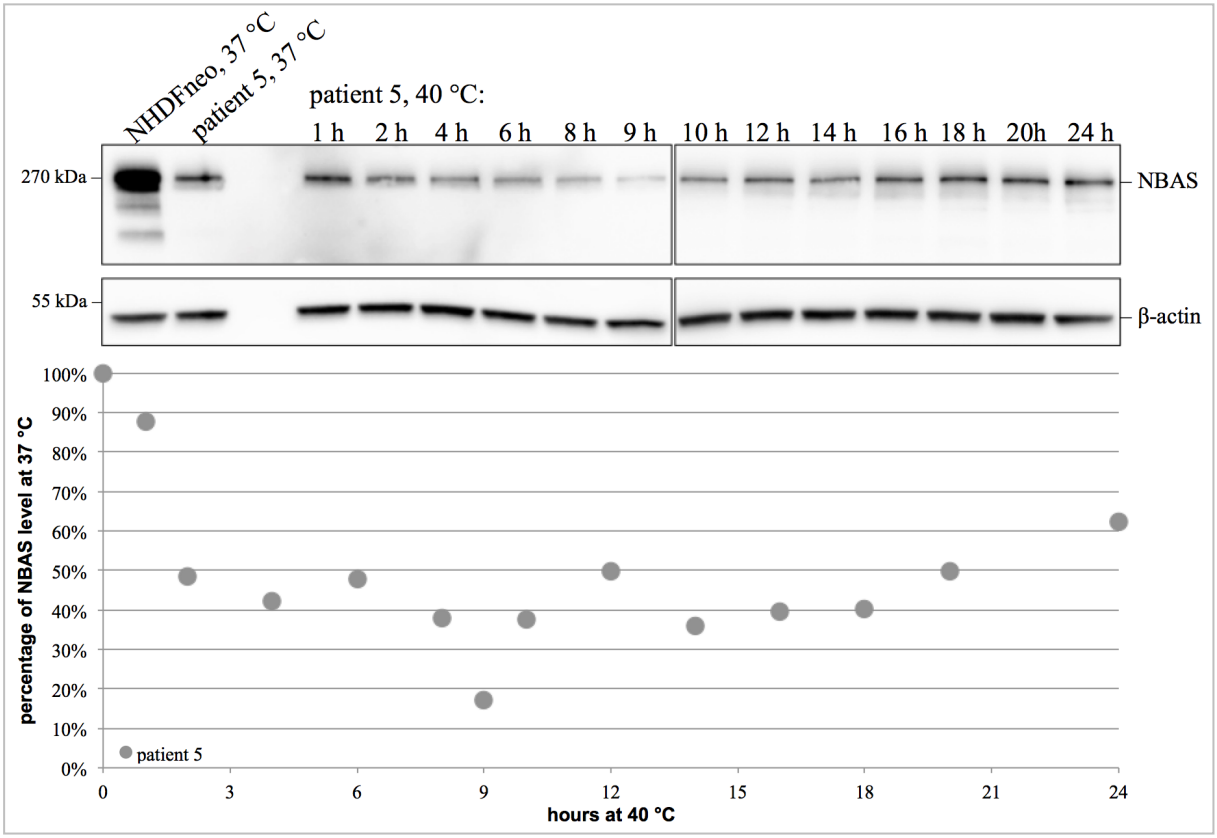

Figure 26: Quantification of NBAS levels after growth at 40 ° C for patient 5. Fibroblast cell lines were cultured until they reached approx. 70 % confluency, consequently harvested, pelleted and processed for Western Blots. Western Blots were incubated overnight with primary antibodies against NBAS and β-actin as loading control and developed using enhanced chemiluminescence. Levels are displayed in percentage of the NBAS level of the cell line at 37 °C.

In a last step, I took samples from all eight patient cell lines and NHDFneo as a control after 3 hours, 9 hours and 18 hours at 40 °C (Figure 27). Quantification of protein levels showed, as in the preceding experiments, a decrease in NBAS in all patient cell lines while remaining unchanged in controls. NBAS levels in NHDFneo remained constant. Protein levels were decreasing variably slowly yet reach a very similar level after 9 h at 40 °C (mean 45 %; SD = 11 %). Nonetheless, after 18 hours at 40 °C, protein levels were widely diverging (mean 47 %; SD 20 %). Levels of p31 were also decreasing in patients, yet slower than NBAS levels, while remaining unaffected in NHDFneo. After three hours, they reached a mean level of 85 % in patients (SD = 14 %), leading to a mean patient level of 72 % (SD = 20 %) after nine hours and eventually ending at a mean level of 68 % with a large standard deviation of 30 % after 18 hours of growth at 40 °C.

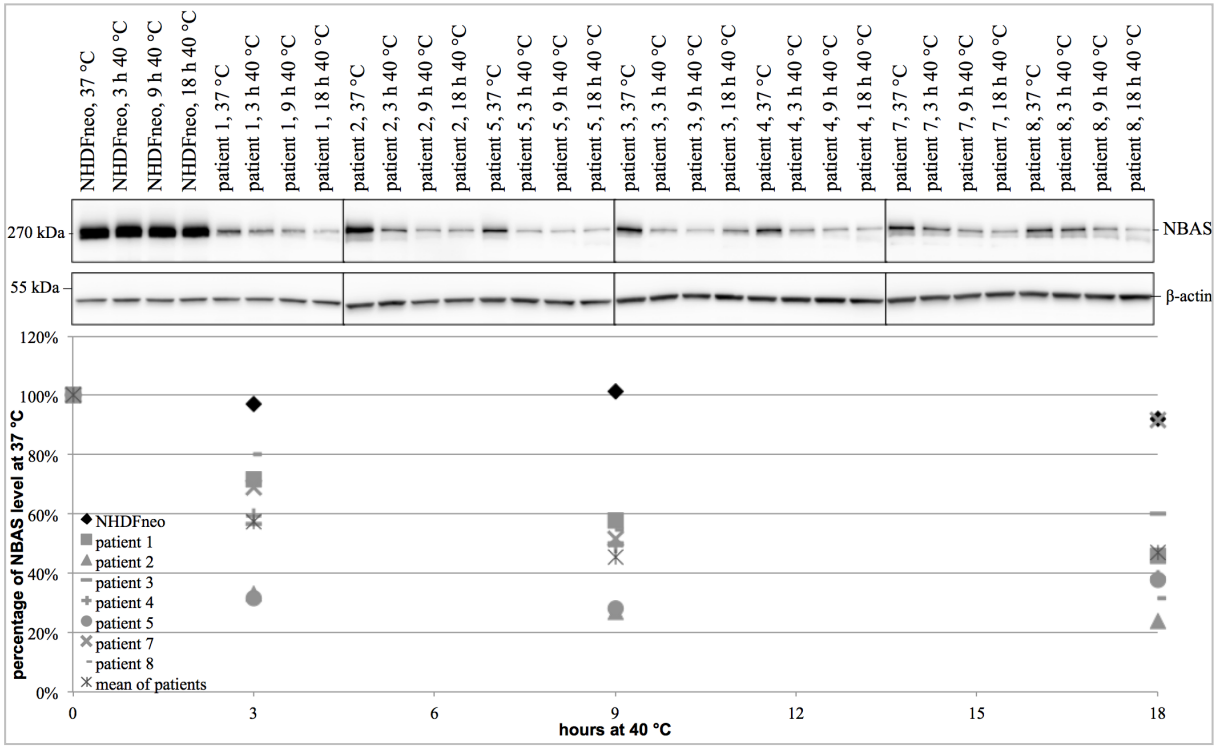

Figure 27: Quantification of NBAS levels after growth at 40 ° C.
Fibroblast cell lines were cultured until they reached approx. 70 % confluency, consequently harvested, pelleted and processed for Western Blots. Western Blots were incubated overnight with primary antibodies against NBAS and β-actin as loading control and developed using enhanced chemiluminescence. Levels are displayed in percentage of the NBAS level of the concerned cell line at 37 °C. Levels of NBAS in NHDFneo cells are used as control.

The fact that NBAS levels persisted unchanged in controls while declining in patient cell lines indicates mutation-dependent thermal instability of the NBAS in patients.

Synthesis of protein level and protein function experiments

The results of both growth curve and the protein level experiments are consistent. Both experiments show that there is sensitivity to temperature in patient cell lines, while control cell lines remain largely unaffected. Protein level experiments indicate that NBAS levels decrease within three hours after the temperature change. This corroborates the finding that a specific growth defect of *NBAS* patient cell lines can already be found shortly after the temperature change.

Conclusion of patient fibroblast experiments

In summary, the experiments show that mutations in *NBAS* leading to infantile liver failure syndrome 2 consistently present with temperature sensitivity on cellular level.

NBAS as part of the syntaxin 18 complex

Summary of previous experiments

As outlined, NBAS is described to function as a component of the syntaxin 18 complex involved in retrograde transport in eukaryotic cells. The complex is supposed to consist of the membrane bound t-SNAREs p31 (USE1), BNIP1 and STX18 at the ER and the membrane-bound v-SNARE Sec22b. NBAS is supposed to interact with p31, ZW10 and RINT1. The protein Sly1 (SCFD1) is supposed to interact with STX18 (Aoki et al. 2009, Uemura et al. 2009, Hong and Lev 2014). With my experiments, I showed that p31 protein levels, another predicted part of this complex, was concomitantly decreasing with NBAS levels in patient cell lines, not only during standard conditions but even more at elevated temperature (please see "Characterization of patient fibroblast cell lines" for presentation of results): I thus confirmed interaction between NBAS and p31, supporting the supposed function of the syntaxin 18 complex. The results I gained from the different experiments with various patients were consistent. This stresses the validity of my results. I tested antibodies of further syntaxin 18 components, however without obtaining a specific result.

Protein interaction

In order to visualize the interactions between the different proteins, I designed Figure 28 showing the syntaxin 18 complex with its components based on my literature research. As can be seen, I display the syntaxin 18 complex while interacting with the v-SNARE Sec22b. I also tried to give an approximate size relation between the different proteins. The proteins BNIP 1, p31 and STX18 are proteins of the endoplasmic reticulum membrane. The other proteins are soluble yet interacting with them, thus can be considered peripheral membrane proteins (UniProt 2017, UniProt 2017, UniProt 2017).

Although the physiologic function of NBAS still remains to be elucidated, my work contributes to the understanding of the protein.

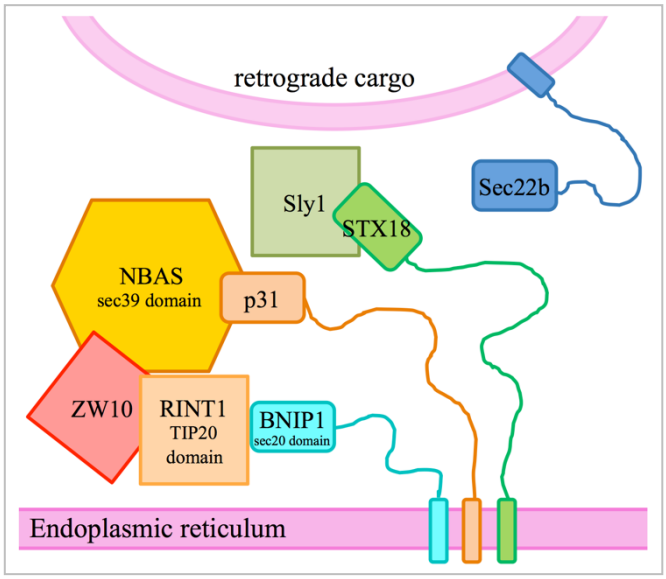

Figure 28: Syntaxin 18 complex.
Figure published in Haack et al. (2015).

Discussion

Preamble

Acute liver failure in children is a rare yet serious and challenging condition. While different triggers such as drugs, infections, autoimmune diseases and inborn disorders may lead to ALF, its cause remains undetermined in one out of two cases. I contributed to the discovery of biallelic mutations in *NBAS* leading to a syndrome of recurrent infantile acute liver failure that we termed "infantile RALF syndrome" (Haack et al. 2015). The syndrome was subsequently named "infantile liver failure syndrome 2" (ILFS2) by OMIM (2015) (OMIM #616483). Infantile liver failure syndrome 2 is characterized by recurrent fever-dependent episodes of liver failure in infancy with full recovery in the interval and reduction of frequency of these episodes with increasing age. The purpose of this work was to validate the effect of mutations in *NBAS* on the patients' cellular and clinical phenotypes, to identify further patients and to characterize this novel monogenic form of liver failure. The work was divided into four parts.

Discussion of results

Firstly, I investigated whether the detected mutations in *NBAS* had an effect on NBAS protein levels in the patients' cell lines to confirm the significance of the mutations. I evaluated the protein levels by conducting Western Blots and quantifying NBAS levels. I have shown that ILFS2 patients only have NBAS levels of approximately 30 % to those of controls. This finding confirms that the mutations in *NBAS* indeed lead to impaired protein levels in all investigated patients. The identification of more than eleven patients by us and further patients reported in literature with acute liver failure and *NBAS* mutations confirmed the causal association.

Secondly, I wanted to examine why patients predominantly present with a liver phenotype while the protein NBAS is present in most tissues. I tried to establish a knockdown of NBAS in hepatocytes in order to consequently challenge the cell lines to find possible tissue-specific differences. Although I successfully transduced control-hepatocytes with shRNA sequences, the knockdown of NBAS levels in the cells was only transient. Even at the time point of lowest levels in transduced cell lines, NBAS levels only decreased to approximately 50 % of controls. As ILFS2 patients presented with NBAS levels of approximately 30 % of controls and did not show a phenotype under normal conditions, it is plausible that transduced cell lines exhibited

no phenotype. In addition, it took two weeks after the transduction to produce the growth curve. This correlates with the findings of the Western Blots showing that NBAS levels are increasing over time. This leads to hypothesize that the growth defect decreases with increasing NBAS levels and vice versa. From these observations follows that this knock-down was not a good model for *NBAS*-induced infantile liver failure and therefore it was not possible to show with this work why *NBAS* patients present predominantly with a liver phenotype.

Thirdly, I chose patient fibroblast cell lines as model cell lines for this disorder. They were the most stable model available since the cell lines have mutations that lead to a reproducible phenotype *in vivo* and there was a lot of experience with the cultivation of fibroblast cell lines in the laboratory. I wanted to characterize the functional consequences of the patients' mutations using these patient cell lines in order to examine whether high temperature had any special effect on the patients. I evaluated protein levels, by the means of Western Blot analysis, and protein function, by the means of protein complex and growth analysis, both at normal and elevated temperature. I have demonstrated that under normal conditions, there is no functional impairment of patients' fibroblasts growth even though I have shown them only to have on average 30 % of NBAS levels compared to controls. However, I have revealed that elevated temperature had a specific impact on cellular level. This has been demonstrated by impaired growth as well as a further decrease of NBAS levels in patients' fibroblasts.

Two mechanisms appear possible to lead to reduced NBAS levels and consequently cell dysfunction when exposed to high temperature. On the one hand, the stability of the protein may be impaired at higher temperatures due to the mutations in *NBAS*. This may lead to impaired proteins which will be degraded, leading to further decreased NBAS levels. On the other hand, the turnover of a number of proteins within a cell, including NBAS, may be increased at elevated temperatures. It thus may also be conjectured that the cell fails to produce sufficient NBAS when under stress of elevated temperature, thus also leading to decreased NBAS levels. The observation that increased temperature leads to impairment in all observed patient cell lines, with different mutations each, yet argues for the latter rather than a temperature-sensitive distortion of *NBAS* itself.

This work nonetheless provides evidence that elevated temperatures have an effect on patients' metabolism. Fibroblast cells are not, of course, an ideal model to study liver disease. However, they are easy to be cultured and examined *in vitro*. Additionally, fibroblast cells are easy to be

obtained directly from the patients, allowing an examination of the patients' mutations and direct effects on their cells. It would neither have been possible to obtain liver cells from the patients nor to culture them without great effort. Also, one may be sceptical whether hepatocytes react *in vitro* as the organ liver does *in vivo*. Another point to be considered is that NBAS appears to be expressed in all tissues at a mean level (Scott et al. 2003, The Human Protein Atlas 2015, GeneCards 2017). The level of expression of NBAS is, at the moment, contradictory in different publications – while the The Human Protein Atlas (2015) found NBAS to be highly expressed in glandular cells and the liver, Fruhwald et al. (2000) found lowest levels of NBAS in the liver. Fibroblasts were described to have low levels of NBAS by The Human Protein Atlas (2015). In my experiments, I did not find a significant difference in NBAS levels between fibroblasts and hepatocytes. Hence, studying patient fibroblasts instead of hepatocytes seemed reasonable and conclusions drawn from the experiments should be taken seriously.

Finally, I assessed the results I had gained on the function of the protein NBAS. As presented in the introduction, NBAS is thought to be involved in retrograde transport. Aoki et al. (2009) provided evidence that NBAS is part of the syntaxin 18 t-SNARE complex together with p31, BNIP1, STX18, ZW10, RINT1 and Sly1 (SCFD1) which interacts with the v-SNARE Sec22b. Aoki et al. (2009) and we (Staufner et al. 2016) both presented evidence that NBAS is linked to the endoplasmic reticulum and that NBAS depletion likely blocks tethering in retrograde transport from Golgi apparatus to ER. This is shown in Staufner et al. (2016) by digitonin treatment of cells making the plasma membrane, yet not Golgi apparatus and ER, permeable. My work indeed confirms that NBAS is in a complex with p31 as I have shown that p31 is concomitantly down regulated in patients with NBAS deficiency. I integrated the acquired knowledge with my findings of the syntaxin 18 complex in Figure 28. Additional experiments to further examine the physiologic function of NBAS had been planned; for example, an assay using the non-toxic Shiga Toxin B-fragment to visualize retrograde transport (Johannes et al. 1997) in patient cell lines. However, this was not possible due to failed delivery of the Shiga Toxin B-fragment. Other functions of NBAS have also been proposed, for example Anastasaki et al. (2011) suggested a role in nonsense-mediated decay, co-regulating a large number of endogenous RNA targets. Hence, it remains for future research to find out the function of NBAS and its pathophysiologic relation to infantile liver failure syndrome 2.

Temperature sensitivity

During fever and inflammatory response, the liver is essential. Its high rate of metabolism is even further accelerated to cope with systemic needs (Speckmann et al. 2013). It may hence be speculated that the liver is the most sensitive organ to be affected by dysfunction of NBAS during the patients' crises, as in many other diseases, although other tissues suffer as well. For example, the fact that the ILFS2 children have presented with vomiting prior to their liver crises can be seen as dysfunction of the gastrointestinal tract, which has a very quick turnover of cells (Marshman et al. 2002), possibly due to impairment of NBAS. Hence, even though the liver does not present with higher NBAS levels than other organs, impairment of NBAS leads to crucial injury of the liver and liver function and consequently to systemic derailment in patients.

In this work, I presented evidence that *NBAS* mutations in patients leading to infantile liver failure syndrome 2 are temperature-sensitive. Temperature-sensitive mutations resulting in inborn disorders are not rare in inborn genetic disorders. Most notably, the widely distributed mutation ΔF508-CFTR leading to cystic fibrosis represents a temperature-sensitive folding defect. A significantly larger amount of CFTR molecules was shown to be present in cultured cells incubated at lower temperatures than in cells incubated at 37 °C (Denning et al. 1992, Ward et al. 1995). This also applies to certain mutations in *PEX13* leading to neonatal adrenoleukodystrophy (peroxisome biogenesis disorder 11B (Shimozawa et al. 1999)). Cases of oculocutaneous albinism have also been linked to temperature-sensitive mutations in the tyrosinase gene with higher activities of tyrosinase at lower temperatures (Giebel et al. 1990, King et al. 1991). In addition, disorders of fatty acid metabolism have also been associated with temperature-sensitive mutations. Fukao et al. (2001) described a myopathic form of very-long chain acyl-CoA dehydrogenase deficiency with two different yet both temperature-sensitive mutations in *ACADVL*. A mutation in *MCAD*, K304E, leading to medium chain acyl-CoA dehydrogenase deficiency has also been shown to be temperature-sensitive (Bross et al. 1995). Grunert et al. (2015) reported on patients with this mutation who presented with decreased protein-activity during febrile infections, suggesting thermal instability of the proteins.

Intriguingly, the significantly reduced levels of NBAS that I have demonstrated in the patients occur to be sufficient under normal conditions. Crises, focussing on the liver only, are only triggered under physiologic stress due to fever. Patients present with almost no obvious phenotypic appearance apart from short stature, that is however not very severe, and

hypertelorism. In contrast to many other inborn metabolic diseases, they do not suffer from cognitive impairment. We have also suggested that cognitive impairment that is present in two patients is due to insufficient management of liver crises at the time (Staufner et al. 2016). Even more intriguing is the fact that infantile ILFS2 patients suffer from few to no crises by the time they have grown to adults. Patients can hence lead a normal life if liver crises are supported properly. Nonetheless, some ILFS2 patients have died in crises, hence the disease must not be underestimated. The knowledge about NBAS is yet very limited and cannot explain why the phenotype is as described.

Diagnosis of pathogenic *NBAS* mutations

Analysis of the frequency of *NBAS* variants showed that the probability for loss of function mutations in the population is approximately 0.3 % and the probability for a rare heterozygous missense mutation is approximately 14 %. Therefore, four persons in 9 000 people are predicted to carry one stop mutation and one rare missense variant. It thus should be presumed that infantile liver failure syndrome 2 is a rather frequent disease in the population. However, many detected mutations in *NBAS*, even some of the known pathogenic ones, are predicted to be benign. Therefore, false-positive results can be found by sequencing patients. The Western Blot I established while working on my thesis may help to differentiate whether mutations in patients are disease-causing or silent as it shows the actual expression of NBAS in patient cells. It can thus be used as a diagnostic tool. Hence, my work helped to validate sequencing results in patients with recurrent acute liver failure and will continue so in future.

Therapy of ILFS2

It is remarkable that mutated NBAS in infantile liver failure syndrome 2 patients is relatively stable at normal body temperature while most of the other known temperature-sensitive mutations are not. It may be deduced that derailment in infantile RALF patients during crises are largely triggered by fever. As a therapeutic consequence, patients should have their temperature, when elevated, strictly brought down. Since patients' livers are highly injured during crises, antipyretic medication which is not or not mainly excreted by the liver should be favoured. Hence, paracetamol, the antipyretic drug of first choice in childhood, should be put aside in favour of metamizole or ibuprofen. Physical measures to bring down fever should also

be applied, as these methods are non-toxic. It is speculative whether consequent antipyresis may ameliorate or even prevent liver crises in patients.

Garcia Segarra et al. (2015), in contrast, proposed that recurrent acute liver failure in patients with NBAS deficiency results from immune dysregulation. They suggested that the liver in patients may be hypersensitive to inflammatory cytokines and thus quickly be injured during infections, leading to crises. Henceforth, the group recommended non-steroidal anti-inflammatory drugs at the onset of a febrile illness, concomitant with our collaborators Staufner et al. (2016), as well as immunoglobulin replacement to reduce the frequency of infections and consequently liver crises.

Our clinical collaborators Staufner et al. (2016) presented an optimised therapy of infantile liver failure syndrome 2 that Professor Hoffmann (director of the university children's hospital Heidelberg) was able to develop during his twenty years of clinical experience with the four index patients. This therapy should be applied early during the course of a liver crisis and is henceforth able to lighten symptoms and even avoid acute liver failure. The therapy includes intravenous administration of high glucose and lipids; patients 1 to 4 received carnitine as well. Parenteral application of lipids was found to lead to a much faster recovery during crises. Most importantly, this therapy includes effective antipyretic therapy by metamizole, supporting the hypothesis that antipyresis in ILFS2 patients may alleviate liver crises.

Liver failure syndromes

Vomiting and failure to thrive have been revealed as markers for inborn metabolic errors in pediatric patients with acute liver failure (Brett et al. 2013), vomiting also being a symptom during crises in patients with infantile liver failure syndrome 2. Recurrent acute liver failure in infancy due to mutations in *NBAS* is one of many inborn liver failure syndromes. Wilson disease, mitochondriopathies and disorders of fatty acid oxidation (FAO), as the most common ones amongst others, were identified as metabolic disorders to cause acute liver failure in childhood (Rinaldo 2001, Squires et al. 2006, Gerner and Hoyer 2009).

There are also mutations in different genes that specifically lead to transient acute liver with recovery in the interval: *TRMU* (transient infantile liver failure (LFIT) (Zeharia et al. 2009), *LARS* (infantile liver failure syndrome 1 (ILFS1) (Casey et al. 2012), *IARS* (growth retardation, intellectual developmental disorder, hypotonia, and hepatopathy (Kopajtich et al. 2016)) and

MARS (interstitial lung and liver disease (ILLD) (van Meel et al. 2013)). All of the resulting proteins are involved in tRNA metabolism. Patients with these diseases present with a clinical picture suggestive of a mitochondriopathy. However, only TRMU is located in the mitochondria (UniProt 2015) while LARS, IARS and MARS are located in the cytoplasm (UniProt 2015, UniProt 2015, UniProt 2017). Hence only LFIT due to mutations in *TRMU* is a mitochondriopathy in strict sense. Patients with LFIT present with acute liver failure and hepatomegaly, concomitant with lactic acidosis, jaundice and hypotonia, in early infancy. Like in ILFS2 patients, LFIT patients can recover spontaneously with supportive care. If they survive the first episode of liver failure, they will show normal development and, unlike ILFS2 patients, no further episodes of ALF. Several families from different origins with members suffering from LFIT have been described by three authors (Lev et al. 2002, Zeharia et al. 2009, Uusimaa et al. 2011). Patients suffering from ILLD due to mutations in *MARS* show, in contrast, not only hepatopathy but also lung disease. They also present with lactic acidosis and hypotonia, however, interstitial lung disease and progressive liver failure are paramount. This presents an important difference to ILFS2 as liver failure is progressive rather than acute. For ILLD, several families from different origins have also been described (van Meel et al. 2013, Hadchouel et al. 2015). ILFS1, lastly, presents the most similarities to infantile liver failure syndrome 2. Patients with ILFS1 also present with recurrent liver failure with recovery in the interval. The most striking similarity is the presentation of acute symptoms under physiologic stress due to illness (Casey et al. 2012). In contrast to ILFS2, ILFS1 has only yet been described in a single family (Casey et al. 2012). Thus, although infantile liver failure syndrome 2 due to mutations in *NBAS* resembles other liver failure syndromes, it presents a distinct disease entity.

Phenotype of patients with *NBAS* mutations

Mutations in *NBAS* had not been linked to liver disease before. As already mentioned, however, a specific mutation in *NBAS* (p.Arg1914His) had been linked to a syndrome of short stature, cone and optic nerve atrophy and Pelger-Huët anomaly in Yakuts in homozygous state (SOPH syndrome) (Maksimova et al. 2010). These patients, though, have not been reported to suffer from any form of liver disease. Additionally, patients with ILFS2 apparently do not present with any of the clinical features of SOPH syndrome apart from short stature (Staufner et al. 2016). Pelger-Huët anomaly, which was present in SOPH syndrome patients, was also present in one ILFS2 patient (patient 8), although we have discussed whether Pelger-Huët anomaly was

due to Crohn's disease in the same patient (Staufner et al. 2016). Ophthalmological findings and specifically optic nerve atrophy were absent in infantile RALF patients apart from one patient who presented with mild cone and optic nerve atrophy (Maksimova et al. 2010). Looking at the gene and protein structure of *NBAS* and the respective patients' mutations, it is striking that the recurrent acute liver failure patients' mutations are clustered in two regions of the protein, both being known domains, the quinoprotein aminedehydrogenase, beta chain like domain and the sec39 domain, while the mutation described to lead to SOPH syndrome (Maksimova et al. 2010) is affecting a protein part of unknown function at the 3'-end of the gene. Therefore, it can be speculated that the different mutation locations have a different impact on protein function and consequently phenotype of the patients. Maksimova et al. (2010) have not, though, examined the present levels of NBAS in SOPH syndrome patients thus they cannot be compared to my results.

Recent publications suggest that the phenotype resulting from *NBAS* mutations may not present as disease entities as distinct as initially suspected. Garcia Segarra et al. (2015) reported on two unrelated patients with multisystem disease involving liver, eye, immune system, connective tissue, and bone, caused by biallelic mutations in *NBAS* after our publication in 2015. The clinical features presented by these two patients bear similarities to both the patients published by us (Haack et al. 2015, Staufner et al. 2016) and by Maksimova et al. (2010). Just as infantile RALF and SOPH syndrome patients, they presented with short stature. Also, they both presented with Pelger-Huët anomaly and ophthalmologic abnormalities (optic atrophy and retinal dystrophy) like the SOPH syndrome patients. One of the two patients only published by Garcia Segarra et al. (2015) presented with acute liver failure. However, both presented with recurrent vomiting during crises. Moreover, Capo-Chichi et al. (2015) reported on three siblings in a consanguineous Lebanese family to suffer from osteoporosis and developmental delay besides recurrent acute liver failure. Bone fragility was also reported by Balasubramanian et al. (2017) who published compound heterozygous mutations in *NBAS* to cause atypical osteogenesis imperfecta. Kortum et al. (2017) reported on a 4-year-old girl who shows both the phenotype of SOPH syndrome as well as recurrent acute live failure. ILFS2 patients have since been reported from further countries, as for example Portugal, Saudi-Arabia and China (Hasosah et al. 2017, Park and Lee 2017, Regateiro et al. 2017).

Moreover, the in-house exome database of the institute of human genetics contains patients with mutations in *NBAS* suffering not from ILFS2, but from other disorders such as developmental delay, Charcot-Marie-Tooth syndrome and mitochondrial diseases. All these reports thus suggest that mutations in *NBAS* will lead to a wider range of disease than previously known. By detecting more patients, the phenotypical spectrum will certainly be expanded. At the same time, the evaluation will be more difficult whether *NBAS* mutations are indeed the cause for the symptoms or just a coincidental finding.

Conclusion

Mutations in *NBAS* appear to be a rather frequent cause of recurrent acute liver failure in infancy. The purpose of this work was to characterize this novel monogenic form of liver failure. The pathophysiology of infantile liver failure syndrome 2 is not yet clear. However, I have shown in this work that patients' mutations are temperature-sensitive and this consequently leads to systemic derailment at elevated body temperatures. I was, though, not able to show a specific hepatocyte phenotype which could help to explain why the organ liver is predominantly involved when NBAS is expressed evenly in all tissues.

Most importantly, it should be highlighted that children with mutations in *NBAS* have a good quality of life outside of liver crises, allowing them to live a normal life. Even more important, they do not suffer from liver crises any more once they have grown to adults. My work presents evidence that elevated temperature in patients itself leads to liver crises. This stresses the importance of diagnosing *NBAS* mutations in children with acute liver failure as they can be provided with a satisfactory therapy and, more importantly, with a benign prognosis. Infringing measures such as liver transplantation can possibly be avoided with the outlook that future liver crises will decrease in frequency and eventually terminate.

As already discussed, mutations in *NBAS* presumably present a frequent cause for infantile acute liver failure with an expanding phenotypic spectrum. Therefore, I suggest *NBAS* to be sequenced in all patients with recurrent acute liver failure, especially when heralded by fever and/or vomiting. Functional consequences of *NBAS* mutations can quickly be examined by conduction of a Western Blot by the protocol I established. Diagnosis of infantile liver failure syndrome 2 is thus possible and consequently adapted therapy hence leads to a better quality of life in patients.

Summary

Introduction

Liver failure in infancy is a rare yet possibly life-threatening condition. The most common causes for acute liver failure are drug-toxicity, metabolic disorders, infections such as hepatitis and autoimmune diseases. However, in approximately half of the cases of acute liver failure in children, a specific cause cannot be found. In four unrelated patients with infantile recurrent acute liver failure, biallelic mutations in *NBAS* were identified as the presumable genetic cause of their disorder. At the start of this thesis, a homozygous *NBAS* mutation had been linked to SOPH syndrome, which does not involve liver disease. NBAS is discussed to play a role in retrograde transport as part of the syntaxin 18 complex, although its exact function is yet unclear.

Purpose

The purpose of this work was to validate the effect of mutations in *NBAS* on the patients' phenotypes, to identify further patients and to characterize this novel monogenic form of liver failure.

Methods

I examined protein levels by Western Blots and protein function by conduction of growth curves. I furthermore conducted the experiments additionally at elevated temperatures. Furthermore, I performed a knockdown of NBAS using shRNA.

Results

I found that mutations in *NBAS* lead to significantly lower levels of NBAS protein in patient cell lines, leading to conjecture that the mutations are the cause of the patients' phenotype. The Western Blot protocol that I established is now a diagnostic tool for *NBAS* mutations of unclear significance. The knockdown of NBAS in Hep-G2 cells did not prove to be a stable system, hence I further examined *NBAS* patient fibroblast cell lines. I detected temperature sensitivity in patient fibroblasts, with both significantly lowered NBAS levels as well as impaired growth at elevated temperatures. Lastly, I added evidence that NBAS is indeed part of the syntaxin 18 complex by also examining p31, another proposed component of the complex.

Discussion

The genetic syndrome caused by *NBAS* mutations has been termed infantile liver failure syndrome 2 by OMIM (#616483). Mutations in *NBAS* may be frequent in the population. Hence, the Western Blot analysis I established may be crucial in diagnosing new patients by detecting possible effects on NBAS levels. My results furthermore support that NBAS is part of the syntaxin 18 complex, although its function is not yet clear. The temperature sensitivity of patients' cell lines suggests that body temperature of ILFS2 patients should be lowered to prevent episodes of liver failure. Moreover, the phenotype between different disorders associated with *NBAS* mutations may not be as distinct as initially anticipated since cases of patients suffering from a range of symptoms, not only liver failure, have been published.

Outlook

More patients will be found in future and thus the phenotypic spectrum associated with *NBAS* mutations will most likely be further expanded. Future research also remains to elucidate the exact function of NBAS.

List of publications

Haack, T. B.*, C. Staufner*, **M. G. Köpke**, B. K. Straub, S. Kolker, C. Thiel, P. Freisinger, I. Baric, P. J. McKiernan, N. Dikow, I. Harting, F. Beisse, P. Burgard, U. Kotzaeridou, J. Kuhr, U. Himbert, R. W. Taylor, F. Distelmaier, J. Vockley, L. Ghaloul-Gonzalez, J. Zschocke, L. S. Kremer, E. Graf, T. Schwarzmayr, D. M. Bader, J. Gagneur, T. Wieland, C. Terrile, T. M. Strom, T. Meitinger, G. F. Hoffmann' and H. Prokisch (2015)'.

"**Biallelic Mutations in *NBAS* Cause Recurrent Acute Liver Failure with Onset in Infancy**."

Am J Hum Genet **97**(1): 163-169.

** co-first authors*

' co-senior authors

Staufner, C., T. B. Haack, **M. G. Köpke**, B. K. Straub, S. Kolker, C. Thiel, P. Freisinger, I. Baric, P. J. McKiernan, N. Dikow, I. Harting, F. Beisse, P. Burgard, U. Kotzaeridou, D. Lenz, J. Kuhr, U. Himbert, R. W. Taylor, F. Distelmaier, J. Vockley, L. Ghaloul-Gonzalez, J. A. Ozolek, J. Zschocke, A. Kuster, A. Dick, A. M. Das, T. Wieland, C. Terrile, T. M. Strom, T. Meitinger, H. Prokisch, G. F. Hoffmann, T. B. Haack, C. Staufner, M. G. Kopke, B. K. Straub, S. Kolker, C. Thiel, P. Freisinger, I. Baric, P. J. McKiernan, N. Dikow, I. Harting, F. Beisse, P. Burgard, U. Kotzaeridou, J. Kuhr, U. Himbert, R. W. Taylor, F. Distelmaier, J. Vockley, L. Ghaloul-Gonzalez, J. Zschocke, L. S. Kremer, E. Graf, T. Schwarzmayr, D. M. Bader, J. Gagneur, T. Wieland, C. Terrile, T. M. Strom, T. Meitinger, G. F. Hoffmann and H. Prokisch (2016).

"**Recurrent acute liver failure due to NBAS deficiency: phenotypic spectrum, disease mechanisms, and therapeutic concepts**."

J Inherit Metab Dis **39**(1): 3-16.

Bibliography

AceView, N. (2017). "Homo sapiens complex locus NBAS, encoding neuroblastoma amplified sequence." Retrieved January 7, 2017, 2017, from https://www.ncbi.nlm.nih.gov/IEB/Research/Acembly/av.cgi?db=human&l=NBAS.

Aktories, K., U. Förstermann, F. Hofmann and K. Starke (2013). Allgemeine und spezielle Pharmakologie und Toxikologie. Elsevier Urban & Fischer, München.

American Type Culture Collection. "Hep G2 [HEPG2] (ATCC® HB-8065™)." Retrieved August 27, 2014, from http://www.lgcstandards-atcc.org/products/all/HB-8065.aspx?geo_country=de.

Anastasaki, C., D. Longman, A. Capper, E. E. Patton and J. F. Caceres (2011). "Dhx34 and Nbas function in the NMD pathway and are required for embryonic development in zebrafish." Nucleic Acids Res **39**(9): 3686-3694.

Aoki, T., S. Ichimura, A. Itoh, M. Kuramoto, T. Shinkawa, T. Isobe and M. Tagaya (2009). "Identification of the neuroblastoma-amplified gene product as a component of the syntaxin 18 complex implicated in Golgi-to-endoplasmic reticulum retrograde transport." Mol Biol Cell **20**(11): 2639-2649.

Balasubramanian, M., J. Hurst, S. Brown, N. J. Bishop, P. Arundel, C. DeVile, R. C. Pollitt, L. Crooks, D. Longman, J. F. Caceres, F. Shackley, S. Connolly, J. H. Payne, A. C. Offiah, D. Hughes, M. J. Parker, W. Hide and T. M. Skerry (2017). "Compound heterozygous variants in NBAS as a cause of atypical osteogenesis imperfecta." Bone **94**: 65-74.

Bartsakoulia, M., J. S. Mupsilonller, A. Gomez-Duran, P. Y. Man, V. Boczonadi and R. Horvath (2016). "Cysteine Supplementation May be Beneficial in a Subgroup of Mitochondrial Translation Deficiencies." J Neuromuscul Dis **3**(3): 363-379.

Bhatia, V., A. Bavdekar and S. K. Yachha (2013). "Management of acute liver failure in infants and children: consensus statement of the pediatric gastroenterology chapter, Indian academy of pediatrics." Indian Pediatr **50**(5): 477-482.

Bourgoin, P., A. Merouani, V. Phan, C. Litalien, M. Lallier, F. Alvarez and P. Jouvet (2014). "Molecular Absorbent Recirculating System therapy (MARS(R)) in pediatric acute liver failure: a single center experience." Pediatr Nephrol **29**(5): 901-908.

Brassier, A., C. Ottolenghi, A. Boutron, A. M. Bertrand, S. Valmary-Degano, J. P. Cervoni, D. Chretien, J. B. Arnoux, L. Hubert, D. Rabier, F. Lacaille, Y. de Keyzer, V. Di Martino and P. de Lonlay (2013). "Dihydrolipoamide dehydrogenase deficiency: a still overlooked cause of recurrent acute liver failure and Reye-like syndrome." Mol Genet Metab **109**(1): 28-32.

Brett, A., C. Pinto, L. Carvalho, P. Garcia, L. Diogo and I. Goncalves (2013). "Acute liver failure in under two year-olds--are there markers of metabolic disease on admission?" Ann Hepatol **12**(5): 791-796.

Bross, P., C. Jespersen, T. G. Jensen, B. S. Andresen, M. J. Kristensen, V. Winter, A. Nandy, F. Krautle, S. Ghisla, L. Bolundi and et al. (1995). "Effects of two mutations detected in medium chain acyl-CoA dehydrogenase (MCAD)-deficient patients on folding, oligomer assembly, and stability of MCAD enzyme." J Biol Chem **270**(17): 10284-10290.

Bucuvalas, J., N. Yazigi and R. H. Squires, Jr. (2006). "Acute liver failure in children." Clin Liver Dis **10**(1): 149-168, vii.

Canbay, A., F. Tacke, J. Hadem, C. Trautwein, G. Gerken and M. P. Manns (2011). "Acute liver failure: a life-threatening disease." Dtsch Arztebl Int **108**(42): 714-720.

Capo-Chichi, J. M., C. Mehawej, V. Delague, C. Caillaud, I. Khneisser, F. F. Hamdan, J. L. Michaud, Z. Kibar and A. Megarbane (2015). "Neuroblastoma Amplified Sequence (NBAS) mutation in recurrent acute liver failure: Confirmatory report in a sibship with very early onset, osteoporosis and developmental delay." Eur J Med Genet **58**(12): 637-641.

Casey, J. P., P. McGettigan, N. Lynam-Lennon, M. McDermott, R. Regan, J. Conroy, B. Bourke, J. O'Sullivan, E. Crushell, S. Lynch and S. Ennis (2012). "Identification of a mutation in LARS as a novel cause of infantile hepatopathy." Mol Genet Metab **106**(3): 351-358.

Danhauser, K., A. Iuso, T. B. Haack, P. Freisinger, K. Brockmann, J. A. Mayr, T. Meitinger and H. Prokisch (2011). "Cellular rescue-assay aids verification of causative DNA-variants in mitochondrial complex I deficiency." Mol Genet Metab **103**(2): 161-166.

Denning, G. M., M. P. Anderson, J. F. Amara, J. Marshall, A. E. Smith and M. J. Welsh (1992). "Processing of mutant cystic fibrosis transmembrane conductance regulator is temperature-sensitive." Nature **358**(6389): 761-764.

Devictor, D., P. Tissieres, P. Durand, L. Chevret and D. Debray (2011). "Acute liver failure in neonates, infants and children." Expert Rev Gastroenterol Hepatol **5**(6): 717-729.

Dhawan, A., P. Cheeseman and G. Mieli-Vergani (2004). "Approaches to acute liver failure in children." Pediatr Transplant **8**(6): 584-588.

Encyclopedia of Cancer (2012). Knockdown. M. Schwab. Berlin Heidelberg, Springer-Verlag.

Engelmann, G., J. Meyburg, N. Shahbek, M. Al-Ali, M. H. Hairetis, A. J. Baker, R. J. Rodenburg, D. Wenning, C. Flechtenmacher, S. Ellard, J. A. Smeitink, G. F. Hoffmann and C. R. Buchanan (2008). "Recurrent acute liver failure and mitochondriopathy in a case of Wolcott-Rallison syndrome." J Inherit Metab Dis **31**(4): 540-546.

ExAC. (2017). "Gene: NBAS." Retrieved February 4, 2017, from http://exac.broadinstitute.org/gene/ENSG00000151779.

Ford, A. (2009). Modeling the environment, Second Edition. Island Press, Washington, DC.

Fruhwald, M. C., M. S. O'Dorisio, L. J. Rush, J. L. Reiter, D. J. Smiraglia, G. Wenger, J. F. Costello, P. S. White, R. Krahe, G. M. Brodeur and C. Plass (2000). "Gene amplification

in PNETs/medulloblastomas: mapping of a novel amplified gene within the MYCN amplicon." J Med Genet **37**(7): 501-509.

Fukao, T., H. Watanabe, K. Orii, Y. Takahashi, A. Hirano, T. Kondo, S. Yamaguchi, T. Aoyama and N. Kondo (2001). "Myopathic form of very-long chain acyl-coa dehydrogenase deficiency: evidence for temperature-sensitive mild mutations in both mutant alleles in a Japanese girl." Pediatr Res **49**(2): 227-231.

Ganschow, R. (2011). "Pediatric Liver Transplantation 2011." Transplantationsmedizin.

Garcia Segarra, N., D. Ballhausen, H. Crawford, M. Perreau, B. Campos-Xavier, K. van Spaendonck-Zwarts, C. Vermeer, M. Russo, P. Y. Zambelli, B. Stevenson, B. Royer-Bertrand, C. Rivolta, F. Candotti, S. Unger, F. L. Munier, A. Superti-Furga and L. Bonafe (2015). "NBAS mutations cause a multisystem disorder involving bone, connective tissue, liver, immune system, and retina." Am J Med Genet A.

Gee, P. and M. Ardagh (1998). "Paediatric exploratory ingestions of paracetamol." N Z Med J **111**(1066): 186-188.

GeneCards. (2017). "Neuroblastoma amplified sequence." Retrieved January 7, 2017, from http://www.genecards.org/cgi-bin/carddisp.pl?gene=NBAS.

Gerhard, D. S., L. Wagner, E. A. Feingold, C. M. Shenmen, L. H. Grouse, G. Schuler, S. L. Klein, S. Old, R. Rasooly, P. Good, M. Guyer, A. M. Peck, J. G. Derge, D. Lipman, F. S. Collins, W. Jang, S. Sherry, M. Feolo, L. Misquitta, E. Lee, K. Rotmistrovsky, S. F. Greenhut, C. F. Schaefer, K. Buetow, T. I. Bonner, D. Haussler, J. Kent, M. Kiekhaus, T. Furey, M. Brent, C. Prange, K. Schreiber, N. Shapiro, N. K. Bhat, R. F. Hopkins, F. Hsie, T. Driscoll, M. B. Soares, T. L. Casavant, T. E. Scheetz, M. J. Brown-stein, T. B. Usdin, S. Toshiyuki, P. Carninci, Y. Piao, D. B. Dudekula, M. S. Ko, K. Kawakami, Y. Suzuki, S. Sugano, C. E. Gruber, M. R. Smith, B. Simmons, T. Moore, R. Waterman, S. L. Johnson, Y. Ruan, C. L. Wei, S. Mathavan, P. H. Gunaratne, J. Wu, A. M. Garcia, S. W. Hulyk, E. Fuh, Y. Yuan, A. Sneed, C. Kowis, A. Hodgson, D. M. Muzny, J. McPherson, R. A. Gibbs, J. Fahey, E. Helton, M. Ketteman, A. Madan, S. Rodrigues, A. Sanchez, M. Whiting, A. Madari, A. C. Young, K. D. Wetherby, S. J. Granite, P. N. Kwong, C. P. Brinkley, R. L. Pearson, G. G. Bouffard, R. W. Blakesly, E. D. Green, M. C. Dickson, A. C. Rodriguez, J. Grimwood, J. Schmutz, R. M. Myers, Y. S. Butterfield, M. Griffith, O. L. Griffith, M. I. Krzywinski, N. Liao, R. Morin, D. Palmquist, A. S. Petrescu, U. Skalska, D. E. Smailus, J. M. Stott, A. Schnerch, J. E. Schein, S. J. Jones, R. A. Holt, A. Baross, M. A. Marra, S. Clifton, K. A. Makowski, S. Bosak and J. Malek (2004). "The status, quality, and expansion of the NIH full-length cDNA project: the Mammalian Gene Collection (MGC)." Genome Res **14**(10B): 2121-2127.

Gerner, P. and P. F. Hoyer (2009). "Acute Liver Failure in Children." Monatsschrift Kinderheilkunde: 1157-1167.

Giebel, L. B., K. M. Strunk, R. A. King, J. M. Hanifin and R. A. Spritz (1990). "A frequent tyrosinase gene mutation in classic, tyrosinase-negative (type IA) oculocutaneous albinism." Proc Natl Acad Sci U S A **87**(9): 3255-3258.

GnomAD. (2017). "Gene: NBAS." Retrieved July 14, 2017, from http://gnomad.broadinstitute.org/gene/ENSG00000151779.

Gortner, L., S. Meyer and F. C. Sitzmann (2012). Pädiatrie. Georg Thieme Verlag, Stuttgart.

Grunert, S. C., A. Wehrle, P. Villavicencio-Lorini, E. Lausch, B. Vetter, K. O. Schwab, S. Tucci and U. Spiekerkoetter (2015). "Medium-chain acyl-CoA dehydrogenase deficiency associated with a novel splice mutation in the ACADM gene missed by newborn screening." BMC Med Genet **16**(1): 56.

Guder, W. G. and J. Nolte (2009). Das Laborbuch für Klinik und Praxis. Elsevier Urban & Fischer, München.

Guénet, J. L., F. Benavides, J.-J. Panthier and X. Montagutelli (2015). Genetics of the Mouse. Springer-Verlag, Berlin Heidelberg.

Haack, T. B., C. Staufner, M. G. Köpke, B. K. Straub, S. Kolker, C. Thiel, P. Freisinger, I. Baric, P. J. McKiernan, N. Dikow, I. Harting, F. Beisse, P. Burgard, U. Kotzaeridou, J. Kuhr, U. Himbert, R. W. Taylor, F. Distelmaier, J. Vockley, L. Ghaloul-Gonzalez, J. Zschocke, L. S. Kremer, E. Graf, T. Schwarzmayr, D. M. Bader, J. Gagneur, T. Wieland, C. Terrile, T. M. Strom, T. Meitinger, G. F. Hoffmann and H. Prokisch (2015). "Biallelic Mutations in NBAS Cause Recurrent Acute Liver Failure with Onset in Infancy." Am J Hum Genet **97**(1): 163-169.

Häberle, J. (2012). UCD Guideline "Harnstoffzyklusstörungen, Diagnostik und Therapie". Deutsche Gesellschaft für Kinder- und Jugendmedizin e.V.

Hadchouel, A., T. Wieland, M. Griese, E. Baruffini, B. Lorenz-Depiereux, L. Enaud, E. Graf, J. C. Dubus, S. Halioui-Louhaichi, A. Coulomb, C. Delacourt, G. Eckstein, R. Zarbock, T. Schwarzmayr, F. Cartault, T. Meitinger, T. Lodi, J. de Blic and T. M. Strom (2015). "Biallelic Mutations of Methionyl-tRNA Synthetase Cause a Specific Type of Pulmonary Alveolar Proteinosis Prevalent on Reunion Island." Am J Hum Genet **96**(5): 826-831.

Halwachs-Baumann, G. (2011). Labormedizin. Springer-Verlag, Wien.

Harms, E. and B. Olgemoller (2011). "Neonatal screening for metabolic and endocrine disorders." Dtsch Arztebl Int **108**(1-2): 11-21; quiz 22.

Hasosah, M. Y., A. I. Iskandarani, A. I. Shawli, A. F. Alsahafi, G. A. Sukkar and M. A. Qurashi (2017). "Neuroblastoma amplified sequence gene mutation: A rare cause of recurrent liver failure in children." Saudi J Gastroenterol **23**(3): 206-208.

Hermann, W. (2012). AWMF Leitlinie für Diagnostik und Therapie in der Neurologie: Morbus Wilson. Deutsche Gesellschaft für Neurologie.

Ho, C. M., P. H. Lee, W. T. Cheng, R. H. Hu, Y. M. Wu and M. C. Ho (2016). "Succinct guide to liver transplantation for medical students." Ann Med Surg (Lond) **12**: 47-53.

HomoloGene. (2015). "HomoloGene:41073. Gene conserved in Euteleostomi." Retrieved February 27, 2015, from http://www.ncbi.nlm.nih.gov/homologene/?term=nbas.

Hong, W. and S. Lev (2014). "Tethering the assembly of SNARE complexes." Trends Cell Biol **24**(1): 35-43.

Hussain, E., M. Grimason, J. Goldstein, C. M. Smith, E. Alonso, P. F. Whitington and M. S. Wainwright (2014). "EEG abnormalities are associated with increased risk of transplant or poor outcome in children with acute liver failure." J Pediatr Gastroenterol Nutr **58**(4): 449-456.

Jhamb, R., B. Kashyap, G. S. Ranga and A. Kumar (2011). "Dengue fever presenting as acute liver failure--a case report." Asian Pac J Trop Med **4**(4): 323-324.

Johannes, L., D. Tenza, C. Antony and B. Goud (1997). "Retrograde transport of KDEL-bearing B-fragment of Shiga toxin." J Biol Chem **272**(31): 19554-19561.

Kim, T. Y. and D. J. Kim (2013). "Acute-on-chronic liver failure." Clin Mol Hepatol **19**(4): 349-359.

King, R. A., D. Townsend, W. Oetting, C. G. Summers, D. P. Olds, J. G. White and R. A. Spritz (1991). "Temperature-sensitive tyrosinase associated with peripheral pigmentation in oculocutaneous albinism." J Clin Invest **87**(3): 1046-1053.

Kopajtich, R., K. Murayama, A. R. Janecke, T. B. Haack, M. Breuer, A. S. Knisely, I. Harting, T. Ohashi, Y. Okazaki, D. Watanabe, Y. Tokuzawa, U. Kotzaeridou, S. Kolker, S. Sauer, M. Carl, S. Straub, A. Entenmann, E. Gizewski, R. G. Feichtinger, J. A. Mayr, K. Lackner, T. M. Strom, T. Meitinger, T. Muller, A. Ohtake, G. F. Hoffmann, H. Prokisch and C. Staufner (2016). "Biallelic IARS Mutations Cause Growth Retardation with Prenatal Onset, Intellectual Disability, Muscular Hypotonia, and Infantile Hepatopathy." Am J Hum Genet **99**(2): 414-422.

Kortum, F., I. Marquardt, M. Alawi, G. C. Korenke, S. Spranger, P. Meinecke and K. Kutsche (2017). "Acute Liver Failure Meets SOPH Syndrome: A Case Report on an Intermediate Phenotype." Pediatrics **139**(1).

Kraynack, B. A., A. Chan, E. Rosenthal, M. Essid, B. Umansky, M. G. Waters and H. D. Schmitt (2005). "Dsl1p, Tip20p, and the novel Dsl3(Sec39) protein are required for the stability of the Q/t-SNARE complex at the endoplasmic reticulum in yeast." Mol Biol Cell **16**(9): 3963-3977.

Kulkarni, S., C. Perez, C. Pichardo, L. Castillo, M. Gagnon, C. Beck-Sague, R. Gereige and E. Hernandez (2015). "Use of Pediatric Health Information System database to study the trends in the incidence, management, etiology, and outcomes due to pediatric acute liver failure in the United States from 2008 to 2013." Pediatr Transplant **19**(8): 888-895.

Larsen, F. S. and P. N. Bjerring (2011). "Acute liver failure." Curr Opin Crit Care **17**(2): 160-164.

Lee, J. Y., S. Sarowar, H. S. Kim, H. Kim, I. Hwang, Y. J. Kim and H. S. Pai (2013). "Silencing of Nicotiana benthamiana Neuroblastoma-Amplified Gene causes ER stress and cell death." BMC Plant Biol **13**: 69.

Lee, W. M. (2003). "Acute liver failure in the United States." Semin Liver Dis **23**(3): 217-226.

Lee, W. M. (2003). "Drug-induced hepatotoxicity." N Engl J Med **349**(5): 474-485.

Lee, W. M., R. H. Squires, Jr., S. L. Nyberg, E. Doo and J. H. Hoofnagle (2008). "Acute liver failure: Summary of a workshop." Hepatology **47**(4): 1401-1415.

Lee, W. S., P. McKiernan and D. A. Kelly (2005). "Etiology, outcome and prognostic indicators of childhood fulminant hepatic failure in the United kingdom." J Pediatr Gastroenterol Nutr **40**(5): 575-581.

Lek, M., K. J. Karczewski, E. V. Minikel, K. E. Samocha, E. Banks, T. Fennell, A. H. O'Donnell-Luria, J. S. Ware, A. J. Hill, B. B. Cummings, T. Tukiainen, D. P. Birnbaum, J. A. Kosmicki, L. E. Duncan, K. Estrada, F. Zhao, J. Zou, E. Pierce-Hoffman, J. Berghout, D. N. Cooper, N. Deflaux, M. DePristo, R. Do, J. Flannick, M. Fromer, L. Gauthier, J. Goldstein, N. Gupta, D. Howrigan, A. Kiezun, M. I. Kurki, A. L. Moonshine, P. Natarajan, L. Orozco, G. M. Peloso, R. Poplin, M. A. Rivas, V. Ruano-Rubio, S. A. Rose, D. M. Ruderfer, K. Shakir, P. D. Stenson, C. Stevens, B. P. Thomas, G. Tiao, M. T. Tusie-Luna, B. Weisburd, H.-H. Won, D. Yu, D. M. Altshuler, D. Ardissino, M. Boehnke, J. Danesh, S. Donnelly, R. Elosua, J. C. Florez, S. B. Gabriel, G. Getz, S. J. Glatt, C. M. Hultman, S. Kathiresan, M. Laakso, S. McCarroll, M. I. McCarthy, D. McGovern, R. McPherson, B. M. Neale, A. Palotie, S. M. Purcell, D. Saleheen, J. M. Scharf, P. Sklar, P. F. Sullivan, J. Tuomilehto, M. T. Tsuang, H. C. Watkins, J. G. Wilson, M. J. Daly, D. G. MacArthur and C. Exome Aggregation (2016). "Analysis of protein-coding genetic variation in 60,706 humans."

Leonis, M. A. and W. F. Balistreri (2008). "Evaluation and management of end-stage liver disease in children." Gastroenterology **134**(6): 1741-1751.

Lev, D., E. Gilad, E. Leshinsky-Silver, S. Houri, A. Levine, A. Saada and T. Lerman-Sagie (2002). "Reversible fulminant lactic acidosis and liver failure in an infant with hepatic cytochrome-c oxidase deficiency." J Inherit Metab Dis **25**(5): 371-377.

Lexmond, W. S., C. M. Van Dael, R. Scheenstra, J. F. Goorhuis, E. Sieders, H. J. Verkade, P. F. Van Rheenen and M. Komhoff (2015). "Experience with molecular adsorbent recirculating system treatment in 20 children listed for high-urgency liver transplantation." Liver Transpl **21**(3): 369-380.

Lin, X., C. C. Liu, Q. Gao, X. Zhang, G. Wu and W. H. Lee (2007). "RINT-1 serves as a tumor suppressor and maintains Golgi dynamics and centrosome integrity for cell survival." Mol Cell Biol **27**(13): 4905-4916.

Liu, E., T. MacKenzie, E. L. Dobyns, C. R. Parikh, F. M. Karrer, M. R. Narkewicz and R. J. Sokol (2006). "Characterization of acute liver failure and development of a continuous risk of death staging system in children." J Hepatol **44**(1): 134-141.

Longman, D., N. Hug, M. Keith, C. Anastasaki, E. E. Patton, G. Grimes and J. F. Caceres (2013). "DHX34 and NBAS form part of an autoregulatory NMD circuit that regulates endogenous RNA targets in human cells, zebrafish and Caenorhabditis elegans." Nucleic Acids Res **41**(17): 8319-8331.

Lopez-Terrada, D., S. W. Cheung, M. J. Finegold and B. B. Knowles (2009). "Hep G2 is a hepatoblastoma-derived cell line." Hum Pathol **40**(10): 1512-1515.

Maksimova, N., K. Hara, I. Nikolaeva, T. Chun-Feng, T. Usui, M. Takagi, Y. Nishihira, A. Miyashita, H. Fujiwara, T. Oyama, A. Nogovicina, A. Sukhomyasova, S. Potapova, R. Kuwano, H. Takahashi, M. Nishizawa and O. Onodera (2010). "Neuroblastoma amplified sequence gene is associated with a novel short stature syndrome characterised by optic nerve atrophy and Pelger-Huet anomaly." J Med Genet **47**(8): 538-548.

Mallard, F. and L. Johannes (2003). "Shiga toxin B-subunit as a tool to study retrograde transport." Methods Mol Med **73**: 209-220.

Marshman, E., C. Booth and C. S. Potten (2002). "The intestinal epithelial stem cell." Bioessays **24**(1): 91-98.

Mellinger, J. L., L. Rossaro, W. E. Naugler, S. N. Nadig, H. Appelman, W. M. Lee and R. J. Fontana (2014). "Epstein-Barr virus (EBV) related acute liver failure: a case series from the US Acute Liver Failure Study Group." Dig Dis Sci **59**(7): 1630-1637.

Meyburg, J. and G. F. Hoffmann (2010). "Liver, liver cell and stem cell transplantation for the treatment of urea cycle defects." Mol Genet Metab **100 Suppl 1**: S77-83.

Narkewicz, M. R., D. Dell Olio, S. J. Karpen, K. F. Murray, K. Schwarz, N. Yazigi, S. Zhang, S. H. Belle, R. H. Squires and G. Pediatric Acute Liver Failure Study (2009). "Pattern of diagnostic evaluation for the causes of pediatric acute liver failure: an opportunity for quality improvement." J Pediatr **155**(6): 801-806 e801.

Odaib, A. A., B. L. Shneider, M. J. Bennett, B. R. Pober, M. Reyes-Mugica, A. L. Friedman, F. J. Suchy and P. Rinaldo (1998). "A defect in the transport of long-chain fatty acids associated with acute liver failure." N Engl J Med **339**(24): 1752-1757.

OMIM. (2015). "INFANTILE LIVER FAILURE SYNDROME 2; ILFS2." Retrieved August 14, 2015, 2015, from http://omim.org/entry/616483.

OMIM. (2015). "NEUROBLASTOMA-AMPLIFIED SEQUENCE; NBAS." Retrieved February 27, 2015, from http://omim.org/entry/608025.

Pape, H.-C., A. Kurtz and S. Silbernagl (2014). Physiologie. Georg Thieme Verlag, Stuttgart.

Park, J. W. and S. J. Lee (2017). "Foveal hypoplasia in short stature with optic atrophy and Pelger-Huet anomaly syndrome with neuroblastoma-amplified sequence (NBAS) gene mutation." J aapos.

Polson, J., W. M. Lee and D. American Association for the Study of Liver (2005). "AASLD position paper: the management of acute liver failure." Hepatology **41**(5): 1179-1197.

Psacharopoulos, H. T., A. P. Mowat, M. Davies, B. Portmann, D. B. Silk and R. Williams (1980). "Fulminant hepatic failure in childhood: an analysis of 31 cases." Arch Dis Child **55**(4): 252-258.

Regateiro, F. S., S. Belkaya, N. Neves, S. Ferreira, P. Silvestre, S. Lemos, M. Venancio, J. L. Casanova, I. Goncalves, E. Jouanguy and L. Diogo (2017). "Recurrent elevated liver transaminases and acute liver failure in two siblings with novel bi-allelic mutations of NBAS." Eur J Med Genet **60**(8): 426-432.

Renz-Polster, H. and S. Krautzig (2013). Basislehrbuch Innere Medizin. Elsevier Urban & Fischer, München.

Rinaldo, P. (2001). "Fatty acid transport and mitochondrial oxidation disorders." Semin Liver Dis **21**(4): 489-500.

Sandvig, K., M. Ryd, O. Garred, E. Schweda, P. K. Holm and B. van Deurs (1994). "Retrograde transport from the Golgi complex to the ER of both Shiga toxin and the nontoxic Shiga B-fragment is regulated by butyric acid and cAMP." J Cell Biol **126**(1): 53-64.

Scott, D. K., J. R. Board, X. Lu, A. D. Pearson, R. M. Kenyon and J. Lunec (2003). "The neuroblastoma amplified gene, NAG: genomic structure and characterisation of the 7.3 kb transcript predominantly expressed in neuroblastoma." Gene **307**: 1-11.

Scott, T. R., V. T. Kronsten, R. D. Hughes and D. L. Shawcross (2013). "Pathophysiology of cerebral oedema in acute liver failure." World J Gastroenterol **19**(48): 9240-9255.

Shi, G., M. Azoulay, F. Dingli, C. Lamaze, D. Loew, J. C. Florent and L. Johannes (2012). "SNAP-tag based proteomics approach for the study of the retrograde route." Traffic **13**(7): 914-925.

Shimozawa, N., Y. Suzuki, Z. Zhang, A. Imamura, R. Toyama, S. Mukai, Y. Fujiki, T. Tsukamoto, T. Osumi, T. Orii, R. J. Wanders and N. Kondo (1999). "Nonsense and temperature-sensitive mutations in PEX13 are the cause of complementation group H of peroxisome biogenesis disorders." Hum Mol Genet **8**(6): 1077-1083.

Sitarz, K. S., H. R. Elliott, B. S. Karaman, C. Relton, P. F. Chinnery and R. Horvath (2014). "Valproic acid triggers increased mitochondrial biogenesis in POLG-deficient fibroblasts." Mol Genet Metab **112**(1): 57-63.

Speckmann, E.-J., J. Hescheler and R. Köhling (2013). Physiologie. Elsevier Urban & Fischer, München.

Speer, C. P. and M. Gahr (2013). Pädiatrie. Springer-Verlag, Berlin Heidelberg.

Sponholz, C., K. Matthes, D. Rupp, W. Backaus, S. Klammt, D. Karailieva, A. Bauschke, U. Settmacher, M. Kohl, M. G. Clemens, S. Mitzner, M. Bauer and A. Kortgen (2016). "Molecular adsorbent recirculating system and single-pass albumin dialysis in liver failure--a prospective, randomised crossover study." Crit Care **20**: 2.

Squires, R. H., A. Dhawan, E. Alonso, M. R. Narkewicz, B. L. Shneider, N. Rodriguez-Baez, D. D. Olio, S. Karpen, J. Bucuvalas, S. Lobritto, E. Rand, P. Rosenthal, S. Horslen, V. Ng, G. Subbarao, N. Kerkar, D. Rudnick, M. J. Lopez, K. Schwarz, R. Romero, S. Elisofon, E. Doo, P. R. Robuck, S. Lawlor and S. H. Belle (2013). "Intravenous N-acetylcysteine in pediatric patients with nonacetaminophen acute liver failure: a placebo-controlled clinical trial." Hepatology **57**(4): 1542-1549.

Squires, R. H., Jr., B. L. Shneider, J. Bucuvalas, E. Alonso, R. J. Sokol, M. R. Narkewicz, A. Dhawan, P. Rosenthal, N. Rodriguez-Baez, K. F. Murray, S. Horslen, M. G. Martin, M. J. Lopez, H. Soriano, B. M. McGuire, M. M. Jonas, N. Yazigi, R. W. Shepherd, K. Schwarz, S. Lobritto, D. W. Thomas, J. E. Lavine, S. Karpen, V. Ng, D. Kelly, N. Simonds and L. S. Hynan (2006). "Acute liver failure in children: the first 348 patients in the pediatric acute liver failure study group." J Pediatr **148**(5): 652-658.

Staufner, C., T. B. Haack, M. G. Köpke, B. K. Straub, S. Kolker, C. Thiel, P. Freisinger, I. Baric, P. J. McKiernan, N. Dikow, I. Harting, F. Beisse, P. Burgard, U. Kotzaeridou, D. Lenz, J. Kuhr, U. Himbert, R. W. Taylor, F. Distelmaier, J. Vockley, L. Ghaloul-Gonzalez, J. A. Ozolek, J. Zschocke, A. Kuster, A. Dick, A. M. Das, T. Wieland, C. Terrile, T. M. Strom, T. Meitinger, H. Prokisch, G. F. Hoffmann, T. B. Haack, C. Staufner, M. G. Kopke, B. K. Straub, S. Kolker, C. Thiel, P. Freisinger, I. Baric, P. J. McKiernan, N. Dikow, I. Harting, F. Beisse, P. Burgard, U. Kotzaeridou, J. Kuhr, U. Himbert, R. W. Taylor, F. Distelmaier, J. Vockley, L. Ghaloul-Gonzalez, J. Zschocke, L. S. Kremer, E. Graf, T. Schwarzmayr, D. M. Bader, J. Gagneur, T. Wieland, C. Terrile, T. M. Strom, T. Meitinger, G. F. Hoffmann and H. Prokisch (2016). "Recurrent acute liver failure due to NBAS deficiency: phenotypic spectrum, disease mechanisms, and therapeutic concepts." J Inherit Metab Dis **39**(1): 3-16.

Tan, S. S. and M. A. Bujang (2013). "The clinical features and outcomes of acute liver failure associated with dengue infection in adults: a case series." Braz J Infect Dis **17**(2): 164-169.

The Human Protein Atlas. (2015). "NBAS." Retrieved August 16, 2015, 2015, from http://www.proteinatlas.org/ENSG00000151779-NBAS/tissue.

UCSC Genome Browser. (2017). "Neuroblastoma amplified sequence." Retrieved January 7, 2017, from http://genome-euro.ucsc.edu/cgi-bin/hgTracks?db=hg19&position=chr2%3A15307032-15701472&hgsid=202826444_gaFAMzNwswphGgqLX6R9sbMatXKJ.

Uemura, T., T. Sato, T. Aoki, A. Yamamoto, T. Okada, R. Hirai, R. Harada, K. Mori, M. Tagaya and A. Harada (2009). "p31 deficiency influences endoplasmic reticulum tubular morphology and cell survival." Mol Cell Biol **29**(7): 1869-1881.

Unal, F., M. Cakir, M. Baran, C. Arikan, H. A. Yuksekkaya and S. Aydogdu (2012). "Liver involvement in children with Familial Mediterranean fever." Dig Liver Dis **44**(8): 689-693.

UniProt. (2015). "P56192 - SYMC_HUMAN." Retrieved August 10, 2015, from http://www.uniprot.org/uniprot/P56192.

UniProt. (2015). "Q2PPL5 - Q2PPL5_HUMAN." Retrieved August 10, 2015, from http://www.uniprot.org/uniprot/Q2PPL5.

UniProt. (2015). "Q9P2J5 - SYLC_HUMAN." Retrieved August 10, 2015, from http://www.uniprot.org/uniprot/Q9P2J5.

UniProt. (2017). "A2RRP1 - NBAS_HUMAN." Retrieved January 7, 2017, from http://www.uniprot.org/uniprot/A2RRP1.

UniProt. (2017). "Q9NZ43 (USE1_HUMAN)." Retrieved July 6, 2017, from http://www.uniprot.org/uniprot/Q9NZ43.

UniProt. (2017). "Q9P2W9 (STX18_HUMAN)." Retrieved July 6, 2017, from http://www.uniprot.org/uniprot/Q9P2W9.

UniProt. (2017). "Q12981 (SEC20_HUMAN)." Retrieved July 6, 2017, from http://www.uniprot.org/uniprot/Q12981.

UniProt. (2017). "UniProtKB - P41252 (SYIC_HUMAN)." Retrieved January 10, 2017, 2017, from http://www.uniprot.org/uniprot/P41252.

Uusimaa, J., H. Jungbluth, C. Fratter, G. Crisponi, L. Feng, M. Zeviani, I. Hughes, E. P. Treacy, J. Birks, G. K. Brown, C. A. Sewry, M. McDermott, F. Muntoni and J. Poulton (2011). "Reversible infantile respiratory chain deficiency is a unique, genetically heterogenous mitochondrial disease." J Med Genet **48**(10): 660-668.

van Meel, E., D. J. Wegner, P. Cliften, M. C. Willing, F. V. White, S. Kornfeld and F. S. Cole (2013). "Rare recessive loss-of-function methionyl-tRNA synthetase mutations presenting as a multi-organ phenotype." BMC Med Genet **14**: 106.

Vilarinho, S., M. Choi, D. Jain, A. Malhotra, S. Kulkarni, D. Pashankar, U. Phatak, M. Patel, A. Bale, S. Mane, R. P. Lifton and P. K. Mistry (2014). "Individual exome analysis in diagnosis and management of paediatric liver failure of indeterminate aetiology." J Hepatol **61**(5): 1056-1063.

Ward, C. L., S. Omura and R. R. Kopito (1995). "Degradation of CFTR by the ubiquitin-proteasome pathway." Cell **83**(1): 121-127.

Wimmer, K., X. X. Zhu, B. J. Lamb, R. Kuick, P. F. Ambros, H. Kovar, D. Thoraval, S. Motyka, J. R. Alberts and S. M. Hanash (1999). "Co-amplification of a novel gene, NAG, with the N-myc gene in neuroblastoma." Oncogene **18**(1): 233-238.

Young, S., E. Kwarta, R. Azzam and T. Sentongo (2013). "Nutrition assessment and support in children with end-stage liver disease." Nutr Clin Pract **28**(3): 317-329.

Zeharia, A., A. Shaag, O. Pappo, A. M. Mager-Heckel, A. Saada, M. Beinat, O. Karicheva, H. Mandel, N. Ofek, R. Segel, D. Marom, A. Rotig, I. Tarassov and O. Elpeleg (2009). "Acute infantile liver failure due to mutations in the TRMU gene." Am J Hum Genet **85**(3): 401-407.

Appendix

List of tables

List of figures

Reference ranges and explanations of the laboratory parameters

The following laboratory parameters are measured in blood plasma. Reference ranges present the range of the middle 95 % values that are found in a healthy control population. Reference ranges may vary between different age groups for some parameters (indicated with *). If this applies, reference ranges for adults are displayed below in Table 21.

Table 21: Reference ranges and explanations of laboratory parameters (Guder and Nolte 2009, Halwachs-Baumann 2011)

parameter	unit	reference range	explanation
alanin transaminase (alt, gpt)	U/l	women: 10-35 men: 10-50	Enzyme located mainly in the cytosol of hepatocytes. Liver specific. When elevated, indicates liver injury.
aspartate transaminase (ast, got)	U/l	women: 10-35 men: 10-50	Enzyme located mainly in the mitochondria of hepatocytes. Also present in many other tissues. When elevated, indicates liver injury.
ast/alt ratio	ratio	< 1.0 → minor liver damage > 1.0 → severe liver damage	Indicates the extent of liver injury.
alkaline phosphatase (ap) *	U/l	women: 35-104 men: 40-130	Enzyme located in hepatocytes and epithelial cells of bile ducts as well as in bones and placenta. When elevated, indicates liver injury.
γ-glutamyl transferase (γ-gt) *	U/l	women: 6-42 men 10-71	Enzyme located in epithelial cells of bile ducts. When elevated, indicates liver injury.
albumin in plasma *	g/l	35-51	Protein mainly synthesized by the liver. When lowered, indicates failure of liver protein synthesis.
bilirubin, total *	mg/dl	≤ 1.0	Decomposition product of haemoglobin. When elevated, indicates liver failure.
bilirubin, indirect	mg/dl	≤ 0.8	Decomposition product of haemoglobin. Indirect bilirubin is conjugated in the liver to direct bilirubin. Hence elevated indirect bilirubin indicates intrahepatic liver failure.

Table 21, continued

bilirubin, direct	mg/dl	≤ 0.2	Decomposition product of haemoglobin. Indirect bilirubin is conjugated in the liver to direct bilirubin. Hence elevated direct bilirubin indicates posthepatic liver failure.
prothrombin time	%	80-130	Assay evaluating the extrinsic pathway of haemostasis. Since the liver is responsible for the synthesis of many proteins required for haemostasis, the decrease of prothrombin time indicates failure of liver protein synthesis.
International Normalized Ratio (INR)	ratio	1.0	Calculated by putting the patient's prothrombin time into ratio with a normal control sample, raised to the power of the ISI value for the analytical system being used. When elevated, indicates failure of liver protein synthesis.

Acknowledgements

In first place, I want to thank Dr. Holger Prokisch for giving me the opportunity to do my doctoral dissertation in his laboratory group. I very much appreciate his encouragement, positive energy and guidance along the way. I also want to thank Prof. Dr. Thomas Meitinger for being my Doktorvater and letting me re-think aspects of my thesis through his advice.

Moreover, my heartfelt thanks go to all Prokisch group members (Eliška Koňaříková, Robert Kopajtich, Arcangela Iuso, Birgit Repp, Marieta Borzes, Katharina Schramm, Caterina Terrile, Caroline Biagosch, Riccardo Berutti, Sabine Schäfer and Lena Protzmann) who were amazing colleagues, always supportive, helpful and made the best working environment. I especially want to thank Caterina Terrile, Sabine Schäfer and Lena Protzmann for their valuable technical assistance in many experiments. Furthermore, thank you to Eliška Koňaříková, who always answered my stupid questions and annotated my thesis.

I am also very grateful to Martina Kuhnert for all the administrative help and shortcuts to Prof. Meitinger.

Last but not least, thank you ever so much to my family, who enabled my medical studies and supported me all the way. Without you, all of this would not have been possible.